# JOURNAL OF FOOD PROCESS ENGINEERING



D.R. HELDMAN
and
R.P. SINGH
COEDITORS

FOOD & NUTRITION PRESS, INC.

VOLUME 15, NUMBER 4 DECEMBER 1992

# JOURNAL OF FOOD PROCESS ENGINEERING





All articles for publication and inquiries regarding publication should be sent to DR. D.R. HELDMAN, COEDITOR, *Journal of Food Process Engineering,* Weinberg Consulting Group Inc., 1220 19th St., N.W., Washington, D.C. 20036 USA: or DR. R.P. SINGH, COEDITOR, *Journal of Food Process Engineering,* University of California, Davis, Department of Agricultural Engineering, Davis, CA 95616 USA.

All subscriptions and inquiries regarding subscriptions should be sent to Food & Nutrition Press, Inc., 2 Corporate Drive, P.O. Box 374, Trumbull, CT 06611 USA.

One volume of four issues will be published annually. The price for Volume 15 is $120.00 which includes postage to U.S., Canada, and Mexico. Subscriptions to other countries are $139.00 per year via surface mail, and $148.00 per year via airmail.

Subscriptions for individuals for their own personal use are $100.00 for Volume 15 which includes postage to U.S., Canada, and Mexico. Personal subscriptions to other countries are $119.00 per year via surface mail, and $128.00 per year via airmail. Subscriptions for individuals should be sent direct to the publisher and marked for personal use.

The *Journal of Food Process Engineering* (ISSN: 0145-8876) is published quarterly (March, June, September and December) by Food & Nutrition Press, Inc.—Office of Publication is 2 Corporate Drive, P.O. Box 374, Trumbull, Connecticut 06611 USA.

Second class postage paid at Bridgeport, CT 06602.

POSTMASTER: Send address changes to Food & Nutrition Press, Inc., 2 Corporate Drive, P.O. Box 374, Trumbull, CT 06611.

# JOURNAL OF FOOD PROCESS ENGINEERING

# JOURNAL OF FOOD PROCESS ENGINEERING

# Journal of FOOD PROCESS ENGINEERING

VOLUME 15
NUMBER 4

**Coeditors:** **D.R. HELDMAN**
**R.P. SINGH**

FOOD & NUTRITION PRESS, INC.
TRUMBULL, CONNECTICUT 06611 USA

ISSN 0145-8876

Printed in the United States of America

## CONTENTS

# EFFECT OF PULPER-FINISHER OPERATION ON QUALITY OF TOMATO JUICE AND TOMATO PUREE

ATHAPOL NOOMHORM and AMPAWAN TANSAKUL

*Division of Agricultural and Food Engineering*
*Asian Institute of Technology*
*G.P.O. Box 2754, Bangkok 10501, Thailand*

Accepted for Publication March 5, 1992

## ABSTRACT

*Preliminary tests were done on the performance of an existing pulper finisher design with two unadjustable blades. Quality parameters such as consistency index and yield were determined at screen sizes of 0.5, 1.0, 1.5 mm and speeds: 100, 300, 500 and 700 rpm. Design modifications were made on the pulper finisher by addition of another blade and slide tapering of blades to allow smooth flow of material on one direction. Quality parameters such as consistency index, pulp/serum ratio, particle size distribution, total solids and total yield were evaluated.*

*A maximum quality index in terms of total solids, pulp/serum, consistency, particle size distribution was achieved at screen size 1.0 mm and a speed of 700 rpm. Maximum yield of tomato juice however, was obtained with screen size of 1.5 mm and a speed of 700 rpm. Results of the comparative tests done on existing and modified pulper finisher showed that quality and quantity of tomato juice and puree from the modified unit is better and higher. A 3% increase in yield was observed from the modified unit.*

## INTRODUCTION

Tomato (*Lycopersicon esculentum*) is one of the most important vegetables in Thailand and in terms of commercial production, ranks first among all processed vegetables. Tomatoes are used in enormous quantities in fresh state, as canned and peeled tomatoes, as canned tomato juice and canned concentrated tomatoes (paste, puree, sauce). Preparation of tomato puree involves size reduction, heating to either soften tissue and/or to inactivate enzymes, and straining of the heated

Journal of Food Process Engineering **15** (1992) 229–239. 

mass through the pulper-finisher. The juice from the pulper-finisher is then concentrated, sterilized and packaged.

The pulper-finisher's operational parameters, i.e., screen size and speed, have significant influence on the quality of tomato puree. Previous studies done on concentrated tomato have focused mainly on the thermal break temperature, pH and method of concentration. Studies on the effect of screen size and speed on quality of tomato juice and puree are quite limited.

This research aims to study the effect of different screen sizes and speed of the laboratory scale pulper-finisher on quality of tomato juice and puree. The results from this study can be applied for improvement of tomato puree quality in food processing plants.

## LITERATURE REVIEW

### Tomato Juice and Puree Processing

In the hot break process, the preliminary heating given to the tomatoes completely destroys the pectic enzymes and protects the constituents of the tomato from enzymatic changes. The tomatoes are crushed with a minimum inclusion of air and quickly heated to as high as 104C. The yield of cyclone juice is greater than that obtained for cold break system. The tomatoes are crushed at temperatures below 66C and allowed to fall in a holding tank, where they remain static for some time. The enzyme liberated during crushing can catalyze the breakdown of pectin.

### Effect of Processing Factors on Tomato Juice and Puree

Maintenance of cloud along with prolonged suspension of solids with proper rheological properties and appearance (consistency) is a primary goal in the production of comminuted tomato products. Attainment of stable consistency is particularly important since thickeners cannot be added to the products. The principal factors contributing are thermobreak temperature, pH and pulper-finisher.

**Pulper-Finisher Performance.** The pulper-finisher consists of a horizontal cylinder made of a fine sieve of stainless steel, inside are heavy paddles that revolve rapidly, causing the fine pulp to pass through the screen and the piece of skin, seeds, fiber, etc., to pass out the end of the machine (Luh and Kean 1988). Whittenberger and Nutting (1957) concluded that consistency depends largely on the quantity, shape and degree of subdivision of the cell walls present, and on the characteristics of the walls as determined by the occurrence of pectin. The finisher

is an important unit for controlling the gross viscosity of tomato juice. With a paddle-type finisher, adjustment of the speed of the paddle provides a wide range of gross viscosity regardless of the preheating temperatures (Hand *et al.* 1955). The use of fine screens for reduction of particle size would enhance oxidation because of the relatively large surface exposed to air and metal. Therefore, increase in the screen size increased the retention of color and ascorbic acid (Kattan *et al.* 1956).

The beating action of the finisher may incorporate more air into the juice and thus destroy some vitamin C (Moyer *et al.* 1959). The quantity and quality of insoluble material present in tomato juice had a very important bearing on consistency and the related property of settling. Rao *et al.* (1986) found that the finishing operation (screen size and finisher speed) can be expected to have significant influence on the consistency of apple sauce due to its effect on the quantity and the dimensions of the pulp. Pulp content and average particle size of the solids affected the magnitude of the yield stress of apple sauce (Qiu and Rao 1988). Small screen sizes can affect the gross viscosity of tomato concentrates in two opposite manners. One is enhancing gross viscosity due to the large surface area of small particles and the other is diminishing the gross viscosity due to the exclusion of large particles (Tanglertpaibul and Rao 1987).

## MATERIALS AND METHODS

### Tomato Juice and Puree Preparation

Tomatoes (*Lycopersicom esculentum* L., var VF-134) were harvested fresh from Chiangmai province, Thailand. The whole tomatoes were sorted, washed and heated in hot water bath at 80C for 5 min. The heated tomatoes were fed to the pulper finisher at a rate of 5 kg/5 s. The heated tomatoes were crushed and extracted by the pulper finisher operating at 100, 300, 500 and 700 rpm with screen openings of 0.5, 1.0, and 1.5 mm. In each trial, the tomato samples (5 kg) was retained in the pulper finisher for 4 min.

In order to obtain tomato puree, the juice from the pulper-finisher was concentrated to 14 Brix by vacuum rotary evaporator at 60 cm Hg and temperature 70C for 35 min in a water bath.

### Pulper Finisher

The cross-sectional diagram of pulper-finisher is shown in Fig. 1. The pulper-finisher was modified from the original design to accommodate three blades and with slight blade angle adjustment into a taper to facilitate smooth flow of the

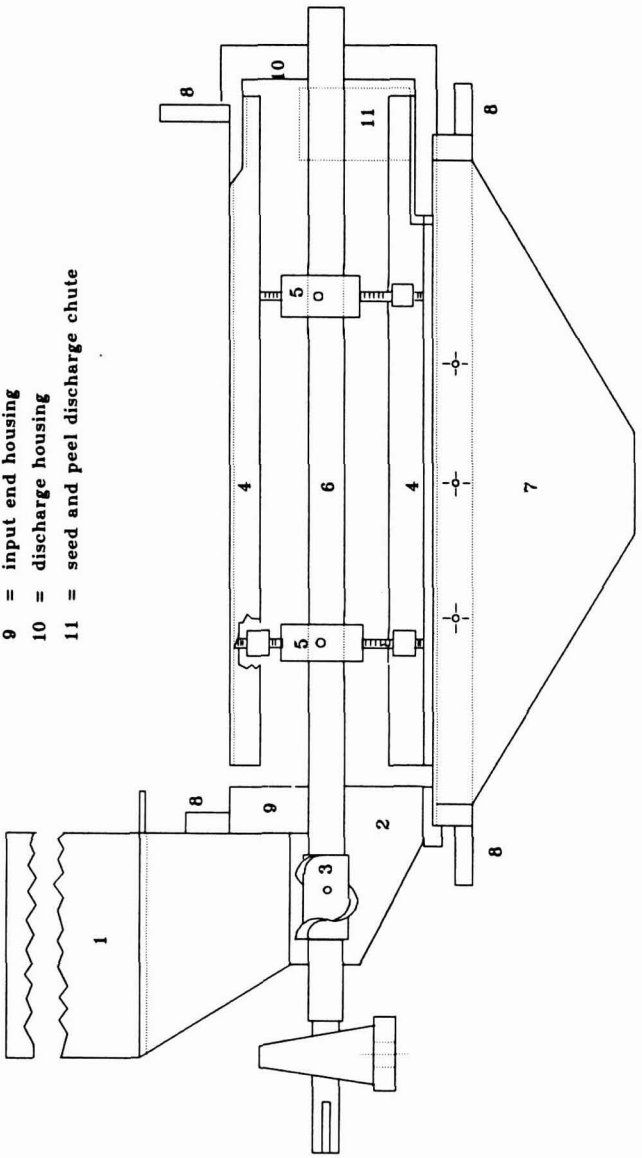


FIG. 1. CROSS SECTION OF A PULP FINISHER

product in one direction. The material moves along the inclined direction of the taper. Increasing the number of blades, helped to push greater quantity of the product through the screen.

### Evaluation of Quality Parameters

**Total Yield and Total Soluble Solid.** The total yield of pulper-finisher was determined by weighing and the product total solids were determined using the AOAC (1975) standard method. The soluble solids of each sample were determined with an Atago refractometer (Atago Co. Ltd., Tokyo, Japan).

**pH.** The pH of samples was determined using pH meter Model HM-26S (TOA Electronics Ltd., Tokyo, Japan).

**Consistency.** The consistency of the tomato juice and puree was determined using a Brookfield Synchro-lectric Viscometer (Model LVF, Brookfield Engineering Laboratories Inc., MA).

**Particle Size Distribution.** The distribution of particle size was determined as suggested by Kimball *et al.* (1952).

**Pulp/Serum Ratio.** The pulp/serum ratio was determined as suggested by Tanglertpaibul and Rao (1987). The sample was centrifuged at 3000 rpm for 30 min using a Centrifuge Model Kokusan Model H-103N Series (Kokusan Ensiki Co. Ltd., Tokyo, Japan).

### Experimental Design and Statistical Analysis

Three sets of experiments were performed on the pulper finisher with three replications at: 100, 300, 500 and 700 rpm speed of rotation and 0.5, 1.0 and 1.5 mm screen sizes. Analyses of variance (ANOVA) was carried out with a Statgraphic software on a microcomputer. Significant difference between means were determined by using Duncan's Multiple Range Test (DMRT) at 5% confidence level ($P < 0.05$).

## RESULTS AND DISCUSSION

### Effect of Screen Size and Speed of Pulper-Finisher on Yield of Tomato Juice

Increasing yield of tomato juice was observed with speed and screen size of pulper-finisher with two blades as shown in Fig. 2. It was observed that at any

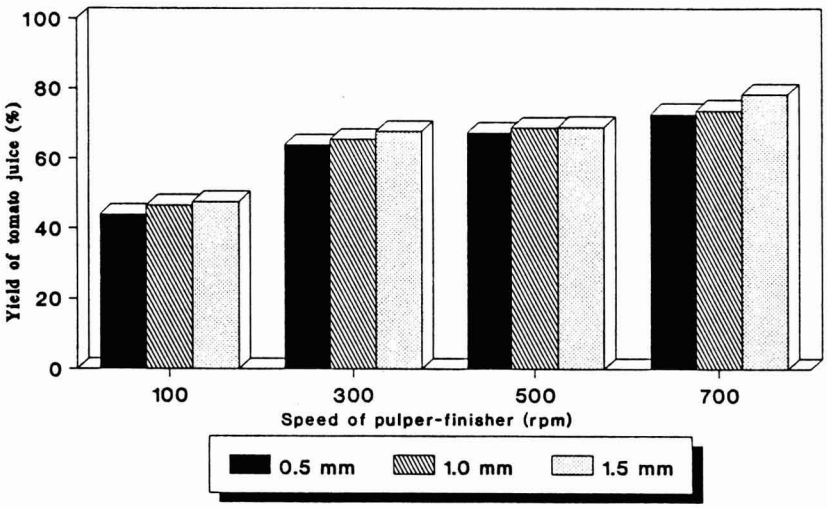


FIG. 2. YIELD OF TOMATO JUICE FROM EXISTING PULPER-FINISHER

given speed, the larger screen size allowed not only more than tomato pulp but also tomato serum to flow through the sieve, which resulted in higher yield. Furthermore, the higher rotating speed resulted in greater centrifugal force, which allowed more tomato juice and serum to pass through. Highest tomato juice yield was obtained at the maximum experimental conditions of 1.5 mm screen size of 700 rpm on both of the existing pulper-finisher with two blades and the modified pulper-finisher with three blades at 78.2 and 80.9%, respectively.

## Effect of Screen Size and Speed of the Existing Pulper-Finisher on the Consistency of Tomato Juice and Puree

At any given speed of rotation, lower consistency of tomato juice and puree was observed for screen size of 0.5 and 1.5 mm than that of 1.0 mm (Fig. 3). At 0.5 mm screen size resulted in small particle size thereby lowering the consistency because gross viscosity was diminished due to exclusion of large particles (Tanglertpaibul and Rao 1987). Use of 1.5 mm screen size resulted in tomato seeds and other large particles mining with the juice. However, the 1.0 mm screen size produced small particles and allowed most of the large particles to remain, thereby resulting in higher consistency. The use of 1.0 mm screen size therefore resulted in tomato juice and puree of optimum particle size with highest consistency. Furthermore, it was observed that at any given screen size, the higher speed

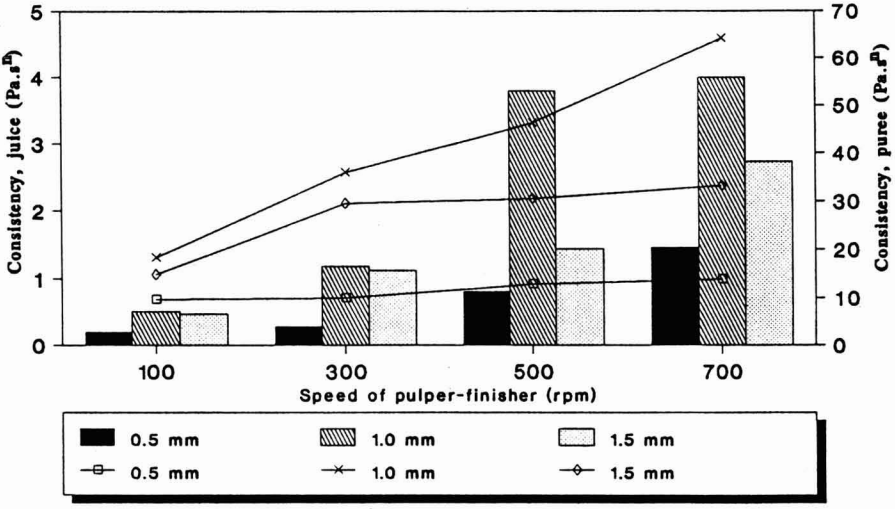


FIG. 3. CONSISTENCY INDEX OF TOMATO JUICE AND PUREE FROM EXISTING PULPER-FINISHER

of finisher resulted in better consistency of tomato juice and puree. At optimum screen size of 1.0 mm, the consistency index increased by approximately threefold and fivefold with increase in speed of 100 to 700 rpm for juice and puree, respectively.

Results of the experiments on the existing pulper-finisher showed satisfactory quality of tomato juice and puree with respect to consistency and yield; however, it was observed that flow and yield of products could be further improved by modification of the existing pulper-finisher design.

## Effect of Screen Size and Speed of Modified Pulper-Finisher on Total Solids of Tomato Juice and Puree

Results showed that total solids of tomato juice and puree increased with speed of pulper-finisher (Fig. 4). Furthermore, it was observed that 1.0 mm screen size gave the highest total solids for any given speed. At 700 rpm and 1.0 mm screen size highest total solids of 6.11% and 16.18% were obtained for tomato juice and puree, respectively. Optimum proportion of tomato pulp and serum were observed for 1.0 mm screen size thereby resulting in higher total solids. Analysis of variance (ANOVA) and DMRT test showed significant differences of total with speed and screen size for juice and puree.

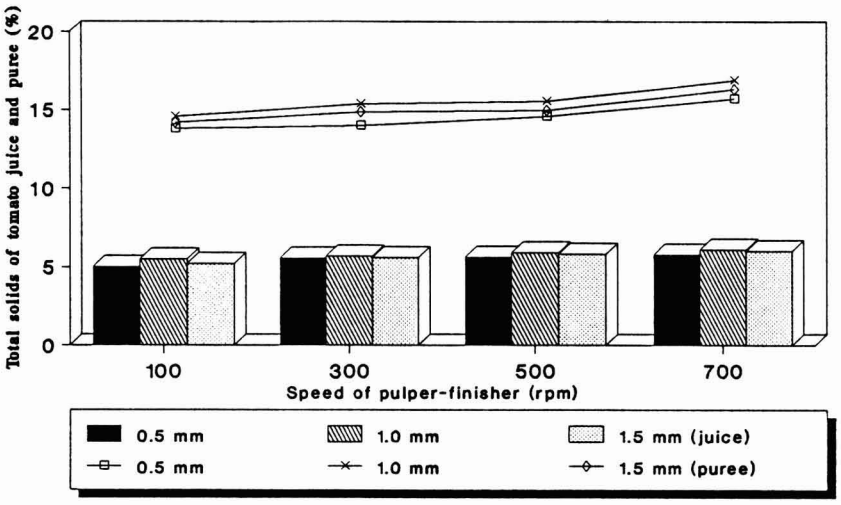


FIG. 4. TOTAL SOLIDS OF TOMATO JUICE AND PUREE FROM MODIFIED PULPER-FINISHER

## Effect of Screen Size and Speed of Modified Pulp/Serum Ratio and Particle Size of Tomato Juice and Puree

Pulp/serum ratio was observed to increased with screen size, but lower for 1.5 mm than for 1.0 mm (Fig. 5). The pulp serum ratio of tomato juice increased from 20.36 to 25.98% at the speed of 100 and 33.60 to 37.19% at 700 rpm when screen size was increased from 0.5 to 1.0 mm. At higher speeds the pulp/serum ratio also increased. Highest pulp serum ratio of 37.19% was obtained for conditions of 1.0 mm screen size and 700 rpm.

Particle size distribution of tomato juice increased with screen size (Fig. 6). Particle size variation was observed (i.e., from .027 to 0.29 mm, 0.34 to 0.35 mm and 0.41 to .043 mm, for screen size of 0.5, 1.0 and 1.5 mm, respectively) when the speed was varied from 100 to 700 rpm.

## Comparative Performance of Existing and Modified Pulper-Finisher

Consistency index from the modified pulper-finisher was consistently higher than the existing machine for both juice and puree (Table 1). Significant increase of consistency index was observed at all treatment combinations of speed and screen size for the modified machine. At the best operating conditions of 700 rpm and 1.0 mm screen size, consistency index increased from 3.00 to 4.75 $Pa.s^n$ and from 64.1 to 151.9 $Pa.s^n$ for tomato juice and puree, respectively.

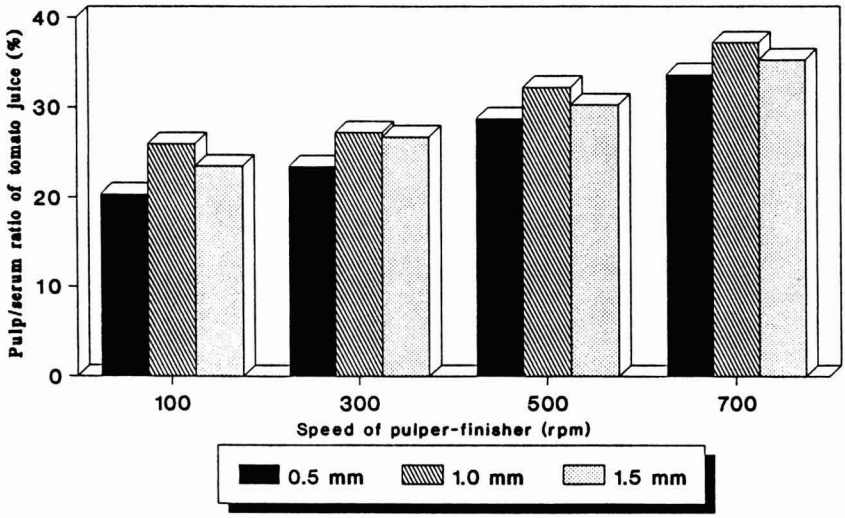


FIG. 5. PULP/SERUM RATIO OF TOMATO JUICE FROM THE MODIFIED PULPER-FINISHER

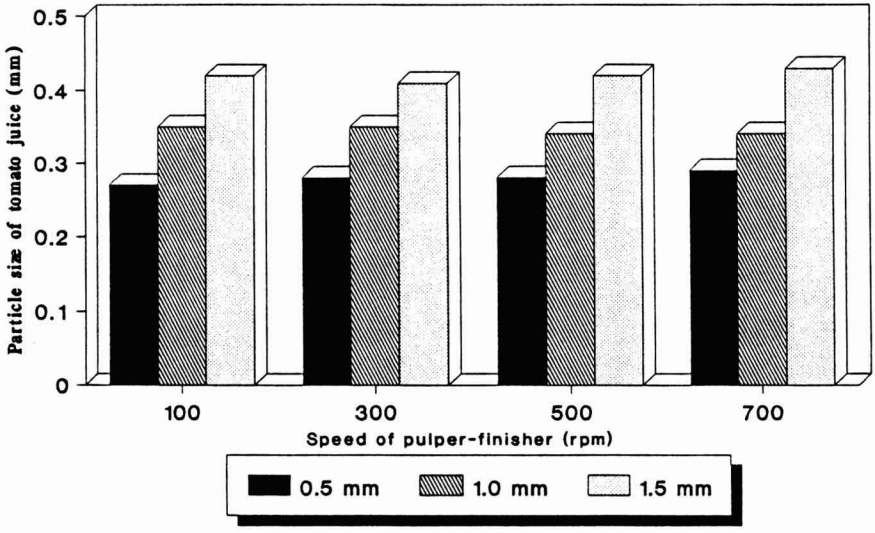


FIG. 6. PARTICLE SIZE OF TOMATO JUICE FROM THE MODIFIED PULPER-FINISHER

TABLE 1.
COMPARATIVE PERFORMANCE OF EXISTING AND MODIFIED PULPER-FINISHER

| rpm | Yield (%) | | | | | | Consistency (Pa.s^n) | | | | | |
|---|---|---|---|---|---|---|---|---|---|---|---|---|
| | existing | | | modified | | | existing | | | modified | | |
| | 0.5 | 1.0 | 1.5 | 0.5 | 1.0 | 1.5 | 0.5 | 1.0 | 1.5 | 0.5 | 1.0 | 1.5 |
| 100 | 43.9 | 46.4 | 47.5 | 44.3 | 46.9 | 47.6 | 0.20 | 0.51 | 0.47 | 0.31 | 1.71 | 0.78 |
| 300 | 63.8 | 65.3 | 67.7 | 66.0 | 67.1 | 67.7 | 0.28 | 1.18 | 1.12 | 0.47 | 2.20 | 1.18 |
| 500 | 67.2 | 68.6 | 68.9 | 76.3 | 76.6 | 76.7 | 0.81 | 3.79 | 1.44 | 1.51 | 4.32 | 2.51 |
| 700 | 72.5 | 73.5 | 78.1 | 78.2 | 79.8 | 80.9 | 1.46 | 3.99 | 2.37 | 1.78 | 4.75 | 3.10 |

Note: Pa.S = Pascal *second; n = Flow behavior index

Furthermore, yield of tomato juice increased with the modified pulper finisher. At the best tomato yield conditions of 700 rpm and 1.5 mm, approximately 3% increase was observed in tomato juice yield. The higher number of paddles could beat tomato macerate to pass through the screen easily. Further improvements on the yield is expected with higher rpm and number of blades; however, in consideration of the quality aspect, specifically consistency, conditions of 700 rpm and from 1.0 to 1.5 mm screen size should be maintained.

## CONCLUSIONS

(1) Screen size and speed of pulper-finisher have significant effect on the quality parameters, i.e., consistency, total solids, pulp/serum ration, particle size distribution and on the yield of tomato juice. (2) Highest consistency and quality parameters can be obtained with 1.0 mm screen size and 700 rpm. (3) For maximum yield conditions of 1.5 mm and 700 rpm should be maintained.

It is therefore recommended that the modified pulper finisher with three blades be used under conditions of 700 rpm and 1.0 and 1.5 mm screen size for best yield and quality considerations.

## REFERENCES

A.O.A.C. 1975. *Official Methods of Analysis*, 14th Ed., Association of Agricultural Chemists, Washington, D.C.

HAND, D.B., MOYER, J.C., RANSFORD, J.R., HENSING, J.C. and WHITTENBERGER, R.T. 1955. Effect of processing conditions on the viscosity of tomato juice. Food Technol. *9*, 228–235.

KATTAN, A.A., OGLE, W.L. and KRAMER, A. 1956. Effect of process variable on quality of canned tomato juice. Proc. Am. Soc. Hort. Sci. *68*, 470.

KIMBALL, L.B., LILLIAN, B. and KERTESZ, Z.I. 1952. Practical determination of size distribution of suspended particles in macerated tomato products. Food Technol. *6*, 68–71.

LUH, B.S. and KEAN, C.E. 1988. *Commercial Vegetable Processing*, 2nd Ed. Van Nostrand Reinhold/AVI, New York.

MOYER, J.C., ROBINSON, W.B., RANSFORD, J.R., LABELLE, R.L. and HAND, D.B. 1959. Processing Conditions Affecting the Yield of Tomato Juice. Food Technol. May, 270–272.

QIU, C.G. and RAO, M.A., COOLEY, H.J., NOQUEIRA, J.N. and MCLELLAN, M.R. 1986. Rheology of apple sauce: Effect of apple cultivar, firmness and processing parameters. J. Food Sci. *51*, 176–179.

RAO, M.A., COOLEY, H.J., NOQUEIRA, J.N. and MCLELLAN, M.R. 1986. Rheology of apple sauce: Effect of apple cultivar, firmness and processing parameters. J. Food Sci. *51*, 176–179.

TANGLERTPAIBUL, T. and RAO, M.A. 1987. Flow properties of tomato concentrates: Effect of serum viscosity and pulp content. J. Food Sci. *52*(2), 318–321.

WHITTENBERGER, R.T. and NUTTING, G.C. 1957. Effect of tomato cell structures on consistency of tomato juice. Food Technol. *11*, 19–22.

# MATHEMATICAL MODELING AND EXPERIMENTAL STUDIES ON OHMIC HEATING OF LIQUID-PARTICLE MIXTURES IN A STATIC HEATER[1]

SUDHIR K. SASTRY[2] and SEVUGAN PALANIAPPAN

*The Ohio State University*
*Department of Agricultural Engineering*
*590 Woody Hayes Drive*
*Columbus, OH 43210*

Accepted for Publication May 28, 1992

## ABSTRACT

*Understanding of the ohmic heating of liquid-particle mixtures requires preliminary study and model development within a static heater. A mathematical (3D finite element) model was developed for prediction of temperatures of mixtures of liquids and multiple particles within a static heater. Experiments were conducted using cubic potato particles within sodium phosphate solutions, for various particle sizes, orientations, concentrations, and liquid conductivities. The mathematical model was found to yield satisfactory prediction of experimental trends. Critical parameters affecting the relative heating rates of particles and liquid were the conductivities of the two phases, and the volume fraction of each phase. Ohmic heating appears most promising with high-solids concentration mixtures.*

## INTRODUCTION

In recent years, the world's food industry has focused increasing attention on continuous sterilization of liquid-particle mixtures. The conventional process

[1]Salaries and research support provided by State and Federal Funds appropriated to the Ohio Agricultural Research and Development Center, The Ohio State University. Journal Article No. 86-92. References to commercial products and trade names is made with the understanding that no discrimination and no endorsement by The Ohio State University is implied.
[2]Corresponding author.

Journal of Food Process Engineering **15** (1992) 241–261. *All Rights Reserved.*

systems considered typically involve swept-surface heat exchangers for heating, a holding tube for providing residence time, and heat exchangers for cooling. When heterogeneous foods (liquids with large suspended solid particles) are processed by these methods, the liquid acts as an intermediate heat transfer medium, and thermal lags exist within particles. Particle temperatures can be conservatively estimated by models (Sastry 1986; Chandarana and Gavin 1989; Lee and Singh 1988, among others), and the problem reduces to that of accurate estimation of fastest-particle residence times and liquid-to-particle convective heat transfer coefficients. Conservative assumptions will ensure safety at the expense of product quality.

Ohmic heating (Biss *et al.* 1989) is considered promising for liquid-particle mixtures because of the rapidity and uniformity of heating. The principle of ohmic heating is, quite simply, internal generation arising from passage of an electric current through the food material. The process is not yet well-understood, although studies by de Alwis and Fryer (1990), de Alwis *et al.* (1990) and Halden *et al.* (1990) have yielded valuable insights. The electrical conductivities of solid and liquid phases, as well as the size, shape and orientation of particles would be expected to play significant roles in the process.

As in the case of conventional aseptic processing, measurement of particle internal temperatures during continuous flow is difficult; the problems being even more severe for ohmic heating because of the presence of a strong electric field. Fundamental understanding of the process can, however, be obtained using a static ohmic heater before attempting process design on the continuous system. The static heater is particularly important, because it can approximate the geometry of the continuous heater and clearly demonstrate the effects of operational variables on heating rates of liquid and particles. It is also a useful device for verification of mathematical models.

Previous work on ohmic heating is limited, being largely confined to blanching (Mizrahi *et al.* 1975), although the concept is hardly new, having been used in electric pasteurization several decades ago, as discussed by Palaniappan *et al.* (1990). Recently, de Alwis and Fryer (1990) developed a 2-D finite element model for prediction of temperatures of a single rectangular particle within a static ohmic heater. Their study indicated the importance of orientation of thin particles and provided useful insights into the process. In a commercial situation, however, many particles will be present, and the three-dimensional configuration cannot be discounted. It is therefore necessary to develop models to address these considerations. The objectives of this study are therefore: (1) to develop a mathematical model for prediction of particle and liquid temperatures during ohmic heating; (2) to verify the model using a static ohmic heater, and (3) to determine the influence of concentration and electrical conductivity of each phase on the heating rates of liquid-particle mixtures.

## MATERIALS AND METHODS

### Mathematical Model

The static heater under consideration (Fig. 1) consists of a cylindrical chamber filled with the liquid-particle mixture, with the electrodes located at the ends. The mathematical formulation involves interdependent thermal and electrical problems; the former involving determination of liquid and particle temperature fields, and the latter, the voltage field (or electric field strength).

In general, a particle size distribution exists, and the heat transfer problem should be separately solved for each particle, resulting in a computationally prohibitive problem. A more expeditious approach would be to consider the effect of the "average" particle and to assume that the population behavior is similar to that of a collection of particles, all of the average size. In the present study, particles were assumed to be cube-shaped.

**Liquid Temperature.** If the fluid is of low viscosity, permitting rapid mixing, temperature gradients within it can be considered small (this has been verified previously by experiment), and the following energy balance may be used on the fluid.

$$M_f C_{pf} \frac{[T_\infty^{n+1} - T_\infty^n]}{\Delta t} = \dot{u}_f v_f + n_p h_{fp} A_p [T_{sm} - T_{\infty m}] - U A_w [T_{\infty m} - T_a] \quad (1)$$

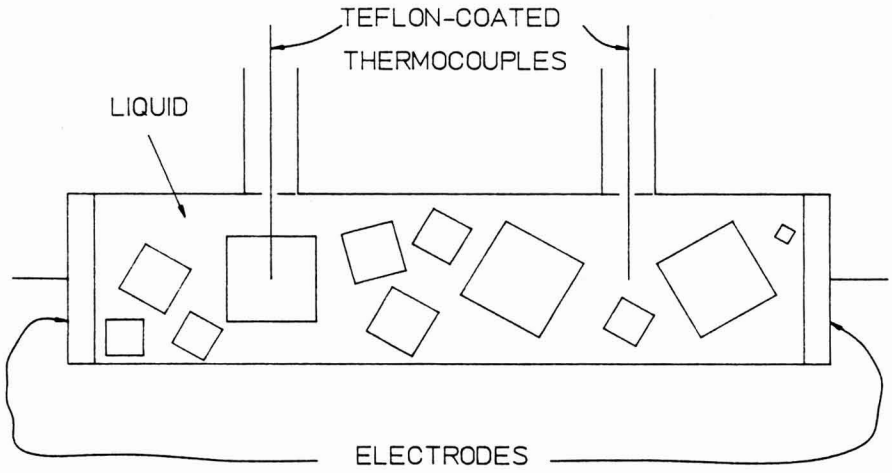


FIG. 1. SCHEMATIC DIAGRAM OF STATIC OHMIC HEATER USED FOR MODELING AND EXPERIMENTAL WORK

where:

$$T_{\infty m} = \frac{T_{\infty}^{n+1} + T_{\infty}^{n}}{2}$$

$$T_{sm} = \frac{T_{s}^{n+1} + T_{s}^{n}}{2}$$

The energy generation rate at each point within a conductor can be derived from basic physical considerations (Mizrahi *et al.* 1975; Sastry 1989), and for the case of constant voltage is:

$$\begin{aligned} \dot{u} &= (\nabla V)\cdot(\nabla V)\sigma \\ &= |\nabla V|^2 \sigma \end{aligned} \tag{2}$$

and for the constant current case:

$$\dot{u} = \frac{J \cdot J}{\sigma} = \frac{|J|^2}{\sigma} \tag{3}$$

The electrical conductivity of most food materials subjected to ohmic heating is a linear function of temperature (Palaniappan and Sastry 1991a,b):

$$\sigma = \sigma_0 [1 + mT] \tag{4}$$

Thus, the energy generation term $\dot{u}_f$ in Eq. (1) is given by:

$$\dot{u}_f = |\nabla V|^2 \sigma_{0f} [1 + m_f T_{\infty m}] \tag{5}$$

The liquid temperature at each successive time increment $(n+1)$ can be calculated from Eq. (1), provided the mean particle surface temperature ($T_{sm}$) and the voltage field ($V$) are known.

**Particle Temperature.** The heat transfer problem for particles is the conduction heat transfer equation with temperature-dependent internal energy generation.

$$\nabla \cdot (k_p \nabla T_p) + \dot{u}_p(T_p) = \rho_p C_{pp} \frac{\partial T_p}{\partial t} \tag{6}$$

with a time-dependent boundary condition:

$$k\nabla T_p \cdot \vec{n} = h_{fp}[T_s - T_\infty(t)] \tag{7}$$

The energy generation term of Eq. (6) is given by:

$$\dot{u}_p = |\nabla V|^2 \sigma_{0p}[1 + m_p T_p] \tag{8}$$

The above problem can be solved using the three dimensional finite element method in space, and Crank-Nicolson finite differencing in time. The approach consists of obtaining the weak variational formulation for the above problem, and using polynomial basis functions to obtain the following system of equations.

$$\sum_{i=1}^{N} M_{ij} \frac{dT_{pi}}{dt} + \sum_{i=1}^{N} K_{ij} T_{pi} = F_j; \tag{9}$$

$$j = 1,2,...N$$

where:

$$M_{ij} = \frac{1}{\alpha} \int_v \phi_i \phi_j dv$$

$$K_{ij} = \int_v [\nabla \phi_i \cdot \nabla \phi_j - \frac{\sigma_{0p} |\nabla V|^2 m_p}{k_p} \phi_i \phi_j] dv$$

for all nonsurface nodes, and:

$$K_{ij} = \int_v [\nabla \phi_i \cdot \nabla \phi_j - \frac{\sigma_{0p} |\nabla V|^2 m_p}{k_p} \phi_i \phi_j] dv$$

$$- \frac{h_{fp}}{k_p} \int_s \phi_i \phi_j \, ds$$

for all surface nodes.

$$F_j = \frac{\sigma_{0p} |\nabla V|^2}{k_p} \int_v \phi_j \, dv$$

for all nonsurface nodes, and:

$$F_j = \frac{\sigma_{0p}|\nabla V|^2}{k_p}\int_v \phi_j\, dv - \frac{h_{fp}T_\infty(t)}{k_p}\int_s \phi_j\, ds$$

for all surface nodes.

In the preceding matrix definitions, the basis functions $\phi_i$ are polynomials chosen such that at the nodal points, $\phi_i(x_j,y_j,z_j) = \delta_{ij}$; where $\delta_{ij}$ is the Kronecker delta function, with the property that $\delta_{ij}$ is unity for $i = j$, and zero for all other $i$, Also implicit in the above development is the assumption that the thermophysical properties of the solid, although functions of temperature, can be expected to be constant within a single time step, permitting the lumping of $k_p$, $\rho_p$ and $C_{pp}$ into an effective thermal diffusivity ($\alpha$).

The system of Eq. (9) can be solved using the Crank-Nicolson algorithm (Strang and Fix 1973). For solution purposes, the cubic particle can be divided into a patchwork of 8-node hexahedra (Fig. 2). Using symmetry considerations, it is necessary only to obtain a solution for a corner segment with three insulated faces at the central planes, as also illustrated in Fig. 2.

**Voltage Field.** The voltage distribution within a conductor can be developed from Maxwell's equations, or by combining Ohm's law and the continuity equation for electric current (Hayt 1981):

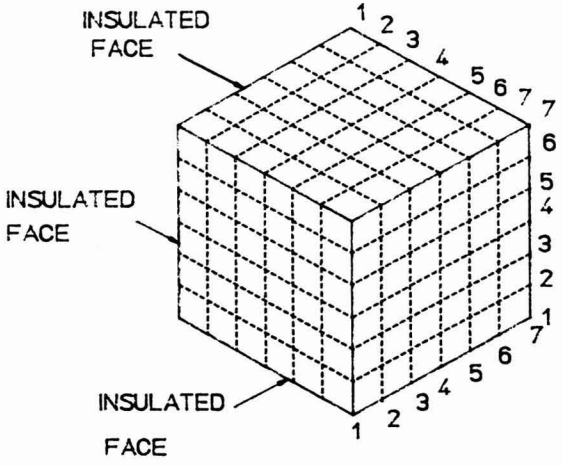


FIG. 2. FINITE ELEMENT GRID USED FOR COMPUTATIONS

$$\nabla\cdot(\sigma\nabla V) + \frac{\partial \rho_c}{\partial t} = 0 \tag{10}$$

For the steady-state case, which is typical:

$$\nabla\cdot(\sigma\nabla V) = 0$$

which must be solved over the domain of the mixture. Such a solution is generally possible in cases of single particles (de Alwis and Fryer 1990), but is difficult for a multiparticle mixture, since it necessitates knowledge of the location and properties of every particle at all points in time. It is possible, however, to obtain a simpler estimate of voltage distribution using the following circuit theory-based approach.

*(a) For Multiparticle Mixtures Involving Large Particle Populations.* The mixture is considered to consist of a continuous (liquid) and a discontinuous (solid) phase. The equivalent electrical circuit is that of parallel liquid ($R_{lP}$) and solid ($R_{sp}$) resistances in series with a liquid resistance ($R_{lS}$) as illustrated in Fig. 3(a). Thus:

$$R = R_{lS} + \frac{R_{lP}R_{sP}}{R_{lP} + R_{sP}} \tag{11}$$

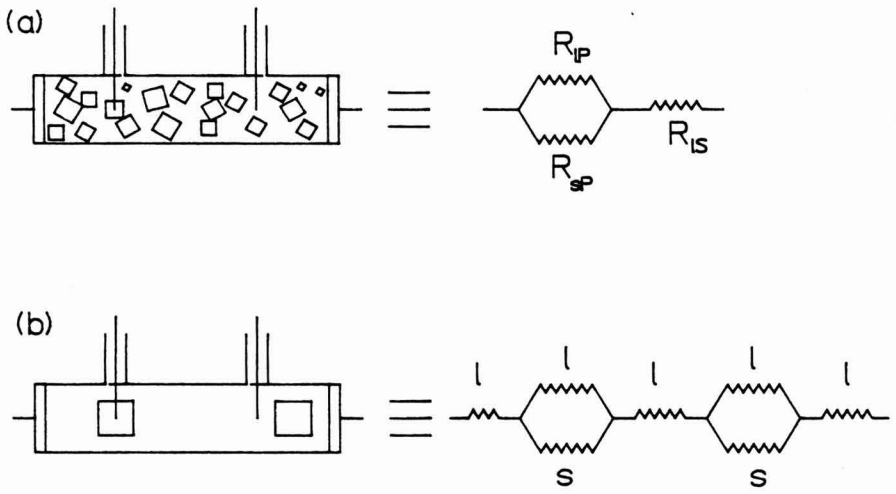


FIG. 3. (a) EQUIVALENT CIRCUIT FOR CONCENTRATED LIQUID-PARTICLE MIXTURE; (b) EQUIVALENT CIRCUIT FOR MIXTURE OF LIQUID AND TWO PARTICLES

where:

$$R_{lS} = \frac{l_{lS}}{A_{lS}\sigma_l} \tag{12}$$

$$R_{sP} = \frac{l_{sP}}{A_{sP}\sigma_s} \tag{13}$$

$$R_{lP} = \frac{l_{lP}}{A_{lP}\sigma_l} \tag{14}$$

In the above set of relations, $A_{lS}$ is equal to the area of cross section of the heater (A), and:

$$A_{lS} = A = A_{sP} + A_{lP} \tag{15}$$

The length of the heater ($l$) is related to the lengths of each phase:

$$l = l_{lS} + l_{lP} \tag{16}$$

and:

$$l_{sP} = l_{lP} \tag{17}$$

For the present case it was assumed (in a manner similar to Kopelman 1966) that the area and length of discontinuous phase could be determined from the volume fraction of that phase ($v_{fs}$) as follows:

$$A_{sP} = A\, v_{fs}^{\frac{2}{3}} \tag{18}$$

and:

$$l_s = l\, v_{fs}^{\frac{1}{3}} \tag{19}$$

The voltage distribution was calculated assuming that all equipotential lines were approximately parallel to electrodes (or perpendicular to tube walls). This is a reasonable approximation when the phases are uniformly mixed. The voltage ($V$) at position $x$ was determined as:

$$V = I R(x) \tag{20}$$

where $R$ is the equivalent resistance up to that position as determined from Eq. (11).

*(b) For a Mixture with Relatively Small Numbers of Particles.* For situations where particle location and orientation were accurately known, the equivalent resistance is calculated by separately considering zones containing particles from those without particles. In particular, for a two-particle case (Fig. 3b), the heater was divided into zones with particles and without, while allowing at least one particle length on either side of each particle to allow distorted equipotential lines to straighten. For zones with particles, the equivalent resistance was calculated as in Eq. (11), while that without particles consisted simply of a liquid resistance, $R_{ls}$, as in Eq. (12). The voltage was then calculated from a relation similar to Eq. (20).

**Solution Procedure and Simulations.** The solution consisted of iterative solution of the voltage field and thermal problems, with the thermal solution being further subdivided into iterative solution for particle and liquid temperatures by the approaches described previously. In all such solutions, due to the cubic shape of particles, the assumption was made that orientation effects did not significantly influence heating rates of individual particles, as demonstrated by Sastry and Palanaiappan (1992).

To permit comparison over a range of experimental conditions, simulations were conducted to correspond to heating of mixtures of potato cubes and sodium phosphate ($NaH_2PO_4 \cdot H_2O$) solutions of various concentrations. Particle populations ranged from two precisely located particles (Fig. 3b) to randomly scattered particles (Fig. 3a). Data inputs included particle, fluid and system properties, as described under the experimental procedure.

## Experimental Procedure

A static ohmic heater with two thermocouple ports (described by Sastry and Palaniappan 1992) was used. Samples of potato cubes of various sizes were tested within the chamber, along with sodium phosphate solutions of various concentrations. Electrical conductivities and their temperature coefficients were determined for these materials using the procedures of Palaniappan and Sastry (1991a,b). These and other measured material properties are presented in Table 1. Other relevant data on physical parameters for the experiments are presented in Table 2.

For experiments involving precise placement of particles, particle samples were placed at the desired locations and a teflon-coated thermocouple wire was inserted

TABLE 1.
MEASURED PROPERTIES OF POTATO AND SODIUM PHOSPHATE SOLUTIONS

| Material | Density (ρ)* (kg/m$^3$) | Sp. Heat ($C_p$)* (kJ/kg C) | El. Cond at 25 C ($\sigma_{25}$) (S/m) | Temp. Coefft. ($m$) ( C$^{-1}$) |
|---|---|---|---|---|
| Sod. Phosphate Solution, 0.1M | 1010 | 3.98 | 0.676 | 0.021 |
| Sod. Phosphate Solution, 0.05M | 1007 | 4.06 | 0.361 | 0.022 |
| Sod. Phosphate Solution, 0.025M | 1002 | 4.11 | 0.189 | 0.027 |
| Potato | 1080 | 3.57 | 0.062 | 0.248 |

* - Experimentally measured properties; density by weight and volume measurements, and specific heat by differential scanning calorimetry.

TABLE 2.
VALUES OF EXPERIMENTAL SYSTEM PARAMETERS AND OTHER PROPERTIES

| Parameter/Property | Value | Source (if not measured) |
|---|---|---|
| Heater chamber diameter | 2.38 cm | |
| Heater chamber length | 10.0 cm | |
| Applied voltage | 230 V | |
| Overall heat transfer coefficient of heater wall* | 56 w/m$^2$ C | |
| Dimension of potato cubes ( 2-particle experiments) | 1.5 cm | |
| Dimension of potato cubes (multiparticle experiments with 20 and 30 particles) | 0.8 cm | |
| Thermal conductivity of potato tissue | 0.55 w/m C | Singh and Heldman (1984) |

* - Measured by heating liquid ohmically till steady-state, equating loss through walls to energy input, and measuring temperature difference between heater interior and surrounding ambient air.

into the center of one of them. Considerable care was required in this operation, since the occurrence of significant damage due to the thermocouple could result

in leakage of liquid medium into the thermocouple vicinity, cause artificially high local electrolyte concentrations and greatly affect the experimental outcome. The position of the unattached sample could be ensured only by making samples large enough to fit snugly within the chamber. For smaller particles, some slight motion may have been unavoidable. For the present set of experiments, all cubes were oriented with faces parallel to the electrodes. For samples involving larger particle numbers, one sample was installed with thermocouple attached, while the rest were placed randomly within the chamber. The other thermocouple was used to monitor liquid temperature. After particle installation, electrodes were inserted to the desired extent, and liquid poured through the thermocouple ports prior to sealing.

Samples were heated using constant voltage treatments, and temperatures of fluid and particle, as well as voltage and current were monitored once every second. All experiments were conducted in triplicate. After each run, samples were examined for mechanical damage and for accurate placement of thermocouples. Thermal lags due to teflon coating (necessary to prevent electrical leakage) of thermocouples were corrected using data from preliminary calibration experiments involving comparison with uncoated thermocouple junctions under conventional heating conditions.

## RESULTS AND DISCUSSION

### Studies Involving Two Particles

Typical experimental data from studies involving two particles are shown in Fig. 4. As expected, samples with higher sodium phosphate concentrations and, consequently, higher electrical conductivities ($\sigma$) heat at more rapid rates. The more interesting observation pertains to the relative heating rates of liquid and particles. With the low conductivity (0.025M) fluid, the particle center generally heated faster than the fluid; for the intermediate conductivity (0.05M) fluid, heating rates were comparable, and for the high conductivity (0.1M) fluid the particle lagged through much of the experiment, but approached fluid temperatures by the end of heating. The obvious explanation for these trends is the difference of $\sigma$ between the phases; however, it is interesting to note that the particle $\sigma$ has a greater temperature coefficient than that of the fluid, and although its conductivity at 25C may be lower, it approaches or exceeds that of the fluid by the end of the experiment (Fig. 5). For the 0.025M solution, the particle conductivity exceeds that of the fluid by 40C, and for the 0.05M solution, by 65C. However, electrical conductivity differences alone do not provide the total explanation. The presence or absence of significant alternative conducting paths through the fluid is an important factor affecting voltage drops and consequently, the energy genera-

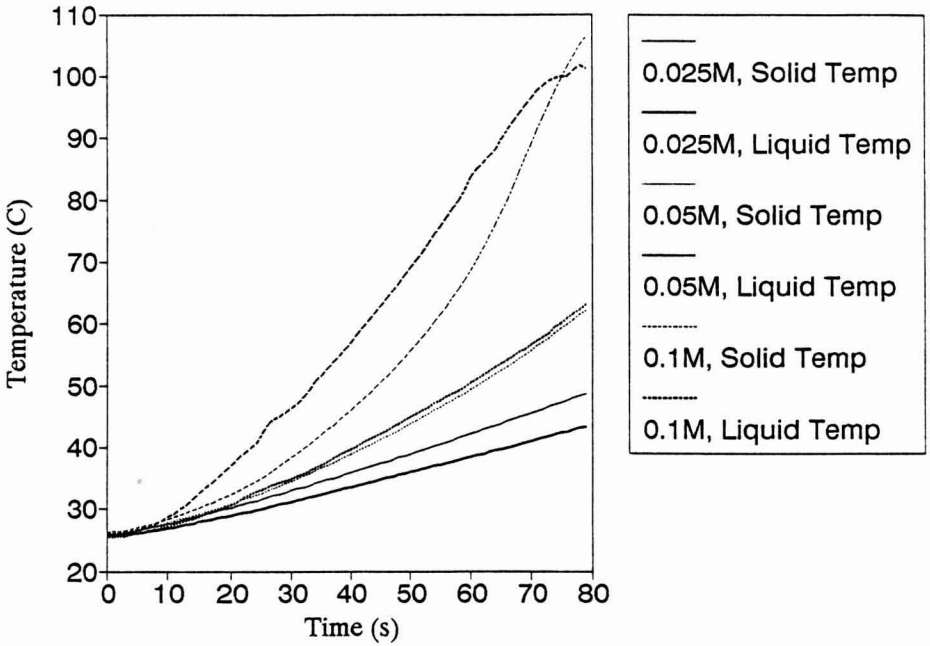


FIG. 4. EXPERIMENTAL DATA FOR HEATING OF TWO 1.5 cm POTATO PARTICLES IN SODIUM PHOSPHATE SOLUTIONS OF VARIOUS CONCENTRATIONS

tion rates within both media, and can be properly understood via mathematical models.

Comparison between model predictions and experimental results are presented in Fig. 6 through 8. In general, satisfactory agreement was obtained for the 0.025M solution. For the 0.05M and 0.1M solution, the predictions were in qualitative agreement, but the temperature differences between phases were slightly greater in the model than in the experiment. The results are still satisfactory given the number of possible errors that could occur in an experiment of this nature. Significant sample-to-sample variations could occur in the $\sigma$ value for potatoes. Leakage of high-conductivity fluid to the thermocouple vicinity could have occurred despite efforts to minimize it (resulting in closer particle-liquid temperatures than predicted). Also, studies of Halden *et al.* (1990) have indicated the possibility of electrohydrodydnamic and electro-osmotic effects, which may increase the values of effective transport properties within a solid food. It was verified beforehand that the presence of the thermocouple did not contribute significantly to the overall circuit resistance, hence its presence cannot be used to account for errors. Model-related limitations are also possible, notably in the approximations inherent in the circuit theory approach to calculation of voltage gradients. The use of circuit theory is useful with large concentrations of particles; however,

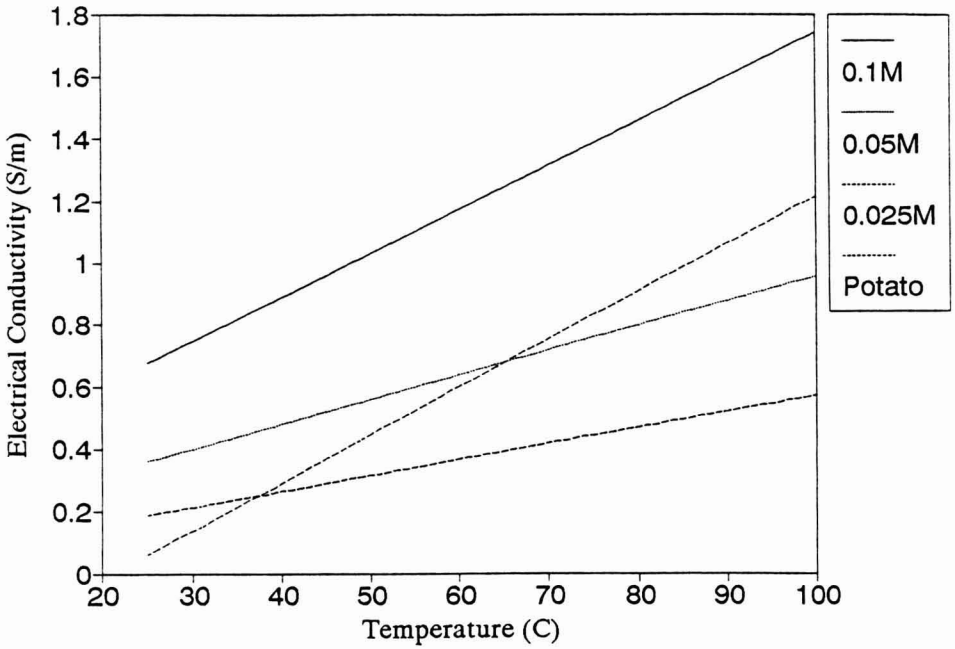


FIG. 5. PLOT OF ELECTRICAL CONDUCTIVITY VERSUS TEMPERATURE FOR POTATO AND SODIUM PHOSPHATE SOLUTIONS

under conditions involving few particles, with significant differences between conductivities of phases, the approach may yield approximate values of voltage gradients, contributing to errors in prediction. Given the possibilities of experimental errors and variations in results, the model does yield predictions that are in reasonably good agreement with experiment.

Since we also measured voltage and current in the above experiments, it was possible to obtain additional verification by determining (a) if the "effective" resistance of the suspension matched that expected from the model; and (b) if the rate of energy input measured matched the thermal energy associated with the temperature rise. The effective resistance was generally in agreement within $\pm 10\%$, variations being primarily due to differences in potato properties. The rate of energy input generally matched the thermal energy dissipation fairly closely, indicating that energy losses through the walls were small. Model predictions also indicated that the system thermal response was not sensitive to variations in the thermal resistance of the wall.

## High Particle Concentrations

Comparison of model versus experimental predictions for cases involving solid volume fractions ($\nu_{fs}$) of 0.23 (20 particles of 0.8 cm side); and 0.345 (30 par-

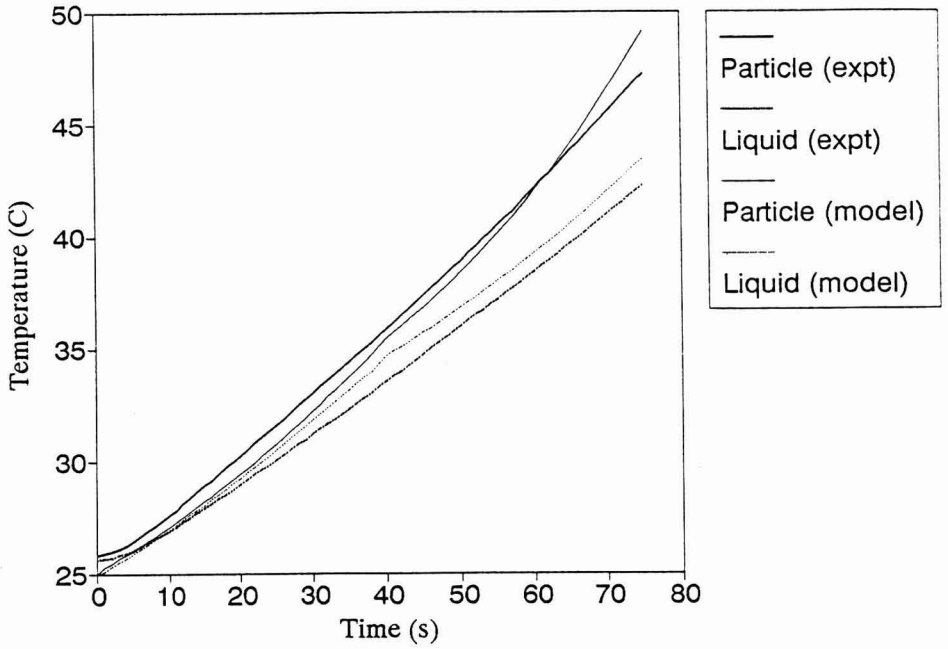


FIG. 6. COMPARISON BETWEEN MODEL AND EXPERIMENT FOR TWO 1.5 cm POTATO PARTICLES IN 0.025M SODIUM PHOSPHATE SOLUTION

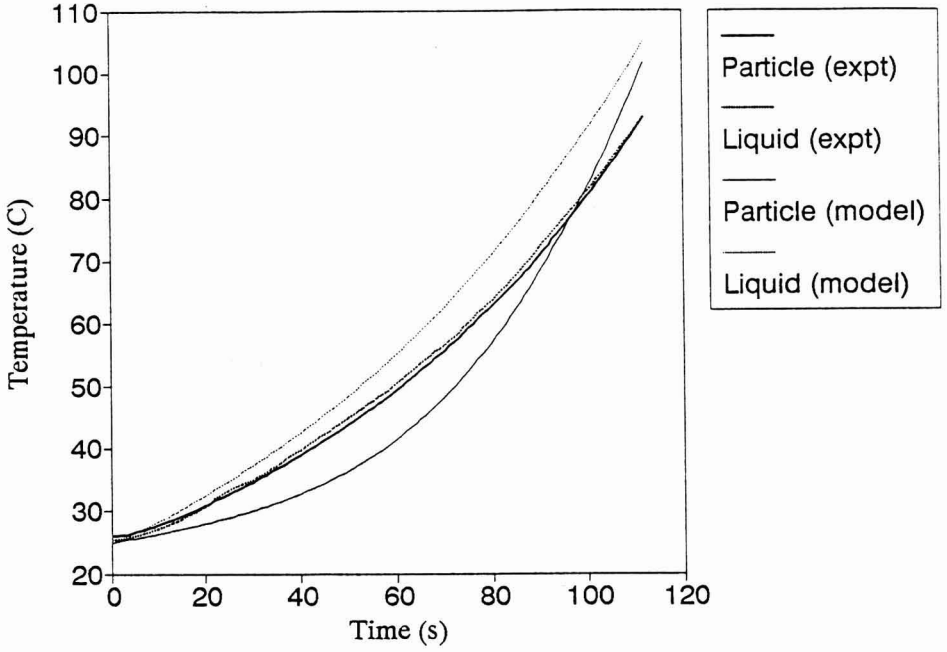


FIG. 7. COMPARISON BETWEEN MODEL AND EXPERIMENT FOR TWO 1.5 cm POTATO PARTICLES IN 0.05M SODIUM PHOSPHATE SOLUTION

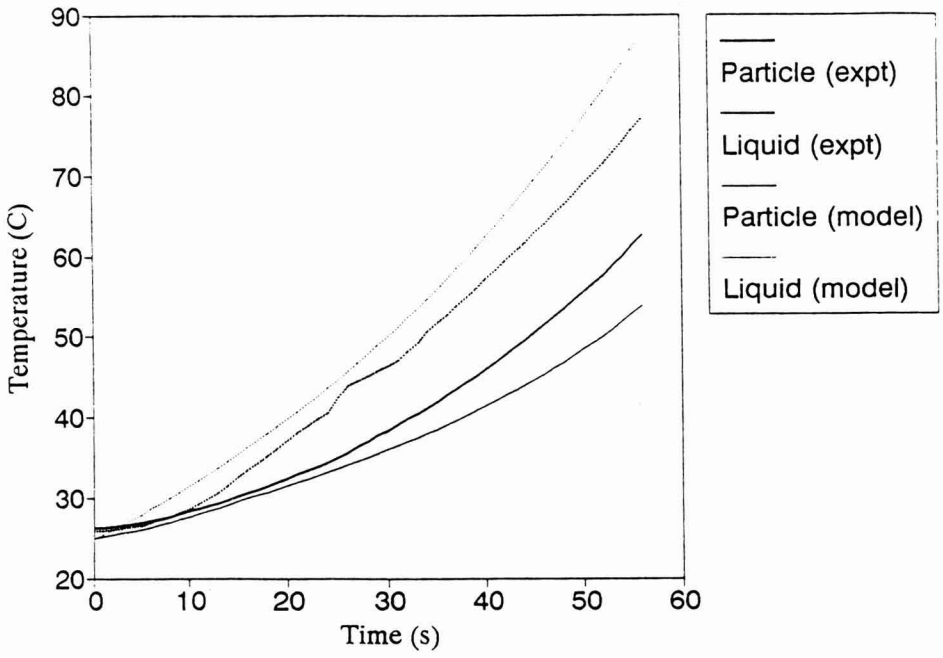


FIG. 8. COMPARISON BETWEEN MODEL AND EXPERIMENT FOR TWO 1.5 cm POTATO PARTICLES IN 0.1M SODIUM PHOSPHATE SOLUTION

ticles of 0.8 cm side) within 0.1M sodium phosphate solution are presented in Fig. 9 and 10, respectively. Interestingly, as solids volume fraction increases, the particle temperature tends to increase relative to that of the fluid. At a $v_{fs}$ of 0.23, particle temperature lagged behind that of the fluid for much of the experiment, but by a lesser extent than that for the 2-particle case (Fig. 8), and eventually caught up after 70 s. At $v_{fs} = 0.345$, particle center temperatures lagged initially, but soon exceeded those of the fluid. Model predictions are also consistent with experimental data, showing an initial lag for the particle, with a change in relative heating rates after some time. The points of transition between particle lagging to particle leading are different between model and experiment. This can be attributed to the same experimental uncertainties discussed with the 2-particle experiments. The use of circuit theory in calculation of voltage gradients is far less likely to be erroneous in these cases, and the generally good agreement between model and experiment tends to bear out this point. Again, the voltage-current data were used to check overall resistances and energy dissipation rates, and results were generally similar to those of the 2-particle experiments.

It must be noted that while particle center temperatures were measured in the above experiments, they may not always represent particle cold spot temperatures. From simulations, when the particle leads the fluid, the cold-spot is typically at

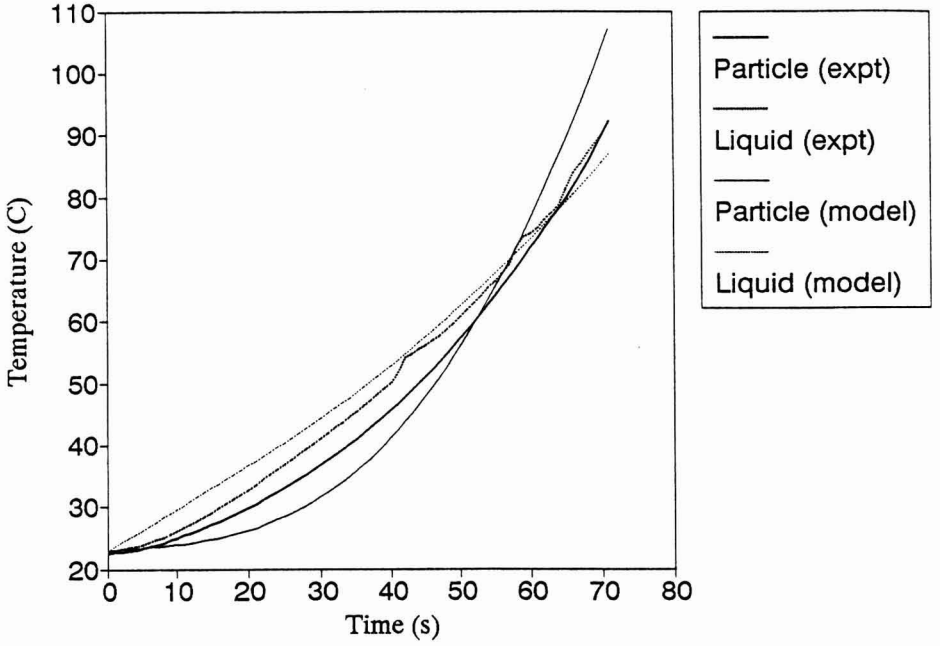


FIG. 9. COMPARISON BETWEEN MODEL AND EXPERIMENT FOR A SUSPENSION OF TWENTY 0.8 cm POTATO PARTICLES ($\nu_{fs}$ = 0.23) IN 0.1M SODIUM PHOSPHATE SOLUTION

the corners, while in the case of particle lagging, the cold spot is at the center. In cases involving transitions from particle-lagging to particle-leading, the cold spot moves diagonally outwards from the center to the corners.

The findings of this study have some important implications. First and foremost, it appears that the use of high solids concentrations is conducive to rapid particle heating, even though the surrounding fluid may have a considerably higher electrical conductivity. This is because as the solids concentration increases, the parallel conduction paths through the fluid are increasingly restricted, forcing a greater proportion of the total current to flow through the particles. This results in higher generation rates within the particles and consequently a greater relative heating rate. This indicates that sterilization via ohmic heating is most suited for high particle concentration mixtures. A second significant point relates to the rate of increase of potato conductivity relative to the fluid. Within the range of conditions of this experiment, as temperature increased, particle conductivities approached and sometimes exceeded fluid condutivities. If this trend continues up to sterilization temperatures for a sufficiently large number of solid foods, the ohmic process is likely to become even more promising.

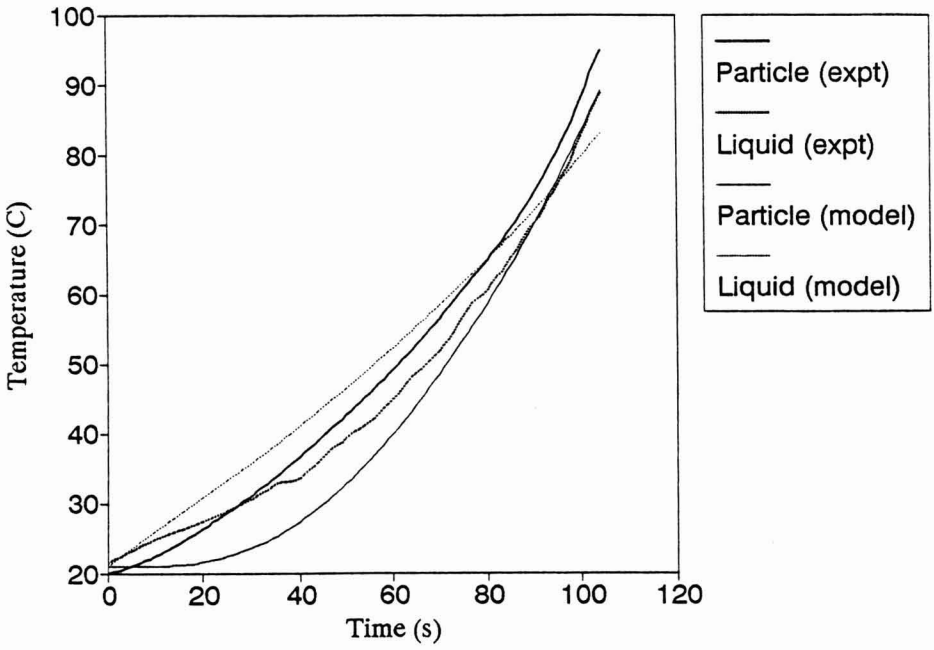


FIG. 10. COMPARISON BETWEEN MODEL AND EXPERIMENT FOR A SUSPENSION OF THIRTY 0.8 cm POTATO PARTICLES ($v_{fs}$ = 0.345) IN 0.1M SODIUM PHOSPHATE SOLUTION

An additional point worthy of discussion relates to the conditions under which a particle may thermally lag or lead the surrounding fluid. It is assumed in the succeeding discussion that particles are generally less electrically conductive than liquids. Based on this work, it appears that if a particle's electrical resistance within a circuit is a significant component of the overall resistance, the particle will likely heat faster than the fluid. This point is borne out by the increase in relative heating rate with increasing particle concentration, even when fluid conductivity significantly exceeds that of the particle. If, on the other hand, the particle represents only a small part of the overall circuit resistance, it may thermally lag the fluid. This occurs with small particle concentrations, when the fluid conductivity is significantly greater than that of the particle, and offers sufficiently wide parallel conduction paths to the current. A similar point is apparent from the studies of de Alwis and Fryer (1990) with respect to orientation of a long thin particle in an electrical field. If the particle is oriented across the current, so that it tends to "block" the current, it then forms a large part of the overall resistance. Under these conditions, the current has relatively few alternative paths, and the particle interior heats faster than the fluid. If, on the other hand, the par-

ticle is oriented parallel to the current, its resistance forms only a small part of the overall resistance, a number of parallel conduction paths become available, and the particle lags behind the fluid. This point is also borne out in simulations on a continuous ohmic heater by Sastry (1992).

The summary of these findings is that ohmic heating appears to show considerable promise in rapid and (nearly) uniform processing of particles and liquids. One of the most attractive features of the process is the potential to control heating rates by product design and formulation. However, further studies need to be conducted with fatty particles and with detailed thermal imaging to ensure that local effects causing slow heating or other unusual phenomena do not exist. Biological tests are obviously also necessary for testing process safety.

## CONCLUSIONS

The mathematical model for ohmic heating is in satisfactory agreement with experimental findings, when considering factors such as potential for experimental error and model assumptions. Particle-liquid mixtures heat at rates which depend on the relative conductivities of the phases, and the volume fractions of the respective phases. Solids of low conductivity relative to fluid will lag behind the fluid if they are in low concentration, but under high-concentration conditions, particles may heat faster than fluid, because of restriction of parallel conduction paths through the fluid. The phenomenon of particle-lagging or particle-leading depends on the significance of particle resistance to the overall circuit resistance. If the particle forms a significant component of overall circuit resistance, it is likely to heat faster than the fluid.

## NOMENCLATURE

$A$ Area
$C_p$ Specific heat
$F_j$ Load vector
$h_{fp}$ Fluid to particle convective heat transfer coefficient
$I$ Current
$J$ Current density vector
$k$ Thermal conductivity
$K_{ij}$ Stiffness matrix
$m$ Temperature coefficient of conductivity
$M$ Mass
$M_{ij}$ Mass or capacitance matrix

$n$ Number
$\vec{n}$ Unit normal vector
$R$ Resistance
$t$ Time
$T$ Temperature
$U$ Overall heat transfer coefficient of heater walls
$iu$ Internal energy generation rate (per unit volume)
$v$ Volume
$V$ Voltage
$v_{fs}$ Volume fraction of solids
$x$ Coordinate dimension

## Greek Letters and Other Symbols

$\alpha$ Thermal diffusivity
$\Delta$ Increment
$\delta_{ij}$ Kronecker delta
$\rho$ Density
$\sigma$ Electrical conductivity
$\phi$ Basis function
$\nabla$ Gradient

## Subscripts and Superscripts

$a$ Ambient air
$c$ Charge
$f$ Fluid
$i$ Node number index
$j$ Node number index
$l$ Liquid
$m$ Mean value
$n$ Time step index
$p$ Particle
$P$ Parallel
$s$ Surface (when used with temperature), solid (when used with resistance)
$S$ Series
$w$ Heater system wall
0 Reference value
$\infty$ Bulk fluid (when used with temperature)

## REFERENCES

BISS, C.H., COOMBES, S.A. and SKUDDER, P.J. 1989. The development and application of ohmic heating for the continuous processing of particulate foodstuffs. In *Process Engineering in the Food Industry*, (R.W. Field and J.A. Howell, eds.) pp. 17–27. Elsevier Applied Science Publishers, New York.

CANDARANA, D.I. and GAVIN III, A. 1989. Establishing thermal processes for heterogeneous foods to be processed aseptically: A theoretical comparison of process development methods. J. Food Sci. *54*(1), 198–204.

DE ALWIS, A.A.P. and FRYER, P.J. 1990. A finite element analysis of heat generation and transfer during ohmic heating of food. Chem. Eng. Sci. *45*(6), 1547–1559.

DE ALWIS, A.A.P., HALDEN, K. and FRYER, P.J. 1990. Shape and conductivity effects in the ohmic heating of foods. Chem. Eng. Res. Des. *67*, 159–168.

HALDEN, K., DE ALWIS, A.A.P. and FRYER, P.J. 1990. Changes in the electrical conductivities of foods during ohmic heating. Int. J. Food Sci. Technol. *25*, 9–25.

HAYT, W.H. 1981. *Engineering Electromagnetics*, 4th Ed., McGraw Hill Book Co., New York.

KOPELMAN, I.J. 1966. Transient Heat Transfer and Thermal Properties in Food Systems, Ph.D. Dissertation, Michigan State University, East Lansing, MI.

LEE, J.H. and SINGH, R.K. 1988. Determination of lethality in a continuous sterilization system containing particulates. Paper no. 88-6600, presented at the 1988 ASAE International Winter Meeting, Chicago, IL, Dec. 13–16.

MIZRAHI, S., KOPELMAN, I.J. and PERLMAN, J. 1975. Blanching by electroconductive heating. J. Food Technol. (Brit.) *10*, 281–288.

PALANIAPPAN, S. and SASTRY, S.K. 1991a. Electrical conductivities of selected solid foods during ohmic heating. J. Food Proc. Eng. *14*, 221–236.

PALANIAPPAN, S. and SASTRY, S.K. 1991b. Electrical conductivity of selected juices: Influences of temperature, solids content, applied voltage and particle size. J. Food Proc. Eng. *14*, 247–259.

PALANIAPPAN, S., SASTRY, S.K. and RICHTER, E.R. 1990. Effects of electricity on microorganisms: A review. J. Food Processing & Preservation *14*, 393–414.

SASTRY, S.K. 1986. Mathematical evaluation of process schedules for aseptic processing of low-acid foods containing discrete particulates. J. Food Sci. *51*, 1323–1328, 1332.

SASTRY, S.K. 1989. A model for continuous sterilization of particulate foods by ohmic heating. Presented at the 5th Int. Cong. Eng. Food, Cologne, Germany, May 28–June 3.

SASTRY, S.K. 1992. A model for heating of liquid-particle mixtures in a continuous flow ohmic heater. J. Food Proc. Eng. *15*, 263–278.

SASTRY, S.K. and PALANIAPPAN, S. 1992. Influence of particle orientation on the effective electrical resistance and ohmic heating rate of a liquid-particle mixture. J. Food Proc. Eng. *15*, 213–227.

SINGH, R.P.and HELDMAN, D.R. 1984. *Introduction to Food Engineering*, Academic Press, Orlando, FL.

STRANG, W.G. and FIX, G.J. 1973. *An Analysis of the Finite Element Method*, Prentice Hall, Englewood Cliffs, NJ.

# A MODEL FOR HEATING OF LIQUID-PARTICLE MIXTURES IN A CONTINUOUS FLOW OHMIC HEATER[1]

SUDHIR K. SASTRY

*The Ohio State University*
*Department of Agricultural Engineering*
*590 Woody Hayes Drive*
*Columbus, OH 43210*

Accepted for Publication May 28, 1992

## ABSTRACT

*Design of safe thermal processes in a continuous flow ohmic heater requires mathematical model development, since temperature monitoring of particles in continuous flow is not presently possible. A mathematical model previously developed and verified for a static heater was modified to predict temperatures of fluids and particles within a continuous heater with high particle concentration suspensions. Results for constant voltage simulations indicate that the presence of large populations of low electrical conductivity particles results in slow heating of the entire mixture rather than a single phase alone. In all these cases, particles tend to heat faster than the liquid. However, if isolated low-conductivity particles enter the system, the danger of underprocessing exists; hence particle conductivity is a critical control point. Simulations also indicate the role played by residence time distribution and liquid-particle heat transfer coefficients in the above cases.*

## INTRODUCTION

The development of a continuous flow ohmic heater with improved electrode systems has opened new possibilities for industries interested in continuous sterilization of liquid-particle mixtures. However, understanding of the ohmic

[1]Salaries and research support provided by State and Federal Funds appropriated to the Ohio Agricultural Research and Development Center, The Ohio State University. Journal Article No. 89-92. References to commercial products and trade names is made with the understanding that no discrimination and no endorsement by The Ohio State University is implied.

Journal of Food Process Engineering **15** (1992) 263–278. 

heating process is still being developed. Models have been developed for static heaters (de Alwis and Fryer 1990; Sastry and Palaniappan 1992b), but for purposes of commercial process design it is necessary to develop models for continuous heaters.

The present study describes a model that can be used to predict particle and liquid temperatures in a continuous flow ohmic heater. The model is based on the experimentally verified static heater model of Sastry and Palaniappan (1992b). The present study involves suspensions with high particle concentrations, since that study indicated that ohmic heating is likely to produce best particle heating results under these conditions. This has also generally been the recommendation of APV Baker, the manufacturers of the ohmic heater. Temperature measurement of particles in continuous flow ohmic heating is even more difficult than under conventional heating because of the presence of a strong electrical field; consequently it is not possible to verify a continuous flow model by itself. However, since the static heater model has been tested against experiment, and continuous flow involves substitution of a time scale with a length scale, the static model can be used with some confidence. The objective of this study is therefore the modeling of ohmic heating of liquid-particle mixtures in a continuous ohmic heater, to identify the critical parameters of the process.

## MATERIALS AND METHODS

A schematic diagram of the heater is presented in Fig. 1 (similar to the ohmic heater manufactured by APV Baker), consisting of three zones with electrodes spaced at intervals between them. The present model assumes that plug flow exists through the heater, although the capability exists to simulate heat transfer to isolated fast-moving particles. The plug flow assumption does need to be verified for individual instances, but is realistic for suspensions of the high solids concentration situations considered herein. As in the case of the static heater (Sastry and Palaniappan 1992b), the problem involves interdependent thermal and electrical problems.

### Thermal Problem

The thermal problem involves separate energy balances on liquid and particles. For the liquid within any incremental section of thickness $\Delta x$, between locations $n$ and $n+1$, the following energy balance is used.

$$\dot{M}_f C_{pf}(T_\infty^{n+1} - T_\infty^n) = \dot{u}_f v_f + n_p h_{fp} A_p (T_{sm} - T_{\infty m}) + UA(T_a - T_{\infty m}) \quad (1)$$

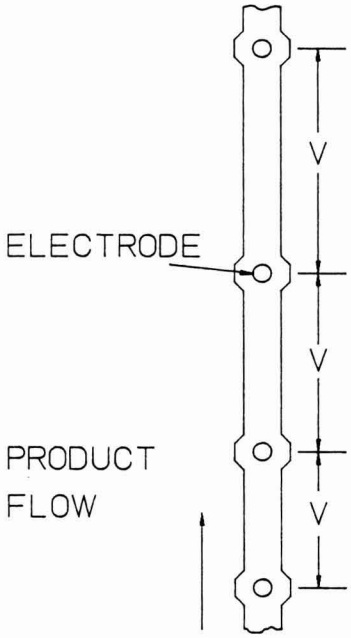


FIG. 1. SCHEMATIC DIAGRAM OF OHMIC HEATER

where the following definitions apply:

$$T_{\infty m} = \frac{T_{\infty}^{n+1} + T_{\infty}^{n}}{2}$$

$$T_{sm} = \frac{T_{s}^{n+1} + T_{s}^{n}}{2}$$

$v_f$ is the volume of fluid in the incremental section:

$$v_f = \frac{\pi}{4} d^2 \Delta x v_{ff}$$

and the energy generation rate is given by:

$$\dot{u}_f = |\nabla V|^2 \sigma_{0f} (1 + m_f T_{\infty m})$$

The liquid temperature at each successive incremental location $(n+1)$ can be determined from Eq. (1) if the voltage field ($V$) and mean particle surface temperature

($T_{sm}$) are known. The heat transfer problem for particles is the conduction heat transfer equation with temperature-dependent internal energy generation.

$$\nabla \cdot (k_p \nabla T_p) + \dot{u}_p(T_p) = \rho_p C_{pp} \frac{\partial T_p}{\partial t} \tag{2}$$

with a time-dependent boundary condition:

$$k \nabla T_p \cdot \vec{n} = h_{fp}[T_s - T_\infty(t)] \tag{3}$$

with the energy generation term of Eq. (6) being given by:

$$\dot{u}_p = |\nabla V|^2 \sigma_{0p}[1 + m_p T_p] \tag{4}$$

The above problem can be solved using the three dimensional finite element method in space, and Crank-Nicolson finite differencing in time. This procedure yields the $n+1$th value of $T_p$, from which $T_{sm}$ can be calculated. However, this requires that $T_\infty^{n+1}$ and $T_\infty^{n}$ both be known. Thus, the following iterative scheme is used. First, Eq. (1) is solved for $T_\infty^{n+1}$ by the approximation: $T_{sm} = T_s^n$; then, Eq. (2) is solved using the value of $T_\infty^{n+1}$ so obtained, to yield a value of $T_s^{n+1}$, which is then used to calculate an updated $T_{sm}$ for another iteration of Eq. (1). This procedure is repeated till convergence.

## Electrical Problem

In principle, the electrical field distribution arises from the continuity equation for current (Hayt 1981):

$$\nabla \cdot (\sigma \nabla V) = 0 \tag{5}$$

which must be solved over the domain of the mixture. Such a solution is generally possible in cases of single particles (de Alwis and Fryer 1990), but is difficult for a multiparticle mixture, since it necessitates knowledge of the location and properties of every particle at all points in time. A more expeditious approach is possible via circuit theory, in the manner described by Sastry and Palaniappan (1992b), where the ohmic heater column is considered to be a set of equivalent resistances in series (Fig. 2). This approximation is useful and realistic in that voltage gradients are likely to occur primarily along the length of the heater, and with high solids concentrations, plug flow is likely. However, the analysis for a continuous heater is somewhat more involved because the product increases in temperature (and consequently conductivity) through the heater; thus the voltage

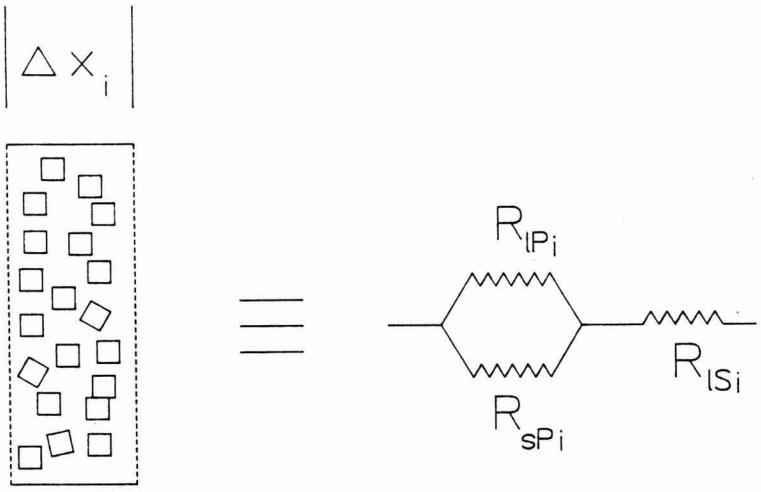


FIG. 2. EQUIVALENT CIRCUIT FOR AN INCREMENTAL SECTION

drop through each incremental section must be determined separately. Thus, for each incremental section $i$ of thickness $\Delta x$ lying between $n$ and $n+1$; the resistance can be determined from that of a continuous (liquid) and a discontinuous (solid) phase as:

$$R_i = R_{lSi} + \frac{R_{lPi} R_{sPi}}{R_{lPi} + R_{sPi}} \tag{6}$$

where:

$$R_{lSi} = \frac{\Delta x_{lSi}}{A_{lSi} \sigma_{li}} \tag{7}$$

$$R_{sPi} = \frac{\Delta x_{sPi}}{A_{sPi} \sigma_{si}} \tag{8}$$

$$R_{lPi} = \frac{\Delta x_{lPi}}{A_{lPi} \sigma_{li}} \tag{9}$$

In the above set of relations, $A_{lS}$ is equal to the area of cross section of the heater ($A = \pi d^2/4$), and:

$$A_{lSi} = \frac{\pi}{4} d^2 = A_{sPi} + A_{lPi} \tag{10}$$

The length of the incremental heater section ($\Delta x$) is related to the lengths of each phase:

$$\Delta x = \Delta x_{lS} + \Delta x_{lP} \tag{11}$$

and:

$$\Delta x_{sP} = \Delta x_{lP} \tag{12}$$

For the present case it was assumed (as described by Sastry and Palaniappan 1992b) that the area and length of discontinuous phase could be determined from the volume fraction of that phase ($v_{fs}$) as follows:

$$A_{sPi} = \frac{\pi}{4} d^2 v_{fs}^{\frac{2}{3}} \tag{13}$$

and:

$$\Delta x_{si} = \Delta x \, v_{fs}^{\frac{1}{3}} \tag{14}$$

The electrical conductivities of liquid ($\sigma_l$) and solid ($\sigma_p$) are calculated from the temperature in the incremental section $i$ as:

$$\sigma_{li} = \sigma_{0l}[1 + m_l T_{\infty mi}] \tag{15}$$

and

$$\sigma_{si} = \sigma_{0p}[1 + m_p T_{pmi}] \tag{16}$$

The total resistance of the ohmic heater column is then:

$$R = \sum_{i=1}^{N} R_i \tag{17}$$

The total current flowing through the system is:

$$I = \frac{\Delta V}{R} \tag{18}$$

The voltage distribution was calculated assuming that all equipotential zones were approximately planar and perpendicular to tube walls (a reasonable approximation when the phases are uniformly mixed). Thus, the voltage drop over increment $i$ was calculated as

$$\Delta V_i = IR_i \tag{19}$$

and the results were used to calculate voltage gradient and energy generation within each incremental section.

Solution of this problem requires that temperatures of continuous and discontinuous phases be known throughout the heater length to determine the current $I$ from which to calculate voltage gradient. The computational effort required for iterative refinement is therefore considerable; but can be decreased by improving the initial estimate of voltage drops by the following procedure.

Since preliminary simulations had indicated reasonable uniformity in temperature of phases, Eq. (2) was replaced with a lumped analysis for the particle temperature. The resulting problem greatly reduced the computational effort required for the thermal problem; and voltage gradients were calculated iteratively with this simplified problem until convergence was obtained. The resulting voltage field was used as the first estimate when Eq. (1), (2) (unmodified) and the electrical problem were solved iteratively in entirety. The program flowchart for these simulations is presented in Fig. 3.

Since this study involved cubic particles, orientation effects were considered small based on results of Sastry and Palaniappan (1992a). Thus the electric field strength for each particle was assumed to be the same within each incremental section. It is recognized that these results would be quite different if long thin particles were used.

## Parametric Simulations

Simulations were performed for a range of scenarios involving various continuous and discontinuous phase conductivities. In addition, a set of special case scenarios were conducted for situations involving (a) a single low-conductivity particle in a high-conductivity mixture; (b) single fast-moving particle; and (c) various values of fluid-to-particle convective heat transfer coefficient ($h_{fp}$) for low-conductivity particles.

The procedure for the isolated low-conductivity particle involved simply solving Eq. (2) using the particle's conductivity in Eq. (4), subject to a time-varying temperature boundary condition (3), which was predetermined from a simulation for a high-conductivity mixture. For cases of fast-moving particles, the values

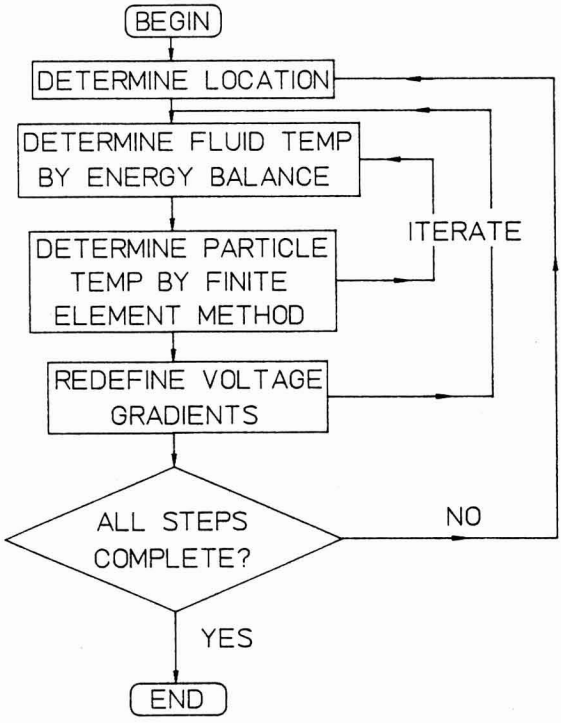


FIG. 3. PROGRAM FLOWCHART

of $T_\infty(t)$ were as determined from previous simulations, with a time scaling factor used for the particle. Similarly, predetermined data on $T_\infty(t)$ were used for the different heat transfer coefficient simulations. Values of product and system parameters used are presented in Table 1. Physical properties of liquid and particles are presented in Table 2.

## RESULTS AND DISCUSSION

The results of a simulation involving equal electrical conductivities for fluid and particle cold spot is shown in Fig. 4. The particle cold-spot temperatures were found to consistently exceed that of the fluid. Temperature variation within individual particles was found to be small ($< 1$C), indicating the uniformity of the heating effect. Cold spots were generally located in the corners. Another notable feature is the rapidity of heating achieved under these conditions. This is not unexpected, as shown by experimental studies (Sastry and Palaniappan (1992b). Also notable is the discontinuity in the curve, arising from a change in

TABLE 1.
SYSTEM PARAMETER VALUES USED IN SIMULATIONS (VALUES ASSUMED)

| Parameter | Value |
|---|---|
| Total length of ohmic heater | 4.7 m |
| Length of first section | 1.12 m |
| Length of second section | 1.57 m |
| Length of third section | 2.01 m |
| Heater tube diameter | 0.08 m |
| Voltage per phase | 2500 - 5000 V |
| Product volumetric flow rate | $4.74 \times 10^{-4}$ $m^3/s$ |
| Particle size | 0.012 - 0.024 m |
| Volume fraction of solids | 0.8 |
| Overall heat transfer coefficient (U) | 20 $w/m^2$ C |
| Initial product temperature | 25 C |
| Fluid-particle heat transfer coefficient | 232 $w/m^2$ C (range 81-1162 $w/m^2$ C) |

TABLE 2.
VALUES OF PHYSICAL PROPERTIES OF LIQUID AND PARTICLES USED IN SIMULATIONS (ALL VALUES ASSUMED)

| Property | Fluid | Particles |
|---|---|---|
| Electrical conductivity (reference value at 0°C) | 0.2 to 1.68 S/m | 0.2 to 1.68 S/m |
| Temperature coefficient of electrical conductivity ($m$) | 0.02 $°C^{-1}$ | 0.02 $°C^{-1}$ |
| Specific heat | 3.76 kJ/kg°C | 3.88 kJ/kg°C |
| Thermal conductivity | 0.5 w/m°C | 0.5 w/m°C |
| Density | 1000 $kg/m^3$ | 1000 $kg/m^3$ |

voltage gradient as the particle passed from one zone of the ohmic heater to another. The other interesting feature relates to the shape of the fluid temperature curve, which has an upward slope in the first stage, and is close to a straight line in subsequent stages. The straight line heating appears to be due to decreasing voltage gradient at downstream locations. If voltage gradients are maintained constant, the fluid temperatures show increasing slopes in all stages.

When all the particles are of low electrical conductivity relative to the fluid,

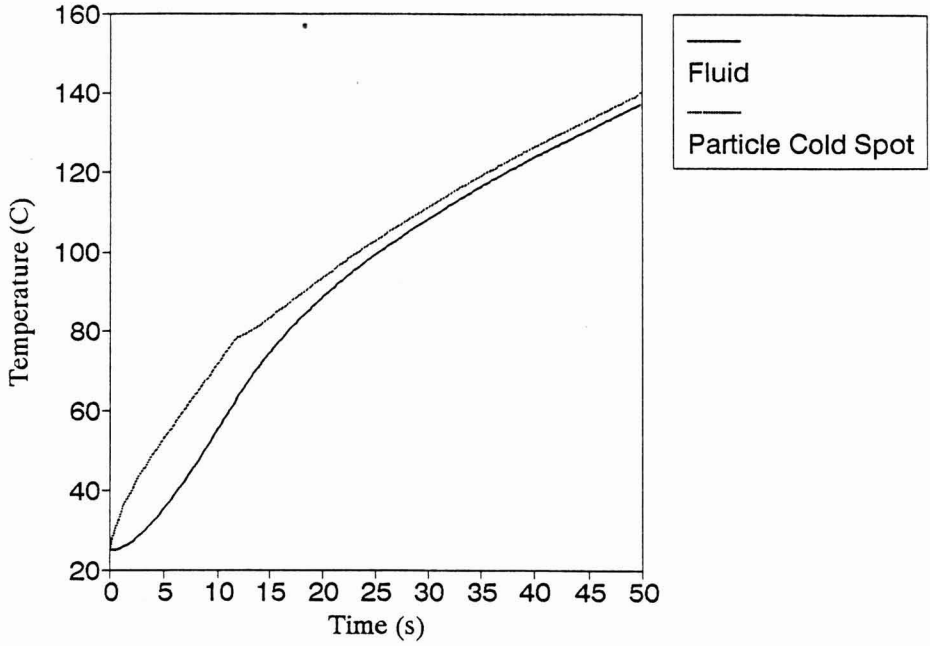


FIG. 4. PARTICLE COLD-POINT AND FLUID TEMPERATURES VERSUS TIME FOR EQUAL ELECTRICAL CONDUCTIVITY CASE
($\sigma_{0f} = \sigma_{0p} = 1.68$ S/m)

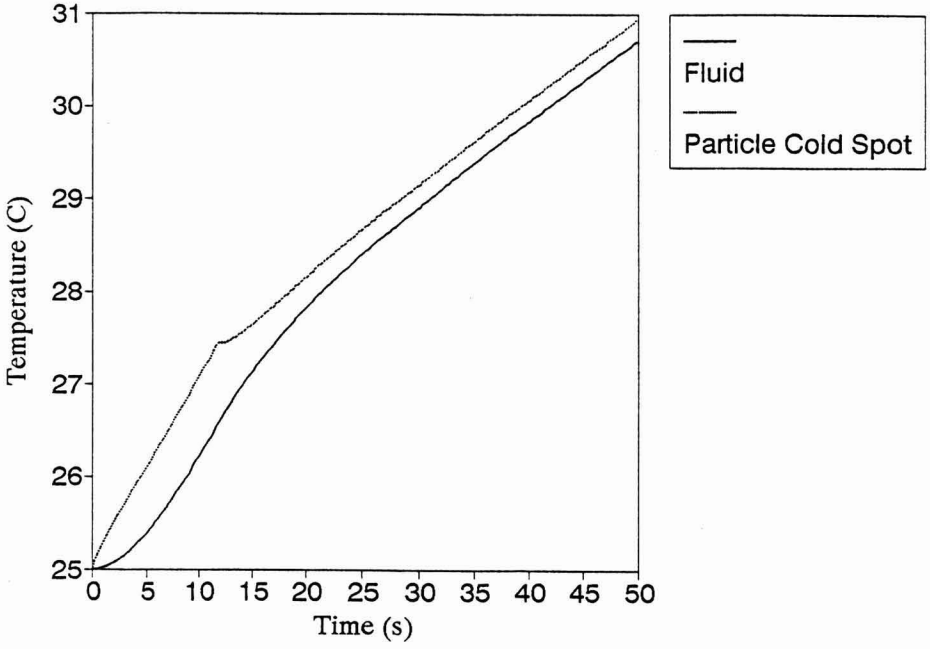


FIG. 5. PARTICLE COLD-POINT AND FLUID TEMPERATURES VERSUS TIME FOR LOW-CONDUCTIVITY PARTICLES
($\sigma_{0f} = 1.68$ S/m; $\sigma_{0p} = 0.2$ S/m)

the results indicate that particles still heat faster than the liquid; however the heating rate of the mixture is now much slower (Fig. 5). The reason is that at the high particle concentrations considered, the particles form a large resistance to current, and parallel conduction paths through the fluid are extremely restricted. The result is a high overall resistance, low current, and slow heating, with particles leading the fluid.

If, however, all particles except one (isolated low-conductivity particle) are of conductivity equal to that of the fluid, the low-conductivity particle will exhibit large thermal lags relative to the rest of the mixture (Fig. 6). This phenomenon is consistent with experimental data of Sastry and Palaniappan (1992b) for two particles in a high conductivity fluid. The low-conductivity particle will then have to be heated via the liquid medium to achieve sterility. This indicates that one of the *critical control points* in ohmic heating is the electrical conductivity of particles. In practice, it will be necessary to ensure that all particles are no less conductive than a certain minimum value.

Results of residence time effects for the equal conductivity case are presented in Fig. 7, and indicate, as expected, that fast-moving particles will tend to thermally lag the fluid, although the extent of lag is far less than that associated with conventional processing. The effects of fluid-particle heat transfer coefficient is

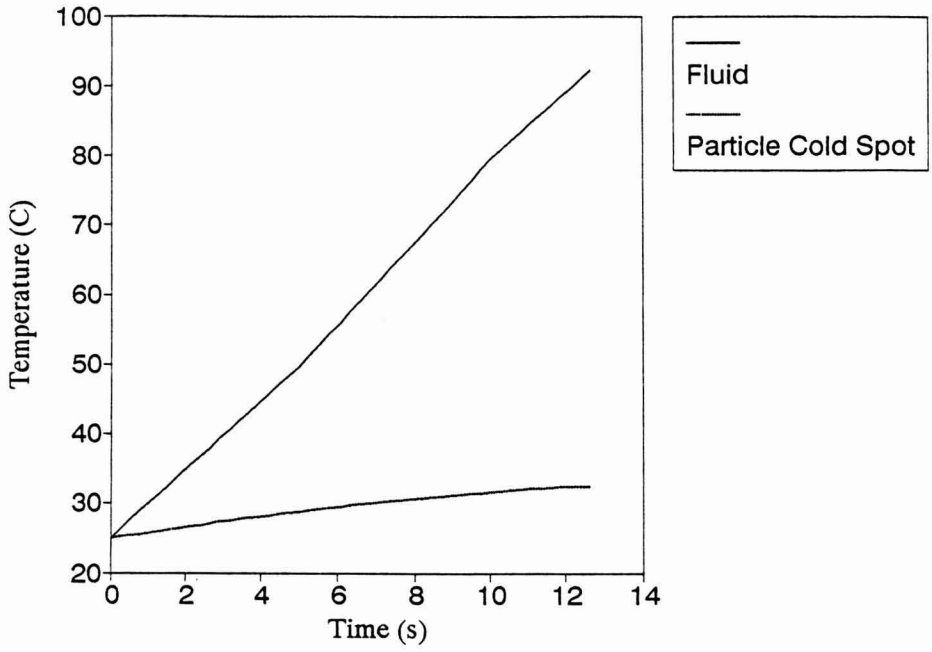


FIG. 6. PARTICLE COLD-POINT AND FLUID TEMPERATURES VERSUS TIME FOR ISOLATED LOW-CONDUCTIVITY PARTICLE
($\sigma_{0p}$ = 0.2 S/m for this particle, $\sigma_{0f}$ = 1.68 S/m, and $\sigma_{0p}$ = 1.68 S/m for all other particles)

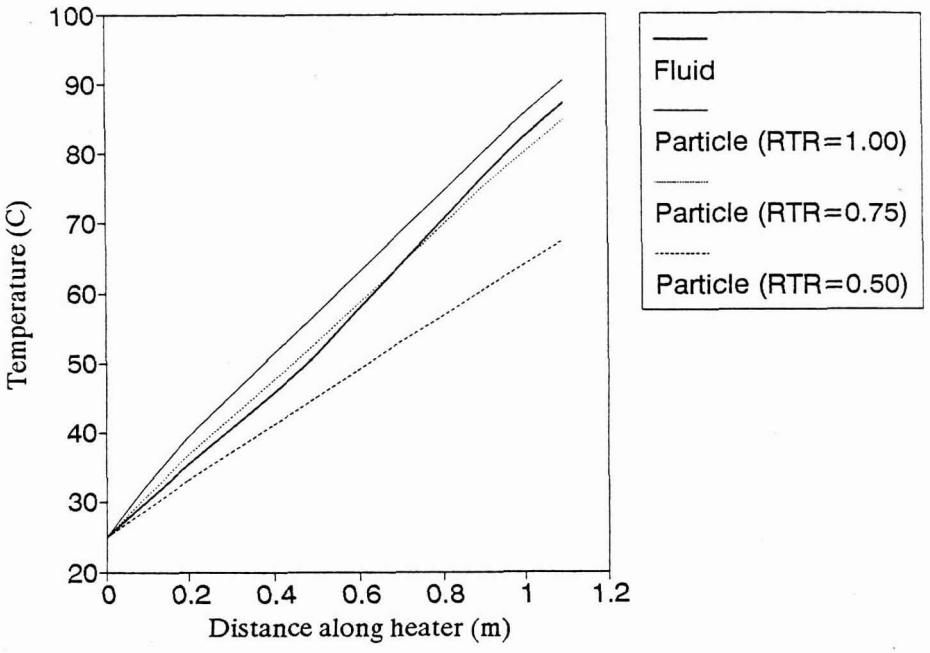


FIG. 7. PARTICLE COLD-POINT AND FLUID TEMPERATURES VERSUS DISTANCE ALONG HEATER FOR EQUAL ELECTRICAL CONDUCTIVITY CASE, ($\sigma_{0f} = \sigma_{0p} = 1.68$ S/m) ILLUSTRAING RESIDENCE TIME EFFECTS
(RTR is residence time ratio = particle residence time/mean fluid residence time.)

shown in Fig. 8 for the case of an isolated low-conductivity particle. The curves for three values of $h_{fp}$ overlap, illustrating the minor role of this parameter over the time scales of the simulations. The benefit of high heat transfer coefficients become more apparent for longer residence times. A notable feature is that inward cold-point migration is faster with high values of $h_{fp}$. As would be expected for an internal generation process, particle size appears to have a relatively small effect on the extent of lag for these particles (Fig. 9).

The observation regarding the isolated low-conductivity particle further illustrates the point made by Sastry and Palaniappan (1992b) regarding the conditions under which a particle may thermally lag or lead the fluid. The isolated low-conductivity particle has a relatively small effect on the overall resistance of the mixture, and may be expected to lag the fluid.

Based on the above findings and those of the literature, the following factors would need to be considered for safe process design.

(a) Thermal process calculation must be based on the lowest conductivity particle in the mixture. Since most mixtures will consist of a range of particle conductivities, it becomes necessary to identify lower limits of these values.

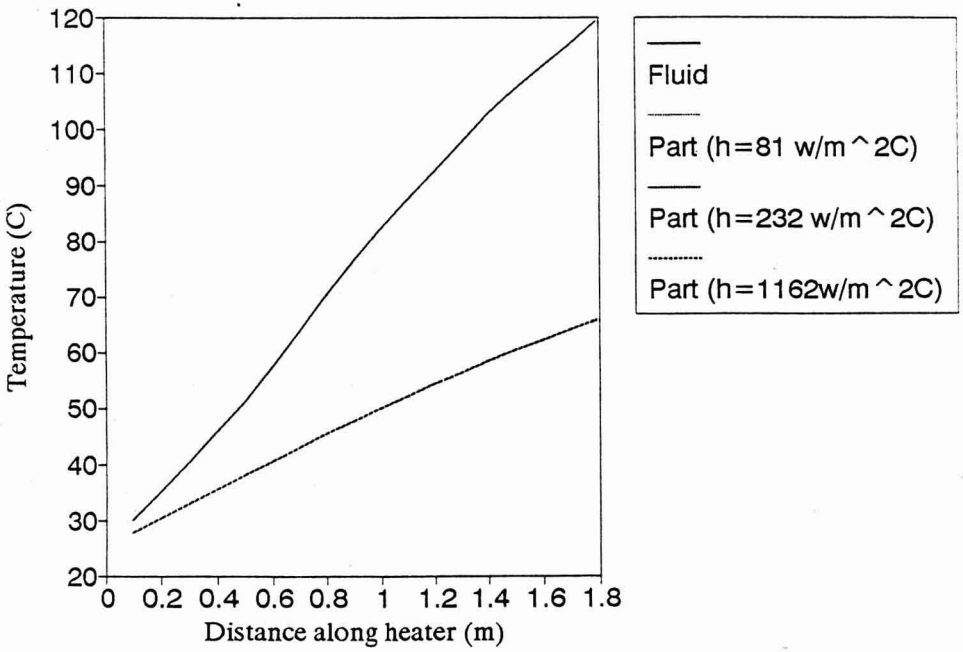


FIG. 8. PARTICLE COLD-POINT AND FLUID TEMPERATURES VERSUS DISTANCE ALONG HEATER FOR FAST-MOVING, ISOLATED LOW-CONDUCTIVITY PARTICLE ($\sigma_{0p}$ = 1.13 S/m FOR THIS PARTICLE, $\sigma_{1f}$ = 1.68 S/m, AND $\sigma_{0p}$ = 1.68 S/m FOR ALL OTHER PARTICLES; RTR = 0.5), ILLUSTRATING THE EFFECT OF FLUID-TO-PARTICLE HEAT TRANSFER COEFFICIENT

NOTE: three particle temperature curves overlap.

(b) Based on the findings of Sastry and Palaniappan (1992b), the lowest conductivity particle will heat most slowly relative to its surroundings if located around fluid (and other particles) of the highest electrical conductivity. Thus, it is important to characterize the range of variation of electrical conductivity for the components of the product.

(c) Based on the work of de Alwis and Fryer (1990), particles heat slowly when oriented in a manner permitting maximum current bypass (e.g., for long-thin particles of low electrical conductivities, orientation parallel to the current). Accordingly, the worst-case scenario would be one involving an isolated low-conductivity particle located in the highest conductivity environment consistent with that product, being oriented with a minimal cross-sectional area exposed to the current.

(d) The above particle would obviously experience an even greater thermal lag if its residence time is shorter than the average: accordingly the lowest-residence time consistent with the above particle would be conservative.

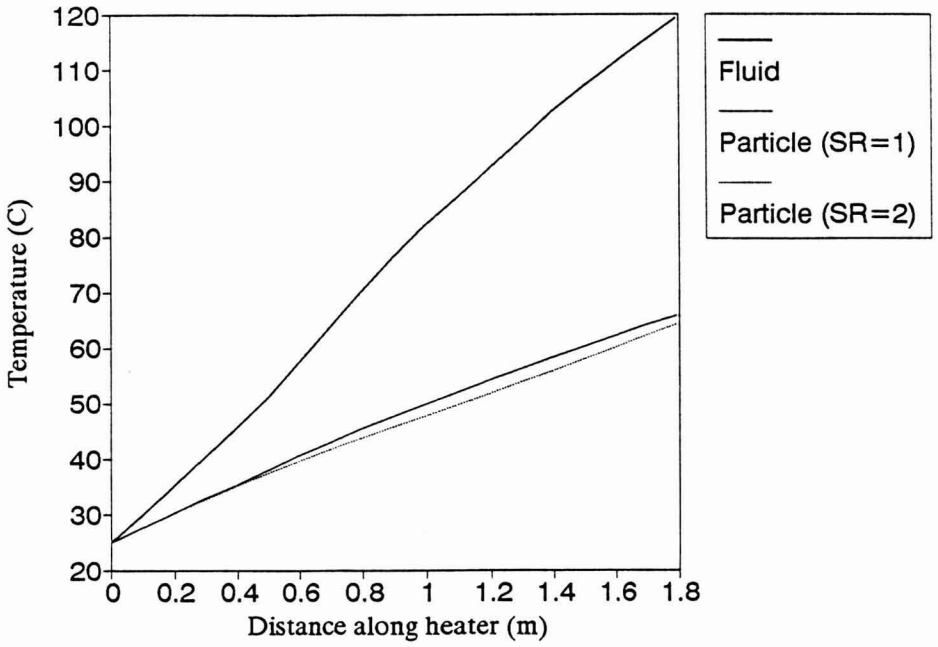


FIG. 9. PARTICLE COLD-POINT AND FLUID TEMPERATURES VERSUS DISTANCE ALONG HEATER FOR FAST-MOVING, ISOLATED LOW-CONDUCTIVITY PARTICLE, ($\sigma_{0p}$ = 1.13 S/m FOR THIS PARTICLE, $\sigma_{0f}$ = 1.68 S/m, AND $\sigma_{0p}$ = 1.68 S/m FOR ALL OTHER PARTICLES; RTR = 0.5) ILLUSTRATING PARTICLE SIZE EFFECTS (SR = size ratio = particle size normalized against 0.012 m.)

(e) It would, of course be conservative to assume a low liquid-particle heat transfer coefficient in the worst case, although this may not be a realistic assumption, based on laboratory data with moving particles (Sastry *et al.* 1990).

From the processors' standpoint, the best way to operate would be to control the range of particle electrical conductivities to the maximum extent possible, and use as high a concentration of particles as possible. This could prevent situations such as an isolated low conductivity particle existing in a high conductivity environment. Precooking treatments and careful product formulation could be used to achieve the desired effect.

The above study is based on a high solids concentration, plug flow scenario. Further modeling efforts are needed to address nonplug flow situations, and situations involving a distribution of electrical conductivities for different components of the mixture. Studies for mixtures exhibiting anisotrophy (long-thin particles) will also be of importance.

## CONCLUSIONS

Model predictions (verified previously for a static heater) indicate that for high solids concentration, ohmic heating will result in particles heating faster than the fluid if they are the same conductivity as the fluid and possess the same residence time. If all particles are of conductivity significantly lower than that of the fluid, the primary effect will be slow heating of the mixture, but particles will still thermally lead the fluid. The potential for underprocessing exists when a particle of low conductivity is surrounded by a high-conductivity environment; this particle will thermally lag the fluid. Residence time effects are also important; fast-moving particles can thermally lag the fluid, but to a lesser extent than expected for conventional process systems. Fluid-to-particle heat transfer coefficients become important in heating particles that exhibit thermal lags.

## NOMENCLATURE

| | |
|---|---|
| $A$ | Area |
| $C_p$ | Specific heat |
| $d$ | Diameter of heater tube |
| $h_{fp}$ | Fluid to particle convective heat transfer coefficient |
| $I$ | Current |
| $k$ | Thermal conductivity |
| $m$ | Temperature coefficient of conductivity |
| $M$ | Product mass flow rate |
| $n$ | Number |
| $\vec{n}$ | Unit normal vector |
| $R$ | Resistance |
| RTR | Residence time ratio = particle residence time/mean fluid residence time |
| SR | Size ratio = particle dimension/(0.012 m) |
| $t$ | Time |
| $T$ | Temperature |
| $U$ | Overall heat transfer coefficient of heater walls |
| $\dot{u}$ | Internal energy generation rate (per unit volume) |
| $v$ | Volume |
| $V$ | Voltage |
| $v_{ff}$ | Volume fraction of fluid |
| $v_{fs}$ | Volume fraction of solids |
| $x$ | Coordinate dimension |

### Greek Letters and Other Symbols

| | |
|---|---|
| $\Delta$ | Increment |
| $\rho$ | Density |
| $\sigma$ | Electrical conductivity |
| $\nabla$ | Gradient |

### Subscripts and Superscripts

| | |
|---|---|
| $a$ | Ambient air |
| $f$ | Fluid |
| $i$ | Index for incremental section |
| $l$ | Liquid |
| $m$ | Mean value |
| $n$ | Time step index |
| $p$ | Particle |
| $P$ | Parallel |
| $s$ | Surface (when used with temperature), solid (when used with resistance) |
| $S$ | Series |
| $w$ | Heater system wall |
| 0 | Reference value |
| $\infty$ | Bulk fluid (when used with temperature) |

## REFERENCES

DE ALWIS, A.A.P. and FRYER, P.J. 1990. A finite element analysis of heat generation and transfer during ohmic heat of food. Chem. Eng. Sci. *45*(6), 1547–1559.

HAYT, W.H. 1981. *Enginering Electromagnetics*, 4th Ed., McGraw Hill Book Co., New York.

SASTRY, S.K., LIMA, M., BRIM, J., BRUNN, TJ. and HESKITT, B.F. 1990. Liquid-to-particle heat transfer during continuous tube flow: Influence of flow rate and particle to tube diameter ratio. J. Food Proc. Eng. *13* 239–253.

SASTRY, S.K. and PALANIAPPAN, S. 1992a. Influence of particle orientation on the effective electrical resistance and ohmic heating rate of a liquid-particel mixture. J. Food Proc. Eng. *15*, 213–227.

SASTRY, S.K. and PALANAIAPPAN, S. 1992b. Mathematical modeling and experimental studies on ohmic heating of liquid-particle mixtures in a static heater. J. Food Proc. Eng. *15*, 241–261.

# PREDICTION OF MASS-AVERAGE AND SURFACE TEMPERATURES, AND THE TEMPERATURE PROFILES AT THE COMPLETION OF FREEZING FOR SHAPES INVOLVING ONE-DIMENSIONAL HEAT TRANSFER

COŞKAN ILICALI, SEMIH TEVFIK ENGEZ and METIN ÇETİN

*Ege University*
*Department of Food Engineering*
*35100 İzmir, Turkey*

Accepted for Publication June 3, 1992

## ABSTRACT

*A model for predicting the temperature profiles of simple-shaped foodstuffs at the end of freezing was developed. It was shown that with appropriate selection of effective thermal diffusivity and initial temperature data, the standard solution of the unidimensional unsteady state heat conduction equation can be used in predicting the average and surface temperatures of infinite slabs at the end of freezing operation. For the calculation of average and surface temperatures in infinite cylinders and spheres, unsteady state solutions were corrected by an empirical factor that was derived from temperature profiles predicted by an accurate finite difference scheme. The temperature profiles calculated from the proposed model were compared with the predicted results obtained from a numerical model. Mean absolute errors between the predictions of the proposed model and the numerical model were 0.54C and 0.46C for average and surface temperatures, respectively.*

## INTRODUCTION

The majority of the simple methods proposed for the calculation of freezing times have been developed to predict the time required for the thermal center of the foodstuff to reach a predetermined value (e.g., Cleland and Earle 1984a; Hung and Thompson 1983; Mascheroni and Calvelo 1982; Pham 1986; Plank 1941). These methods cannot be used to predict the temperature profiles when freezing is terminated. The total heat load on the refrigeration system in freezing

Journal of Food Process Engineering **15** (1992) 279–297. *All Rights Reserved.*

a foodstuff having a uniform initial temperature of $T_i$, to a final center temperature $T_r$ will depend on the temperature profile at the completion of the freezing. The final center temperature may be used in the calculation of the heat load, but this will lead to loss of accuracy (Cleland and Earle 1984b). It may be shown that for a lean beef sphere having an initial temperature of 0C, at a freezing Biot number ($h*D/k_f$) of 2, in an ambient temperature of −40C, for a final center temperature of −10C, the average temperature will be approximately −25C. The enthalpy difference between −10C and −25C is 42 kj/kg for lean beef having 74.5% water (Heldman and Singh 1981). The total heat load between 0C and −25C will be 274 kj/kg. Therefore, using the final center temperature in heat load calculations will lead to the underestimation of the heat load by 15%. This is a significant value that should be accounted for the accurate determination of the heat loads during freezing. The temperature driving force for heat transfer at the onset of the freezing will ($T_i - T_a$). The estimation of the final surface temperature T will lead to determination of the final temperature driving force ($T_s - T_a$). Information about the temperature driving forces during the freezing operation will help the designers of freezing equipments to determine the rate of heat release from foodstuffs (Pham 1984).

Numerical models, finite difference or finite element, have been used successfully by various researchers for the theoretical analysis of freezing and thawing (Cleland and Earle 1977, 1979, 1984b; Cleland *et al.* 1987; Pham and Willix 1990). The temperature profiles during freezing can be computed accurately by numerical models. However, numerical methods require considerable computational power and software. Since these resources are not always available, simplified analytical or empirical methods for the prediction of temperature profiles will be useful.

Schwartzberg (1981) has developed an analytical method for the prediction of the average temperature of the foodstuffs with simple shapes during freezing. The foodstuff was assumed to have a uniform initial temperature that is equal to or less than the initial freezing point. The solution of the unidirectional unsteady state heat conduction equation with constant physical properties for the mass average temperature was first differentiated with respect to time. Only the first term of the series solution was considered. The freezing Biot number was assumed to be less than three. It was possible to represent the first root of the characteristic equation by analytical functions in this low Biot number range. The apparent specific heat for freezing was also represented by an analytical equation in terms of the average temperature. Then, the average temperature was integrated with respect to time assuming that an average thermal conductivity may be used for the freezing period. For an infinite slab, in the Biot number range less than three, the final equation obtained was;

$$t_f = \frac{\rho_f (1+0.34*\overline{Bi})}{h * S} \left[ Cp_f * \ln\left[\frac{T_a - T_1}{T_a - \overline{T}}\right] + \frac{L*(T_o - T_i)}{(T_o - T_a)^2} * \ln\left[\frac{(T_o - \overline{T})*(T_a - T_1)}{(T_o - T_1)*(T_a - \overline{T})}\right] + \left[\frac{T_1 - \overline{T}}{T_o - T_1}\right] * \left[\frac{T_o - T_a}{T_o - \overline{T}}\right] \right] \quad (1)$$

Good agreement with corresponding numerical solution of the governing differential equations and experimental results was observed. However, this method can only be used if the freezing Biot number is less than three and if the foodstuff is at its initial freezing point or at a lower temperature. Simple equations for predicting the temperature profiles of infinite slabs at high Biot numbers were developed for the initial penetration period of freezing. The core was assumed to be at the initial freezing point and the temperature profile was assumed to be linear. This method cannot be used to predict the temperature profiles at the end of freezing, since this method assumes the temperature at the center to be at the initial freezing point of the foodstuff.

Pham (1984) has proposed the following linear equation for the calculation of the mean final temperature $\overline{T}$.

$$\overline{T} = T_r - (T_r - T_a) \; / \; (2+4/Bi) \quad (2)$$

Utilization of the same linear equation for the estimation of the mean final temperature in infinite slabs, infinite cylinders and spheres may lead to loss of accuracy in predictions.

ILICALI and Sağlam (1987), and ILICALI (1989a) have developed a simplified method for predicting the freezing times of foodstuffs having regular shape by applying the analytical solution for heat conduction with constant thermal properties in an empirical manner. The same approach was also applied to the prediction of the thawing times of foodstuffs having simple shape (ILICALI 1989b). It was the aim of this study to extend the freezing time prediction methods to predict the temperature profiles in foodstuffs with simple shapes at the end of freezing operation.

## THEORETICAL DEVELOPMENT

The standard solution for unsteady state one-dimensional heat transfer to solids having constant physical properties, and a uniform initial temperature $T_i$, after exposure to a constant ambient temperature $T_a$ for Fourier numbers greater than 0.1 has the general form (ILICALI 1989b);

$$\frac{T - T_a}{T_i - T_a} = A_1 \, f(\lambda_1 \, R/R_m) \, \exp(-\lambda_1^2 \, Fo) \quad (3)$$

where $A_1$ and $\lambda_1$ are functions of Biot number, R is the radial position, $R_m$ is the characteristic length, Fo is the Fourier number and $f(\lambda_1 R/R_m)$ is a function depending on Biot number and radial position.

The average temperature $\overline{T}$ for unsteady state one-dimensional heat conduction may be calculated from Eq. (4):

$$\frac{\overline{T} - T_a}{T_i - T_a} = A_1 \, d(\lambda_1) \exp(-\lambda_1^2 \, Fo) \tag{4}$$

The characteristic equations for $\lambda_1$, the functions $f(\lambda_1 R/R_m)$ and $d(\lambda_1)$ for the three basic simple shapes are shown in Table 1 (Kutateladze and Borishanskii 1966).

At the center of the solid, the function $f(\lambda_1 R/R_m)$ is equal to one for the three basic shapes. Therefore, Eq. (3) becomes:

$$\frac{T - T_a}{T_i - T_a} = A_1 \exp(-\lambda_1^2 \, Fo) \tag{5}$$

When a foodstuff is frozen the thermal conductivity and the volumetric heat capacity of the foodstuff are strong functions of temperature below the initial freezing point of the foodstuff and Eq. (3), (4) and (5) will be no longer valid. However, ILICALI and Sağlam (1987) have shown that these equations may be used in predicting the freezing times of foodstuffs with simple shapes by assuming (i) the freezing operation may be divided to a cooling period followed by a freezing

TABLE 1.
PARAMETERS FOR SERIES SOLUTION FOR UNSTEADY STATE HEAT TRANSFER AT FINITE BIOT NUMBERS TO SOLIDS WITH A UNIFORM INITIAL TEMPERATURE AFTER EXPOSURE TO A CONSTANT AMBIENT TEMPERATURE

| GEOMETRY | Eq. for $\lambda_1$ | $f(\lambda_1 R/R_m)$ | $d(\lambda_1)$ |
|---|---|---|---|
| Infinite slab | $Bi / (\tan \lambda_1)$ | $\cos(\lambda_1 . R/R_m)$ | $\frac{\sin \lambda_1}{\lambda_1}$ |
| Infinite cylinder | $\frac{Bi . J_0(\lambda_1)}{J_1(\lambda_1)}$ | $J_0(\lambda_1 R/R_m)$ | $\frac{2 J_1(\lambda_1)}{\lambda_1}$ |
| Sphere | $(1-Bi)\tan \lambda_1$ | $\frac{\sin(\lambda_1 . R/R_m)}{\lambda_1 (R/R_m)}$ | $\frac{3(\sin \lambda_1 - \lambda_1 . \cos \lambda_1)}{\lambda_1^3}$ |

period and (ii) Eq. (5); may be used to predict the freezing time for the freezing period if an effective constant thermal diffusivity incorporating the latent heat effects is used. According to their model, the time for the freezing period may be evaluated from Eq. (5) where $T_i$ is replaced by $T_f$, the initial freezing point of the foodstuff:

$$\frac{T_r - T_a}{T_f - T_a} = A_1 \exp(-\lambda_1^2 \, Fo_{eff}) \tag{6}$$

In Eq. (6) $T_r$ is the final center temperature at which the freezing operation is terminated and the effective Fourier Number, $Fo_{eff}$ is defined by:

$$Fo_{eff} = \frac{\alpha_{eff} \cdot t}{R_m^2} \tag{7}$$

where $\alpha_{eff}$ is an effective thermal diffusivity characterizing the freezing period, which is defined in ILICALI and Sağlam (1987) as;

$$\alpha_{eff} = \frac{k_f}{\rho_f * Cp_{eff}} \tag{8}$$

where $Cp_{eff}$ is the effective heat capacity incorporating the latent heat effects for the freezing period.

If one assumes that a similar approach can be used in predicting the average and the surface temperatures when the center temperature reaches $T_r$, then these temperatures may be evaluated from Eq. (9) and (10), respectively.

$$\frac{\overline{T} - T_a}{T_f - T_a} = A_1 \, d(\lambda_1) \exp(-\lambda_1^2 \, Fo_{eff}) \tag{9}$$

$$\frac{T_s - T_a}{T_f - T_a} = A_1 \, g(\lambda_1) \exp(-\lambda_1^2 \, Fo_{eff}) \tag{10}$$

where $T_s$ is the surface temperature and $g(\lambda_1)$ is the function $f(\lambda_1 \, R/R_m)$ at the surface.

If one assumes that the same effective diffusivity and the same Biot number may be used in Eq. (6), (9), and (10), the center, average and surface temperatures may be related by the equations:

$$\frac{\overline{T} - T_a}{T_r - T_a} = d(\lambda_1) \tag{11}$$

$$\frac{T_s - T_a}{T_r - T_a} = g(\lambda_1) \tag{12}$$

The validity of Eq. (11) and (12) will depend on the temperature profiles at the onset of the freezing period and at the termination of the freezing operation. When the temperature profiles are relatively flat, the temperature differences between equally spaced radial positions between the onset and the termination of freezing will be approximately equal, and therefore, the assumption of constant Biot number and effective diffusivity will not lead to serious errors in temperature profile prediction. The temperature profile will be expected to be relatively flat for low Biot numbers and high ambient temperatures. Furthermore, it can be shown that for an infinite slab the temperature profile will be flatter compared to the infinite cylinder and sphere geometry for the same Biot number and ambient temperature. Therefore, the prediction of the average and the surface temperatures by Eq. (11) and (12) will be expected to be in better agreement with the actual average and surface temperatures in infinite slabs compared to infinite cylinders and spheres.

With these considerations, for infinite slabs Eq. (11) and (12) were used without any correction in the prediction of the average and the surface temperatures at the end of freezing, respectively.

For infinite cylinders and spheres, the use of Eq. (11) and (12) lead to erroneous prediction of temperatures as expected. The errors in the predictions were found to depend on $T_r$ and $|T_aBi|$. Such a dependence has also been pointed out by Schwartzberg (1981). It was observed that as $T_r$ or $|T_aBi|$ decreased, the level of agreement between the predicted and numerical values increased. Therefore, by comparison with numerical data, the following corrections were introduced to Eq. (11) and (12):

$$\frac{\overline{T} - T_a}{T_r - T_a} = d(\lambda_1)\, K \tag{13}$$

$$\frac{T_s - T_a}{T_r - T_a} = g(\lambda_1)\, K \tag{14}$$

where K is an empirical correction factor obtained by comparing the predictions of the proposed model with numerical predictions:

$$K = \left[ 1 - \exp\left[-A - \frac{(C+T_r)}{T_aBi}\right] \right] \tag{15}$$

where A and C are the numerical constants shown in Table 2.

TABLE 2.
NUMERICAL VALUES OF THE CONSTANTS IN EQ. (12) FOR INFINITE CYLINDERS AND SPHERES

| GEOMETRY | A | C |
|---|---|---|
| Infinite Cylinder | 0.98 | - 20 |
| Sphere | 0.49 | - 10 |

Eq. (14) could be made the starting point for developing a method for predicting the temperature profile at the completion of freezing. For infinite slabs, Eq. (9) and (10) were utilized for the calculation of average and surface temperatures. An adequate approximation for temperature profiles in infinite slabs may be obtained by replacing $g(\lambda_1)$ in Eq. (10) by $f(\lambda_1\ R/R_m)$ from Eq. (1):

$$\frac{T - T_a}{T_r - T_a} = f(\lambda_1\ R/R_m) \tag{16}$$

For infinite cylinders and spheres, an equation similar to Eq. (16) may be written as,

$$\frac{T - T_a}{T_r - T_a} = f(\lambda_1\ R/R_m)\ K \tag{17}$$

However, for the center, $f(\lambda_1\ R/R_m)$ is equal to one. Therefore, Eq. (17) becomes,

$$\frac{T_c - T_a}{T_r - T_a} = K \tag{18}$$

Since K varies between 0.39 and 1.0, the utilization of Eq. (17) for predicting the temperature profiles for infinite cylinders and spheres will give erroneous results at locations near the center. For the case of a sphere frozen in an ambient temperature of $-40$C to a final center temperature of $-10$C at an infinite Biot number, Eq. (17) predicts a center temperature of $-28.3$C. As illustrated, the predictions of Eq. (17) will be very poor especially for high Biot numbers for locations close to the center. Therefore, for the prediction of the temperature profiles, it was postulated that the temperature profile may be represented by the following parabolic equation:

$$T = (T_s - T_r)*(R/R_m)^n + T_r \tag{19}$$

where n is a constant to be determined. In the models developed for the predictions of freezing and thawing times of foodstuffs with simple shapes, ILICALI and Sağlam (1987) and ILICALI (1989b) have observed that for infinite cylinders, the temperature of the foodstuff at the volume-half radius may be used for the average temperature of the cylinders. If this observation is generalized for the three basic shapes, then the constant n may be evaluated. The average temperatures and the temperatures at the volume-half radius ($R/R_m = 0.5$ for infinite slabs, 0.707 for infinite cylinders and 0.794 for spheres) at the end of freezing were compared with results from the application of a numerical model and very satisfactory agreement was observed. Therefore, n was evaluated as:

$$n = 1.44 * m * \ln \left[ \frac{(T_s - T_r)}{(T - T_r)} \right] \qquad (20)$$

where m has the values of 1, 2 and 3 for infinite slabs, infinite cylinders and spheres, respectively.

For the prediction of the temperature profiles, the average and the surface temperatures are calculated from Eq. (13) and (14), respectively. For infinite slabs K is taken to be equal to unity. The temperature profiles are calculated from Eq. (19).

## Numerical Verification

To test the model developed in a wide range of operational conditions, computer programs utilizing the fully implicit technique were prepared. The basic scheme used in the computation was taken from Carnahan *et al.* (1969). This scheme was modified to take into account the variation in the thermal properties during freezing,and finite convective resistance at the surface. The predictions of the computer programs for the freezing times were compared with experimental infinite slab freezing time data (Cleland and Earle 1977; Hung and Thompson 1983), infinite cylinder and sphere freezing time data (Cleland and Earle 1979). The performance of the numerical model for these data sets is shown in Table 3. The computer programs were also checked by comparing their predictions of the temperature profiles for solids having constant thermal properties with the analytical solution given in Eq. (3). Excellent agreement was observed. Therefore, it was concluded that these programs can be used for the verification of the proposed model.

The test materials chosen were lean beef and mashed potato. The thermophysical properties data used in the numerical model were taken from Cleland and Earle (1984b). The computer programs developed for infinite slab, infinite cylinder and sphere geometry were run in the Biot number range 0.25 to $\infty$ for eight different Biot numbers. The initial temperature of the test objects was assumed to

TABLE 3.
COMPARISON OF THE PREDICTIONS OF THE PRESENT NUMERICAL MODEL WITH EXPERIMENTAL FREEZING DATA

| Data Sources | $\bar{E}(\%)$ | $\sigma_{n-1}$ |
|---|---|---|
| Cleland and Earle (1977) | | |
| 43 Tylose infinite slabs | + 2.2 | 5.0 |
| 6 Potato infinite slabs | - 1.5 | 2.9 |
| 6 Lean Beef infinite slabs | + 0.2 | 5.3 |
| Cleland and Earle (1979) | | |
| 30 Tylose cylinders | + 3.5 | 4.8 |
| 30 Tylose spheres | + 5.0 | 3.5 |
| Hung and Thompson (1983) | | |
| 23 Tylose infinite slabs | - 2.6 | 8.2 |
| 9 Potato infinite slabs | - 3.9 | 10.0 |
| 9 Lean Beef infinite slabs | + 3.2 | 12.5 |

be 20C. The ambient temperatures considered were −20C, −30C and −40C. The programs were run until the center temperatures reached −10C and −18C and the predicted temperature profiles and the mass average temperatures were computed and compared with the predictions of the proposed model. The average temperatures predicted by the numerical model were not found by an enthalpy-based calculation, since the average temperatures predicted by the present model were not enthalpy-based average temperatures.

## RESULTS AND DISCUSSION

The predicted results from the proposed model were compared to the numerical data obtained for the freezing of infinite slabs, infinite cylinders and spheres of mashed potato and ground lean beef.

The comparison of the predicted results from the proposed model with results obtained from the numerical model for the average and the surface temperatures are given in Table 4 and Table 5, respectively. The comparison of the predicted mean final temperatures obtained from the equation proposed by Pham (1984) for shapes involving one dimensional heat transfer with the predicted results from the numerical model are also shown in Table 4. As may be expected, utilization of the same equation in prediction of the mean final temperatures for infinite slabs, infinite cylinders and spheres resulted in loss of accuracy. The predictions were especially poor for the sphere geometry.

Equation (1) suggested by Schwartzberg (1981) to predict the variation of the mean temperature as a function of time during freezing was also tested by comparison to numerical data obtained for lean beef and mashed potato. The initial

TABLE 4.
COMPARISON OF THE ACCURACY OF PREDICTED AVERAGE TEMPERATURES BY THE PROPOSED MODEL AND PHAM'S EQUATION WITH PREDICTED RESULTS FROM THE NUMERICAL MODEL

Proposed Model

| Material | Geometry | M.A.E. ( C) | N.A.E. (%) | Err.Range (%) |
|---|---|---|---|---|
| Lean Beef | Infinite Slab | 0.47 | 2.3 | 0.0 to + 6.3 |
| | Infinite Cylinder | 0.57 | 4.5 | - 6.3 to + 6.0 |
| | Sphere | 0.50 | 4.0 | -12.0 to + 6.5 |
| Mashed Potato | Infinite Slab | 0.44 | 2.1 | 0.0 to + 6.5 |
| | Infinite Cylinder | 0.68 | 5.0 | -15.0 to + 4.9 |
| | Sphere | 0.59 | 4.3 | -11.5 to + 6.9 |

Pham's Model

| Material | Geometry | M.A.E. ( C) | N.A.E. (%) | Err.Range (%) |
|---|---|---|---|---|
| Lean Beef | Infinite Slab | 1.67 | 11.2 | -15.0 to - 6.0 |
| | Infinite Cylinder | 2.19 | 12.5 | - 4.5 to +23.0 |
| | Sphere | 5.32 | 24.5 | - 2.0 to +40.7 |
| Mashed Potato | Infinite Slab | 1.66 | 10.9 | -15.0 to - 4.0 |
| | Infinite Cylinder | 2.47 | 9.6 | - 6.0 to +24.3 |
| | Sphere | 4.35 | 24.4 | - 2.1 to +40.7 |

TABLE 5.
COMPARISON OF NUMERICAL AND PREDICTED SURFACE TEMPERATURES

| Material | Geometry | M.A.E. ( C) | M.A.E. (%) | Err.Range (%) |
|---|---|---|---|---|
| Lean Beef | Infinite Slab | 0.43 | 2.1 | - 3.5 to + 7.1 |
| | Infinite Cylinder | 0.44 | 2.6 | - 6.0 to + 6.3 |
| | Sphere | 0.44 | 3.3 | -11.5 to + 5.0 |
| Mashed Potato | Infinite Slab | 0.39 | 1.9 | - 0.1 to + 6.5 |
| | Infinite Cylinder | 0.52 | 3.1 | - 7.0 to + 7.4 |
| | Sphere | 0.52 | 3.7 | -12.0 to + 7.3 |

temperature of the foodstuff was assumed to be equal to the initial freezing point. The freezing Biot number was kept below three. For five different freezing Biot numbers, the freezing times to reach center temperatures of $-10$C and $-18$C, and the mass average temperatures for these center temperatures were computed. The ambient temperatures utilized in the computations were $-20$C, $-30$C and $-40$C. The freezing times obtained by the numerical method was used in Eq. (1) to predict the final mean temperatures. During this comparison, it was observed that Eq. (1) except for low freezing Biot numbers (e.g., Bi = 0.50) predicted

lower freezing times than the numerical method. This in turn, resulted in mean temperatures that were larger than the mean temperatures calculated by the numerical model. For many cases, Eq. (1) predicted higher mean temperatures than the corresponding numerical center temperature. Therefore, it was concluded that a meaningful comparison to numerical data could not be carried out by Eq. (1). Numerical comparisons reveal that Eq. (1) should be treated as a freezing time prediction method rather than a mean temperature prediction equation.

As may be observed from Tables 4 and 5, the predictions from the proposed model were in good agreement with predictions from the numerical model. These results have shown that the average and surface temperatures for infinite slabs at the termination of freezing can be calculated from the standard series solution for one-dimensional unsteady state heat transfer in solids having constant thermophysical properties. Satisfactory agreement between the results obtained using Eq. (11) and (12) and numerical predictions were also observed for infinite cylinders and spheres when the ambient temperature was high (−20C) and the Biot number was low (0.25). However, when the Biot number was increased and the ambient temperature was decreased, the level of agreement became poorer. Introducing the empirical correction factor given in Eq. (15) significantly improved the agreement between the predicted and numerical results. The mean absolute error between the predictions of the numerical model and the proposed model for average and surface temperatures ranged from 0.39C to 0.68C. The normalized absolute error (N.A.E.) defined as;

$$\frac{\left|\begin{array}{l}\text{Temperature predicted by the proposed model} - \\ \text{Temperature predicted by the numerial model}\end{array}\right|}{|\ \text{Ambient temperature} - \text{Final center temperature}\ |} * 100$$

varied between 1.9% and 5.0%.

To eliminate the necessity of using tabulated values of $\lambda_1$ for the calculation of the functions $d(\lambda_1)$ and $g(\lambda_1)$ in Eq. (13) and (14) for the calculation average temperatures and surface temperatures, the results of the present research were presented in graphical form [Fig. (1), (2), (3) and (4)].

The variation of the dimensionless surface temperature with different Biot number for infinite cylinders and spheres was only slightly influenced by the final center temperature. Therefore, Fig. (4) was prepared for a final center temperature of −10C. However, it can also be used for center temperatures down to −18C. Figure (5) shows the comparison of the temperature profiles predicted by Eq. (19) with the numerical prediction for an ambient temperature of −30C and two different Biot numbers (Bi = 0.25 and $\infty$) for an infinite slab at a final center temperature of −10C. The level of agreement was quite satisfactory. The predictions of the proposed model for the temperature profiles of infinite cylinders and spheres are compared with numerical profiles in Fig. (6) and (7), respectively. Again, satisfactory agreement was observed.

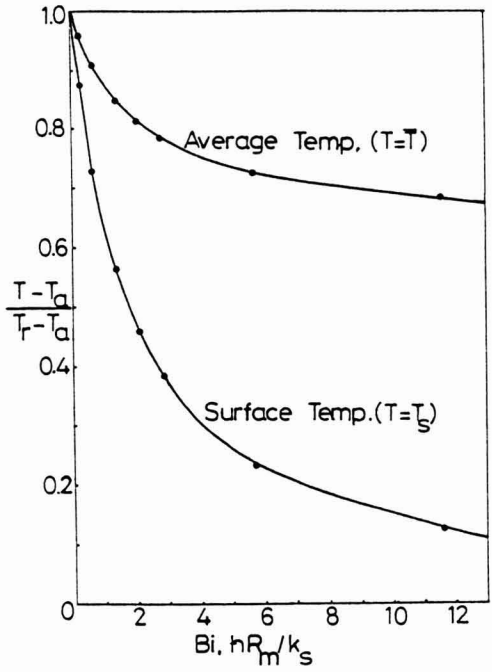


FIG. 1. THE VARIATION IN THE DIMENSIONLESS AVERAGE AND SURFACE TEMPERATURES AS A FUNCTION OF BIOT NUMBER AT THE TERMINATION OF FREEZING FOR INFINITE SLABS
($-20C \leqslant T_a \leqslant -40C$)

The agreement between the temperature profiles predicted by the proposed model and the numerical model was relatively poor for spheres at high Biot numbers at location near the center of the sphere compared to infinite cylinders and slabs. This can be attributed to the steep temperature profiles in spheres near the center.

## CONCLUSION

An empirical method for the determination of temperature profiles, average and surface temperatures at the completion of freezing for foods undergoing one dimensional heat transfer was tested by comparing its predictions with the results of a numerical model and found to be accurate. The proposed model can

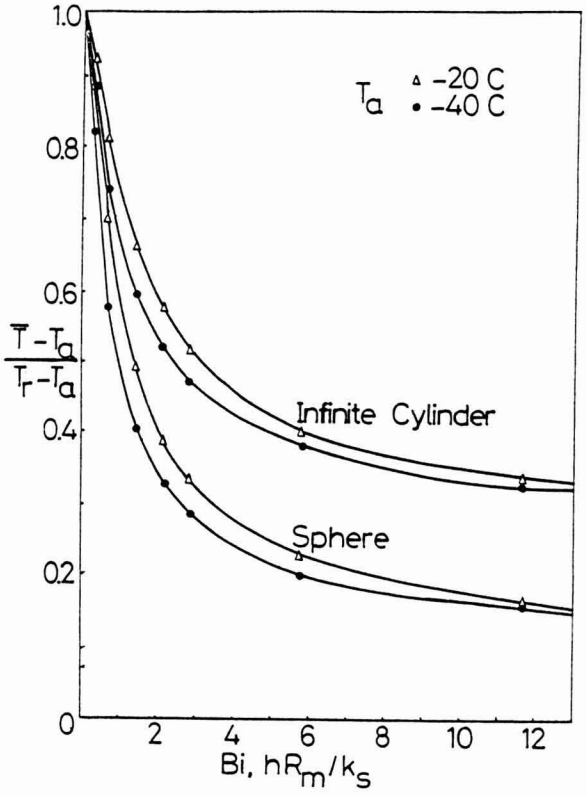


FIG. 2. THE VARIATION IN THE DIMENSIONLESS AVERAGE TEMPERATURE AS A FUNCTION OF BIOT NUMBER AT THE TERMINATION OF FREEZING FOR INFINITE CYLINDERS AND SPHERES ($T_r = -10C$)

be used safely for the estimation of the temperature profiles, average and surface temperatures at the completion of freezing.

## NOMENCLATURE

| | |
|---|---|
| A | Constant in Eq. (15), dimensionless |
| $A_1$ | Constants in Eq. (3), (4), (5), (6), (9) and (10), dimensionless |
| Bi | Biot number, $h*R_m/k_f$ dimensionless |
| $\overline{Bi}$ | Average Biot number, $2h*R_m/(k_f + k_1)$, dimensionless |
| C | Constant in Eq. (15), C |

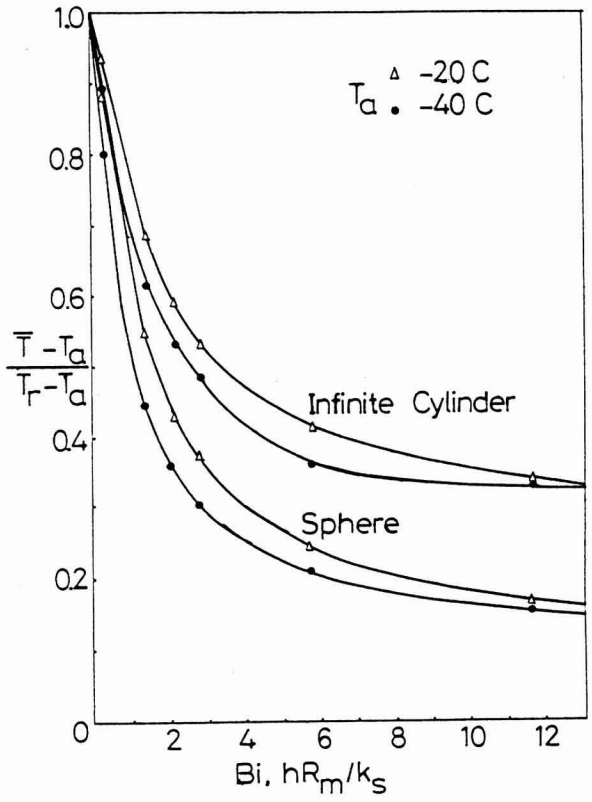


FIG. 3. THE VARIATION IN THE DIMENSIONLESS AVERAGE TEMPERATURE AS A FUNCTION OF BIOT NUMBER AT THE TERMINATION OF FREEZING FOR INFINITE CYLINDERS AND SPHERES
($T_r = -18C$)

| | |
|---|---|
| $d(\lambda_1)$ | Function in Eq. (4), dimensionless |
| $\overline{E}$ | Mean error |
| Err. | Error |
| $f(\lambda_1\ R/R_m)$ | Function in Eq. (3), dimensionless |
| Fo | Fourier number, $\alpha t/R^2_m$, dimensionless |
| $g(\lambda_1)$ | Function in Eq. (10), dimensionless |
| h | Heat transfer coefficient, $W/m^2K$ |
| $J_o$ | Bessel function of the first kind of order zero |
| $J_1$ | Bessel function of the first kind of order one |
| $k_f$ | Thermal conductivity in the fully frozen state, w/mK |
| $k_l$ | Thermal conductivity in the fully thawed state, w/mK |

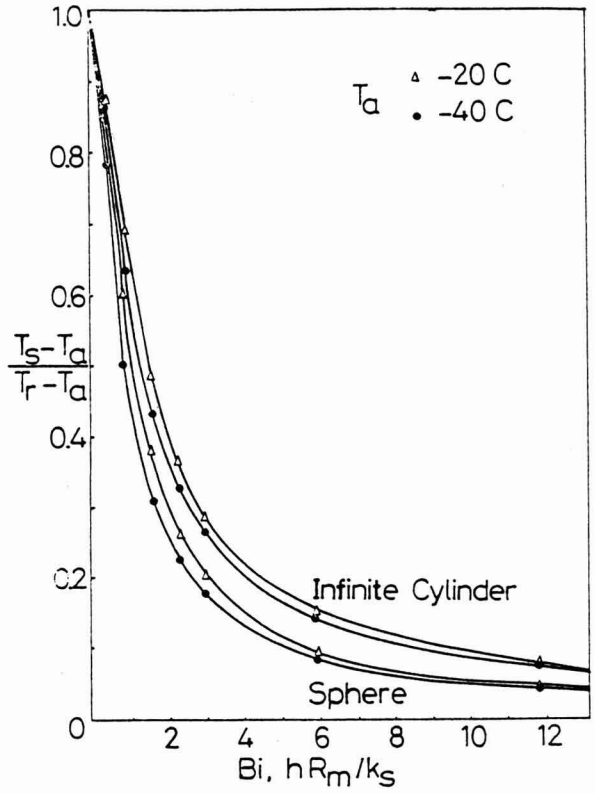


FIG. 4. THE VARIATION IN THE DIMENSIONLESS SURFACE TEMPERATURE AS A FUNCTION OF BIOT NUMBER AT THE TERMINATION OF FREEZING FOR INFINITE CYLINDERS AND SPHERES
($T_r = -10C$)

| | |
|---|---|
| K | Correction factor defined by Eq. (15), dimensionless |
| L | Latent heat of the foodstuff, J/kg |
| m | Constant in Eq. (20), dimensionless |
| M | Mass, kg |
| n | Constant defined by Eq. (20), dimensionless |
| N.A.E. | Normalized absolute error |
| R | Radial position, m |
| $R_m$ | Half-thickness for infinite slab, radius for infinite cylinder and sphere, m |
| S | Area, $m^2$ |
| t | Time, s |
| T | Temperature, C |

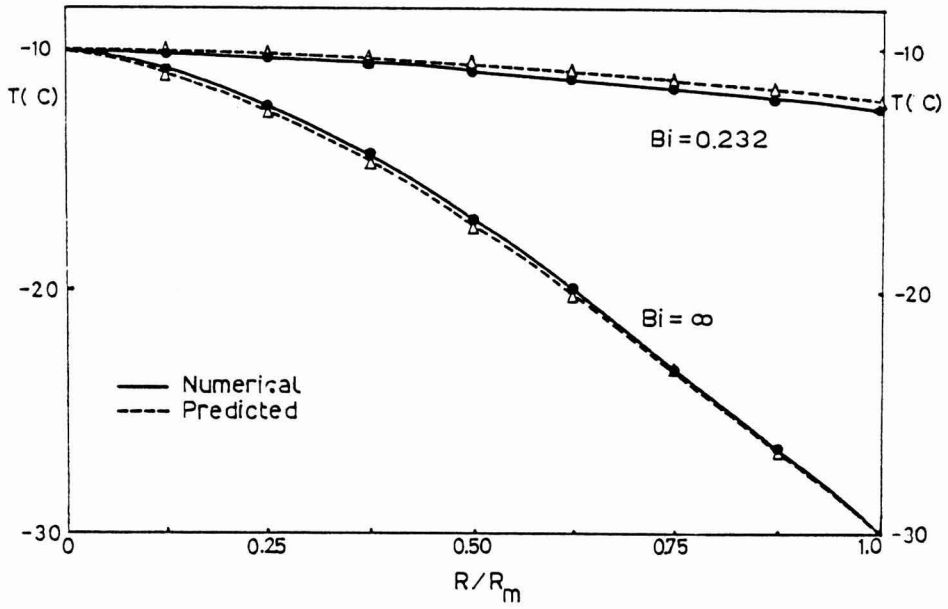


FIG. 5. COMPARISON OF THE PREDICTED TEMPERATURE PROFILES BY THE PROPOSED MODEL WITH THE NUMERICAL TEMPERATURE PROFILES FOR INFINITE SLAB
($T_a = -30C$, $T_r = -10C$)

| | |
|---|---|
| $T_a$ | Ambient temperature, C |
| $T_f$ | Initial freezing point, C |
| $T_i$ | Initial temperature, C, initial freezing point in Eq. (1), C |
| $T_0$ | Freezing point of pure water, 0C |
| $T_r$ | Center temperature at the end of freezing, C |
| $T_s$ | Surface temperature, C |
| $\overline{T}$ | Average temperature, C |
| $T_1$ | Uniform initial temperature in Eq. (1), C |
| V | Volume, $M^3$ |

## Greek Letters

| | |
|---|---|
| $\alpha$ | Thermal diffusivity, $m^2/s$ |
| $\rho$ | Density, $kg/m^3$ |
| $\lambda_1$ | First root of the characteristic equation, rad |

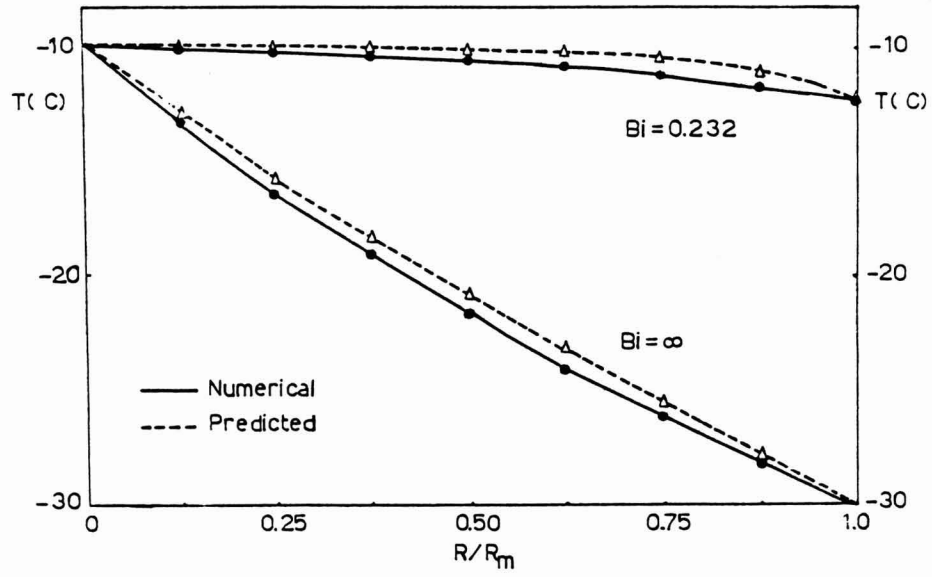


FIG. 6. COMPARISON OF THE PREDICTED TEMPERATURE PROFILES BY THE PROPOSED MODEL WITH THE NUMERICAL TEMPERATURE PROFILES FOR INFINITE CYLINDER
($T_a = -30C$, $T_r = -10C$)

## Subscripts

| | |
|---|---|
| a | Ambient |
| c | Center |
| eff | Effective |
| exp | Experimental |
| f | Fully frozen state |
| i | Initial |
| num | Numerical |
| s | Fully frozen |

## REFERENCES

CARNAHAN, B., LUTHER, H.A. and WILKES, J.O. 1969. *Applied Numerical Methods*, John Wiley & Sons, New York.

CLELAND, A.C. and EARLE, R.L. 1977. A comparison of analytical and numerical methods of predicting the freezing times of food. J. Food Sci. *44*, 1390.

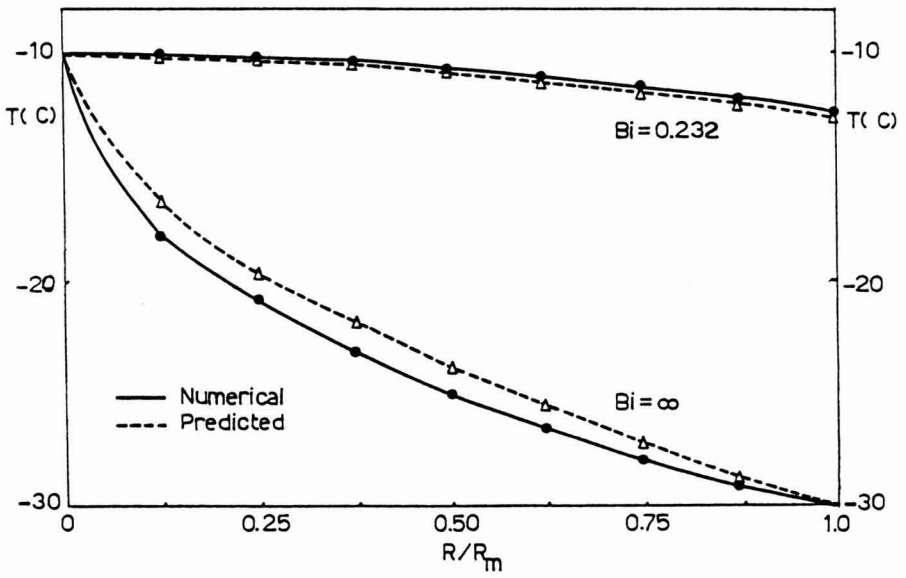


FIG. 7. COMPARISON OF THE PREDICTED TEMPERATURE PROFILES BY THE PROPOSED MODEL WITH THE NUMERICAL TEMPERATURE PROFILES FOR SPHERE ($T_a = -30C$, $T_r = -10C$)

CLELAND, A.C. and EARLE, R.L. 1979. A comparison of methods for predicting the freezing times of cylindrical and spherical foodstuffs. J. Food Sci. *44*, 958.

CLELAND, A.C. and EARLE, R.L. 1984a. Freezing time predictions for different final product temperatures. J. Food Sci. *49*, 1230.

CLELAND, A.C. and EARLE, R.L. 1984b. Assessment of freezing time prediction methods. J. Food Sci. *49*, 1034.

CLELAND, D.J., CLELAND, A.C. and EARLE, R.L. 1987. Prediction of freezing and thawing time for multi-dimensional shapes by simple formulae. Part 1. Regular shapes. Int. J. Refrig. *10*, 156.

HELDMAN, D. and SINGH, R.P. 1981. *Food Process Engineering*, 2nd Ed., Van Nostrand Reinhold/AVI, New York.

HUNG, Y.C. and THOMPSON, D.R. 1983. Freezing time prediction for slab shape foodstuffs by an improved analytical method. J. Food Sci. *48*, 555.

ILICALI, C. 1989a. A simplified analytical model for freezing time calculation in brick-shaped foods. J. Food Proc. Eng. *11*, 177.

ILICALI, C. 1989b. A simplified analytical model for thawing time calculation in foods. J. Food Sci., *54*, 1031.

ILICALI, C. and SAĞLAM, N. 1987. A simplified analytical model for freezing time calculation in foods. J. Food Proc. Eng. *9*, 299.

KUTATELADZE, S.S. and BORISHANSKII, V.M. 1966. *A Concise Encyclopedia of Heat Transfer*, p. 56, Pergamon Press, London.

MASCHERONI, R.H. and CALVELO, A. 1982. A simplified model for freezing time calculation in foods. J. Food Sci. *47*, 1201.

PHAM, Q.T. 1984. Extension to Plank's Equation for predicting freezing times of foodstuffs of simple shapes. Int. J. Refrig. *7*, 377.

PHAM, Q.T. 1986. Simplified equations for predicting the freezing times of foodstuffs. J. Food Technol. *21*, 209.

PHAM, Q.T. and WILLIX, J. 1990. Effect of Biot number and freezing rate on accuracy of some food freezing time prediction methods. J. Food Sci. *55*, 1429.

PLANK, R. 1941. Cited by Ramaswamy, H.S. and Tung, M.A. 1984. A review on predicting freezing times of foods. J. Food Proc. Eng. *7*, 169.

SCHWARTZBERG, H.C. 1981. Mathematical analysis of freezing and thawing. Tutorial presented at AICHE Summer Meeting Detroit, Michigan.

# DESCRIPTION OF LOG PHASE GROWTH FOR SELECTED MICROORGANISMS DURING MODIFIED ATMOSPHERE STORAGE[1]

YANYUN ZHAO, JOHN HENRY WELLS[2] and DOUGLAS L. MARSHALL[3]

*Department of Biological and Agricultural Engineering*
*Louisiana Agricultural Experiment Station*
*Louisiana State University Agricultural Center*
*Baton Rouge, LA 70803*

Accepted for Publication June 8, 1992

## ABSTRACT

*Two mathematical descriptions based on (1) a modified and additive Arrhenius equation and (2) a modified Arrhenius temperature characteristic equation were developed to describe the combined effects of time, temperature and initial gas composition of modified atmosphere storage on the population growth rate coefficients of* Listeria monocytogenes *and* Pseudomonas fluorescens. *Statistical analysis revealed that there was no significant interaction of temperature with* $[O_2]/(1+[CO_2])$ *ratio, such that a combined temperature and gas composition ratio term was not needed in an additive Arrhenius description. The Arrhenius temperature characteristic term* ($\mu$) *was found to be related to the* $[O_2]/(1+[CO_2])$. *Growth rate coefficients of bacterial populations could be estimated by substituting a term functionally relating to* $[O_2]/(1+[CO_2])$ *ratio for the* $\mu$ *coefficient in the Arrhenius expression. The mathematical descriptions were shown applicable for determining bacterial population growth rate coefficients in modified atmosphere storage for oxygen concentration from 0 to 20.99% and carbon dioxide concentration from 0.03 to 80%.*

[1]Approved for publication by the Director of the Louisiana Agricultural Experiment Station as Manuscript No. 91-07-5327.
[2]Corresponding author.
[3]Author Marshall is affiliated with the Department of Food Science, Louisiana Agricultural Experiment Station, Louisiana State University Agricultural Center.

Journal of Process Engineering **15** (1992) 299–317. 

## INTRODUCTION

Mathematical techniques can help predict the effects of environmental variables, such as temperature, water activity, pH and other factors, on bacterial proliferation. Attempts have been made to develop predictive equations to describe the quantitative relationship between bacterial proliferation and important processing and storage factors (Ratkowsky *et al.* 1982, 1983; Broughall *et al.* 1983; Broughall and Brown 1984; McMeekin *et al.* 1987; Thayer *et al.* 1987; Chandler and McMeekin 1989a,b; Davey 1989). Few mathematical descriptions, however, have been proposed for the prediction of bacterial growth on meat products stored under modified atmospheres.

Modified atmosphere storage can inhibit the growth of microorganisms and extend the shelf-life of chilled foods. Studies have confirmed the inhibitory effect of modified atmospheres on the growth of bacteria during low temperature storae of meats (Gill and Tan 1980; Marshall *et al.* 1991; Wimpfhimer *et al.* 1990). Under aerobic storage conditions, spoilage of meat products occurs primarily due to the growth of Gram-negative bacteria like *Pseudomonas fluorescens*. Modified atmosphere packaging (MAP) using reduced oxygen and increased carbon dioxide can inhibit the growth of these microorganisms and significantly increase the shelf-life of meat products (Farber 1991). However, some Gram-positive, facultatively anaerobic bacteria, such as the pathogen *Listeria monocytogenes*, are not substantially inhibited by MAP and would likely predominate during low temperature storage of meat products. Consequently, consumers could judge MAP products as wholesome, since spoilage would not be evident and inadvertently risk exposure to pathogens that may be abundant in the microflora. Precooked convenience items like chicken nuggets provide an especially hazardous risk to consumers since they often require little reheating prior to consumption.

Mathematical techniques can be used to describe the quantitative relationships between population growth rate coefficients at different temperatures and atmospheric environments for a given food. Predictive equations, capable of estimating bacterial proliferation over various temperatures and atmospheric compositions, could provide an understanding of the potential risk of pathogen growth for in-package gas compositions used by manufacturers and temperature conditions during distribution.

The specific objectives of this work were: (1) to review the mathematical descriptions proposed in the literature for predicting microbial population growth rate coefficient; and (2) to develop a mathematical description for the log phase population growth rate coefficient of *Listeria monocytogenes* and *Pseudomonas fluorescens* under varying $[O_2]/(1+[CO_2])$ concentration ratios at refrigeration temperatures.

## MATHEMATICAL DESCRIPTION OF POPULATION GROWTH RATE COEFFICIENT

### Predicting Bacterial Growth

The log (growth) phase of bacterial proliferation can be described by a exponential equation:

$$N(t)=N_0\exp(kt) \quad (1)$$

Where t is time, $N_0$ is initial number (population) of microorganisms at the beginning of log phase growth, N(t) is number (population) of microorganisms at time t, and k is the population growth rate coefficient for a given set of constant conditions (temperature, humidity, pH, water activity, etc.).

Various mathematical descriptions have been used to predict the effects of temperature and other environmental variables, such as water activity and pH, on bacterial population growth rate coefficient (k). Mathematical descriptions based on linear combinations, nonlinear expressions and variations of the Arrhenius relationship have been proposed (Broughall *et al.* 1983; Chandler and McMeekin 1989a,b; Davey 1989; McMeekin *et al.* 1987; Ratkowsky *et al.* 1982, 1983; Thayer *et al.* 1987). The most widely used mathematical descriptions of bacterial growth rate coefficient are summarized below.

### Polynomial Equation

Polynomial equations for describing microbial population growth rate coefficients were given by Roberts (1989) and Thayer *et al.* (1987). In general, these equations involve storage and composition factors including temperature, water activity, pH, level of added preservatives, storage atmosphere and other parameters. For example, Thayer *et al.* (1987) suggested a polynomial equation that combined NaCl, initial pH, temperature, and storage atmosphere. The polynomial expression was:

$$k=c_0+c_1C_N+c_2pH_I+c_3T+c_4C_NpH_I+c_5C_NT+c_6pH_IT+c_7C_N^2+c_8pH_I^2+c_9T^2 \quad (2)$$

where $C_N$ is the concentration of NaCl, $pH_I$ is initial pH value, T is incubation temperature in Centigrade, and coefficients $c_0$ to $c_9$ were calculated by statistical regression techniques. Such an equation has limited biological basis, but might be viewed as a Taylor's series approximation to a true underlying theoretical function (Roberts 1989). The results of polynomial equations remain unique to the product/storage condition combinations for which the regression coefficients were

determined and are useful only in the range of the experimental parameters. Polynomial forms do not typically appear consistent across a wide range of the independent parameters. That is, polynomial descriptions lack universality and contain large numbers of regression coefficients that only can be extrapolated with extreme caution.

## Modified Square-Root Equation

Ratkowsky *et al.* (1982) proposed a linear relationship between the square root of the population growth rate coefficient and the absolute temperature T in Kelvin:

$$\sqrt{k}=b(T-T_{min}) \tag{3}$$

where b is a regression coefficient and $T_{min}$ is a theoretical minimum temperature for growth of a particular microorganism. An extension of the Eq. (3), capable of describing bacterial population growth rate coefficient throughout an entire theoretical temperature range for that organism, was also proposed by Ratkowsky *et al.* (1983):

$$\sqrt{k}=b(T-T_{min})\{1-\exp[c(T-T_{max})]\} \tag{4}$$

where $T_{max}$ is a theoretical maximum temperature for growth and c is a regression coefficient that, in conjunction with b, enables the Eq. (4) to fit experimental data better than Eq. (3).

The modified square root equation was used by McMeekin *et al.* (1987) to describe the combined effect of temperature and water activity on the population growth rate coefficient of *Staphylococcus xylosus*. McMeekin *et al.* (1987) proposed the expression:

$$\sqrt{k}=c\sqrt{(\alpha_w-MIN\alpha_w)}(T-T_{min}) \tag{5}$$

where $\alpha_w$ is water activity, c is a constant and $MIN\alpha_w$ is estimated by extrapolating the fitted line of $b^2$ [in Eq. (3)] versus water activity to the water activity axis (McMeekin *et al.* 1987; Chandler and McMeekin 1989a). This equation has only three coefficients, but the necessary nonlinear form has a disadvantge in that it is difficult to determine an iterative fit to experimental data.

## Arrhenius Equation

The most common and generally valid description of the temperature dependence of population growth rate coefficient is represented by the classic Arrhenius expression:

$$k=A\exp(-\frac{\mu}{RT}) \tag{6}$$

where T is absolute temperature in Kelvin, R is the universal gas constant = 1.987cal/(K mol), $\mu$ is an empirically determined quantity called the activation energy or temperature characteristic term in cal/mole, and A is a constant, independent of temperature, variously referred to as the "collision factor," "frequency factor" (Davey 1989; Ratkowsky *et al.* 1982) or "pre-exponential factor" (Labuza 1984).

The linear form of the classic Arrhenius equation implies that a plot of ln k versus 1/T yields a straight line. However, studies by Ratkowsky *et al.* (1982) indicated that an Arrhenius plot of population growth rate coefficient for selected organisms shows curvature. Ratkowsky *et al.* (1982) has pointed out that "bacterial growth is a complex biological process involving a variety of substrates and enzymes, and it is thus not surprising that the Arrhenius Law does not adequately describe the effect of temperature on the growth of bacteria."

## Modified and Additive Arrhenius Equation

A description for combined temperature and water activity based on a modified and "additive" Arrhenius equation was investigated by Davey (1989). This equation presented a simple yet significant relationship, which permitted prediction of microorganism population growth rate coefficient given the temperature and water activity of a particular substrate. Davey (1989) presented the following equation:

$$lnk=c_0+\frac{c_1}{T}+\frac{c_2}{T^2}+c_3\alpha_w+c_4\alpha_w^2 \tag{7}$$

where $c_0$ through $c_4$ are coefficients to be determined from statistical analyses, T is absolute temperature in Kelvin, $\alpha_w$ is water activity, and k is growth rate coefficient. Advantages over previous equations are that it is relatively easy to fit to data using least square regression and requires only five coefficients.

## Nonlinear Arrhenius Equation

A nonlinear Arrhenius equation, as published by Schoolfield *et al.* (1981), was stated as:

$$\frac{1}{G}=\frac{\rho_{(25)}\frac{T}{298}\exp\{\frac{H_A}{R}(\frac{1}{298}-\frac{1}{T})\}}{1+\exp\{\frac{H_L}{R}(\frac{1}{T_{1/2L}}-\frac{1}{T})\}} \tag{8}$$

where R is the Universal Gas Constant, $\rho_{(25)}$ is the growth rate at 25C, T is the absolute temperature in Kelvin, $H_A$ is a constant describing the enthalpy of activation for microbial growth, $H_L$ is another constant describing the enthalpy of the low temperature inactivation of growth, $T_{1/2L}$ describes the temperature for 50% low temperature inactivation of the growth rate, and G is the generation time relating to population growth rate by:

$$G=\frac{ln2}{k} \tag{9}$$

The generation time G was defined as the time that elapses between the formation of a daughter cell and its division into two new cells. Experimental data during the log phase of bacterial population growth can be used to estimate generation time, since there is a linear relationship between the logarithm of cell numbers and time of incubation (Broughall *et al.* 1983; Marshall and Schmidt 1988).

Broughall *et al.* (1983) adapted the nonlinear Arrhenius equation of Schoolfield *et al.* (1981) as the basis for a two-dimensional model combining temperature and water activity into the population kinetics of both the lag phase and log phase of bacterial growth. The lag phase and growth (log) phase kinetics were treated separately. The four constants in Eq. (8), $\rho_{(25)}$, $H_A$, $H_L$ and $T_{1/2L}$ were described in terms of water activity. Furthermore, a three-dimensional equation (Broughall and Brown 1984) was developed to describe the effects of temperature, water activity, and pH, on the kinetics of bacterial proliferation.

A disadvantage of the nonlinear Arrhenius description is the resulting complexity of the equation, where, i.e., eight coefficients were required to define the growth phase for a two-dimensional equation, and 12 coefficients were required for a three-dimensional equation.

## MATERIALS AND METHODS

### Organisms and Growth Conditions

Dark-meat chicken nuggets were prepared from hand deboned broiler thigh meat. The thigh meat was ground through a 70 mm diameter plate with 3.2 mm holes. One-half percent NaCl by weight was added and tumbled with the ground product under vacuum for 15 min in a rotating 20 L drum (Globus Inject Star MC massager). Massaged meat was tempered to −1.7C with dry ice and formed into 20 g nuggest portions using a Hollymatic Super former. Nuggets were frozen in a carbon dioxide cabinet freezer and stored at −10C until autoclaving and inoculation. Chicken nuggets were precooked in an autoclave at 120C for 15 min and cooled to room temperature prior to inoculation. Precooked chicken nuggets

were inoculated with either *Listeria monocytogenes* Scott A or *Pseudomonas fluorescens* ATCC 13525, according to the procedures described by Marshall *et al.* (1991). Each nugget was packaged in a 7″ × 8″ plastic barrier bag (Koch model 01 46 09, Kansas City, MO) evacuated, and backflushed with air or one of two commercial premixed gas blends. Experimental data were collected from a replicated 3 × 3 factorial design consisting of 3 temperatures (3, 7, and 11C), and 3 initial gases (air containing 0.03% $CO_2$:78.03% $N_2$:20.99% $O_2$, modified atmosphere 1 containing 76% $CO_2$:13.3% $N_2$:10.7% $O_2$, and modified atmosphere 2 containing 80% $CO_2$:20$_7$ $N_2$:0% $O_2$). Two nuggets were sampled for each replication at intervals ranging from 1 to 3 days depending on anticipated population growth rate for a particular storage temperature. Mean values of microbiological populations were reported as averages of duplicate platings of each of 4 nuggets per sampling point. The number of bacteria present was expressed as $\log_{10}$ colony forming units (CFU)/g. Analysis of the comparative growth of *L. monocytogenes* and *P. fluorescens* on precooked dark-meat nuggets has been discussed by Marshall *et al.* (1991) and the reported data set served as the basis for model development.

## Proposed Equations for Population Growth Rate Coefficient

Statistical analysis (F-test) of the experimental data indicated that percent concentration of oxygen [$O_2$] and carbon dioxide [$CO_2$] could not be separated as independent variables for the description of bacterial population growth rate coefficients. Considering the mathematical viability of proposed descriptions when $CO_2$ is absent, (1+[$CO_2$]) term was used instead of [$CO_2$] term. Therefore, the percent concentration ratio of oxygen to carbon dioxide [$O_2$]/(1+[$CO_2$]) was used as the primary independent variable rather than oxygen and carbon dioxide concentration alone. Furthermore, the effect of nitrogen concentration was not included in equation development, as it is usually considered to have no significant effect on the growth of microorganisms (Farber 1991).

After preliminary analysis of the mathematical descriptions relating [$O_2$]/(1+($CO_2$]) to population growth rate coefficient, two mathematical descriptions were proposed. One mathematical description was based on the modified and additive Arrhenius equation (Davey 1989), and the other was based on a modification of the temperature characteristic term in the Arrhenius equation.

The first equation was based on a modified and additive Arrhenius equation of a form used previously by Davey (1989) to describe the effect of temperature and water activity on bacterial proliferation. Inspection of the experimental data portrayed in an Arrhenius plot (ln k vs 1/T, Fig. 1) indicated that the general shape of the curve did not change for different [$O_2$]/(1+[CO2]) percent concentration ratios, suggesting that there was no significant interaction between

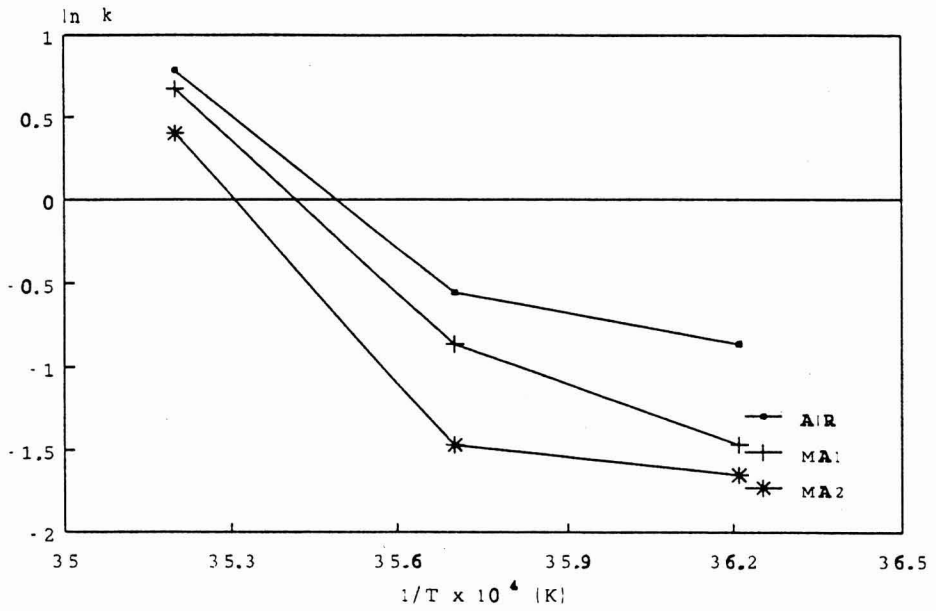


FIG. 1. ARRHENIUS PLOT OF ln k VS INVERSE ABSOLUTE TEMPERATURE 1/T FOR *L. MONOCYTOGENES* AT DIFFERENT $[O_2]/(1+[CO_2])$

$[O_2)/(1+[CO_2])$ and temperature. However, curvature was observed for individual ln k vs 1/T curves at each atmosphere condition. The curvature can be taken into account within a proposed description with a quadratic expression of temperature. Furthermore, the magnitude of ln k appears to be dependent on the gas composition. The dependence also carries over to the frequency factor term such that it is exponentially related to $[O_2]/(1+[CO_2])$ ratio. A description of population growth rate coefficient taking into account these observations was suggested as:

$$\ln k = \beta + \frac{c_2}{T} + \frac{c_3}{T^2} \tag{10}$$

where, the frequency factor in the classic Arrhenius equation has been expressed as an exponential function of the $[O_2]/(1+[CO_2])$ ratio:

$$\beta = c_0 + c_1 \exp\left(-\frac{[O_2]}{1+[CO_2]}\right) \tag{11}$$

Where, T is absolute temperature in Kelvin, $c_0$ through $c_3$ are regression coefficients determined by statistical procedure, $[O_2]$ is percent concentration of oxygen, and $[CO_2]$ is percent concentration of carbon dioxide. As consistent with

the notation by Davey (1989), the temperature characteristic and universal gas constant terms of the Arrhenius equation has been replaced with two coefficients of inverse temperature in the proposed equation.

The second equation was based on the classic Arrhenius equation, with modification of the temperature characteristic term (modified Arrhenius temperature characteristic equation). Previous research (Saguy and Karel 1980; Davey 1989) has suggested that the temperature characteristic term ($\mu$) in the classic Arrhenius equation is not constant over the entire growth temperature range. The empirical temperature characteristic term ($\mu$) can be related to water activity, moisture content, solids concentration, pH, and other composition factors (Saguy and Karel 1980; Davey 1989). Upon examination of the experimental data, it was found that temperature characteristic term changed with the ratio of percent concentration of oxygen and carbon dioxide. A quadratic function curve was observed for individual temperature characteristic terms vs $[O_2]/(1+CO_2])$ at each temperature condition. A proposed description for population growth rate using a modification of the temperature characteristic term was suggested as:

$$lnk = lnA - \frac{\gamma}{RT} \tag{12}$$

where the temperature characteristic term in the classic Arrhenius equation has been expressed as a quadratic function of $[O_2]/(1+[CO_2])$ ratio:

$$\gamma = c_0 + c_1\left(\frac{[O_2]}{1+[CO_2]}\right) + c_2\left(\frac{[O_2]}{1+[CO_2]}\right)^2 \tag{13}$$

where A and $c_0$ through to $c_2$ are coefficients determined by statistical procedure.

## Mathematical and Statistical Analyses

The population growth rate coefficient (k) was determined at each temperature and atmosphere composition from the observed generation time of the microorganisms under study. Generation time was calculated by using selected pairing of data points judged to be in the exponential (log) phase of growth using the techniques described by Marshall and Schmidt (1988). In turn, population growth rate coefficient (k) was calculated from generation time using Eq. (9). The regression coefficients in Eq. (10) through Eq. (13) were determined by statistical procedures (SAS Institute Inc. 1988). Nine sets of experimental data were used in the fitting of Eq. (10) and Eq. (12). Eq. (10) is a linear regression equation that was fitted by least squares regression using the statistical procedure REG (SAS Institute Inc. 1988). The parameters for the nonlinear regression equation, Eq. (12), were determined with the statistical procedure NLIN using a standard Mar-

quardt method (SAS Institute Inc. 1988). Various initial estimatesd for the NLIN procedure were provided all of which resulted in the same estimates for the coefficients.

## RESULTS AND DISCUSSION

The purpose in constructing mathematical descriptions of population growth rate coefficients was to predict the total number of bacteria during log phase multiplication under the atmospheric composition and storage temperature used in MAP. The growth rate coefficient was statistically related to $[O_2]$, $[CO_2]$, and temperature using Eq. (10) and Eq. (12) for both *L. monocytogenes* and *P. fluorescens*. Table 1 presents values of the coefficients determined for Eq. (10), and parameter estimates found for Eq. (12) are listed in Table 2. Since the SAS NLIN procedure did not provide values for the regression coefficient $R^2$ from Eq. (12), $R^2$ was computed to equal (1 − Residual sum of square/Corrected total sum of square). High $R^2$ coefficients indicated that Eq. (12) is an appropriate mathematical formulation for describing the relationship of population growth rate coefficient with temperature and atmospheric composition. Bacterial population growth rate coefficients during log phase were predicted using the regression constants in Eq. (10) and Eq. (12). In turn the growth rate coefficient was

TABLE 1.
PARAMETERS DETERMINED FOR MODEL 1 (EQ. 10)

| Organisms | $c_0$ | $c_1$ | $c_2 x10^{-6}$ | $c_3 x10^{-8}$ | $R^2$ | %V[a] |
|---|---|---|---|---|---|---|
| *L. monocytogenes* | 3116.68016 | -3.403779 | -1.725622 | 2.38993535 | 96.77 | 94.88 |
| *P. fluorescens* | 74.48349 | -3.965879 | -0.019867 | 0 | 96.33 | 94.12 |

[a] Percent variance accounted for (%V) was determined by both the number of observations (n) and the number of terms (N) in the model (N=3 for eq (10) ). Percent variance is more appropriate for relatively few data as a high value for the multiple regression coefficient $R^2$ might give the impression of too good a fit (Davey 1989). The percent variance was calculated as:

$$\%V = 1 - \frac{(1-R^2)(n-1)}{(n-N-1)}$$

For all predictions, temperature range 3-11 C; oxygen concentration range 0%-20.99%; carbon dioxide concentration range 0.03%-80%.

TABLE 2.
PARAMETERS DETERMINED FOR MODEL 2 (EQ. 12)

| Organisms | A | $c_0$ | $c_1$ | $c_2$ | $R^2$ |
|---|---|---|---|---|---|
| *L. monocytogenes* | 1.85759e29 | 37980.27765 | -2243.8291 | 2501.22755 | 86.2 |
| *P. fluorescens* | 5.82307e30 | 39608.04260 | 504.5654 | -11711.47931 | 97.5 |

For all predictions, temperature range 3-11 C; oxygen concentration range 0%-20.99%; carbon dioxide concentration range 0.03%-80%.

used to predict the estimated population from Eq. (1) under constant conditions of temperature and initial atmospheric composition. Figures 2 to 5 illustrate the population estimated by Eq. (1) compared with the actual experimental data. From Tables 1 and 2, as well as Fig. 2 to 5, it is apparent that Eq. (10) and Eq. (12) can be used to predict the growth of *L. monocytogenes* and *P. fluorescens* during log phase accounting for combined effects of temperature and atmospheric composition.

Equation (10) expressed temperature and $[O_2]/(1+[CO_2])$ in terms of an additive equation, i.e., there was no interaction. The good agreement between predication of this equation and the experimental data suggested that temperature and gas composition act independently on microbial growth in the log phase, as shown in Fig. 1 where the data form a series of parallel curves displaced for each value of $[O_2]/(1+[CO_2])$. This indicated that there is no interaction of temperature with gas composition. The finding that storage temperature and $[O_2]/(1+[CO_2])$ act independently was also discussed by Marshall *et al.* (1991). Because Eq. (10) was quadratic in terms of 1/T and $[O_2]/(1+[CO_2])$, the minimum data that can reasonably be fitted must be at least three levels for each of temperature and gas composition. Additional levels of both temperature and gas composition would be desirable for model development.

The results of the present investigation are limited to Eq. (10) and Eq. (12), and do not necessarily represent the best fit equations for the experimental data. The limited amount of experimental data appropriate to model development currently constrains derivation of predictive equations for MAP applications. Further studies explicitly designed for equation development are required. The nonlinear Arrhenius equation, Eq. (8), may be very efficient for predicting bacterial population growth for combined gas atmosphere and temperature. However, it is almost impossible to realize population growth prediction in this case because at least eight parameters need to be determined in Eq. (8). In the

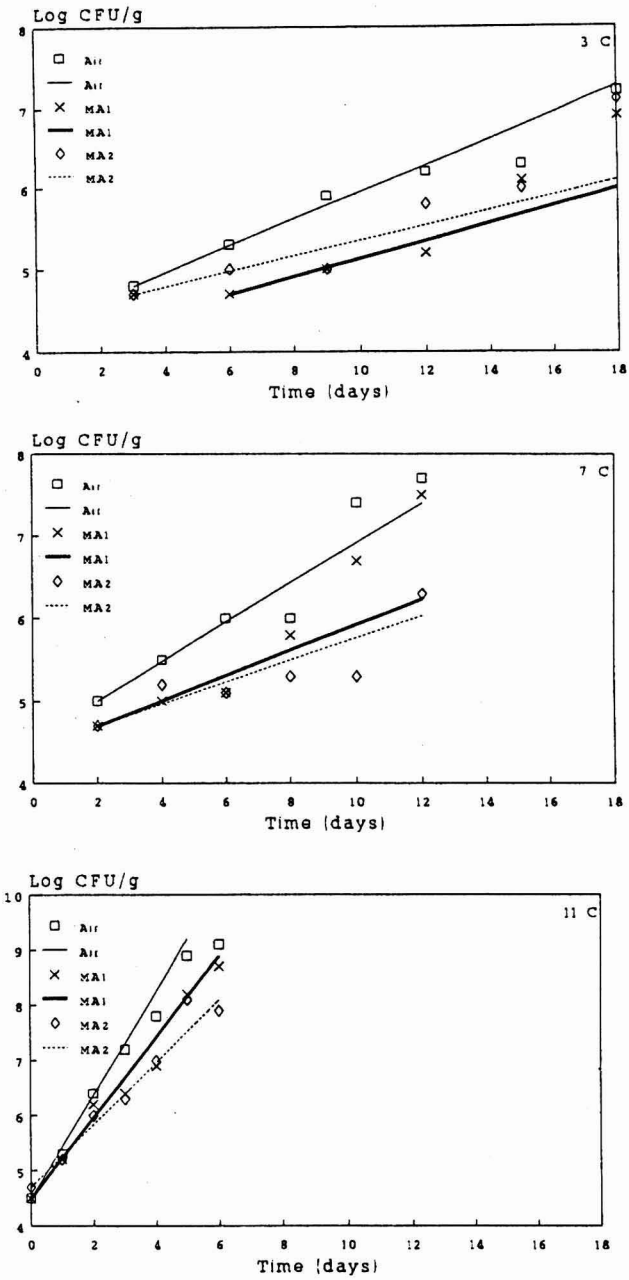


FIG. 2. COMPARISON OF OBSERVED (SYMBOL) AND PREDICTED (LINE) GROWTH OF *L. MONOCYTOGENES* POPULATION AT 3, 7, AND 11C USING A MODIFIED AND ADDITIVE ARRHENIUS EQUATION (EQ. 10)

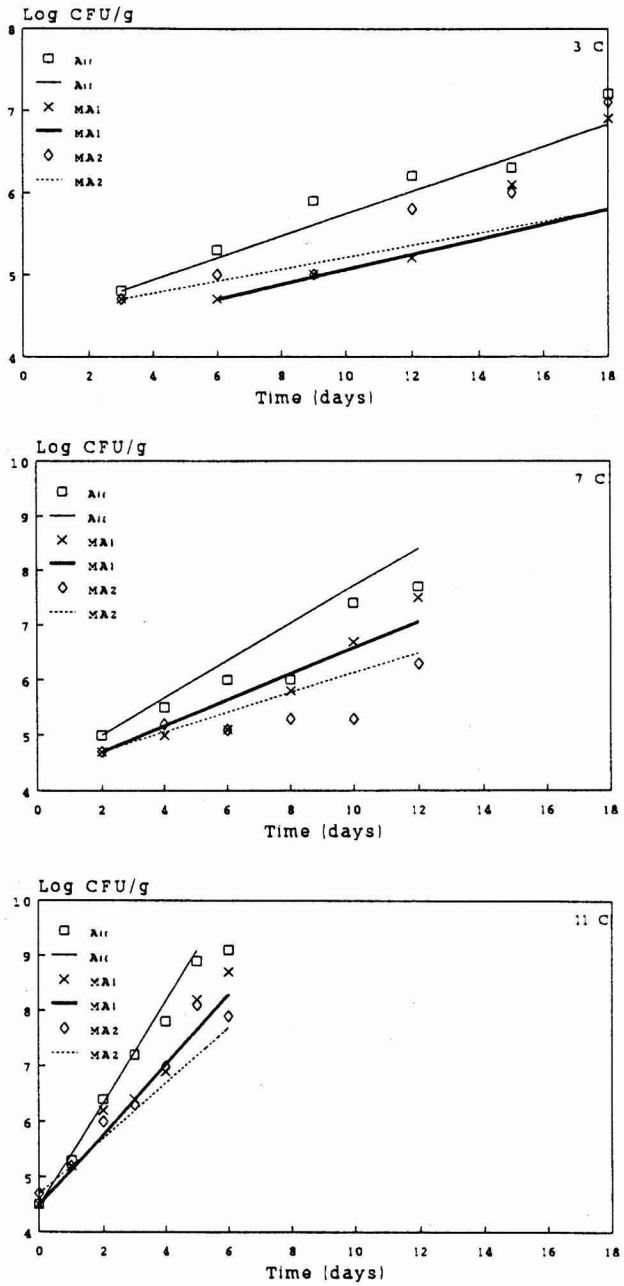


FIG. 3. COMPARISON OF OBSERVED (SYMBOL) AND PREDICTED (LINE) GROWTH OF *L. MONOCYTOGENES* POPULATION AT 3, 7, AND 11C USING MODIFIED ARRHENIUS TEMPERATURE CHARACTERISTIC EQUATION (EQ. 12)

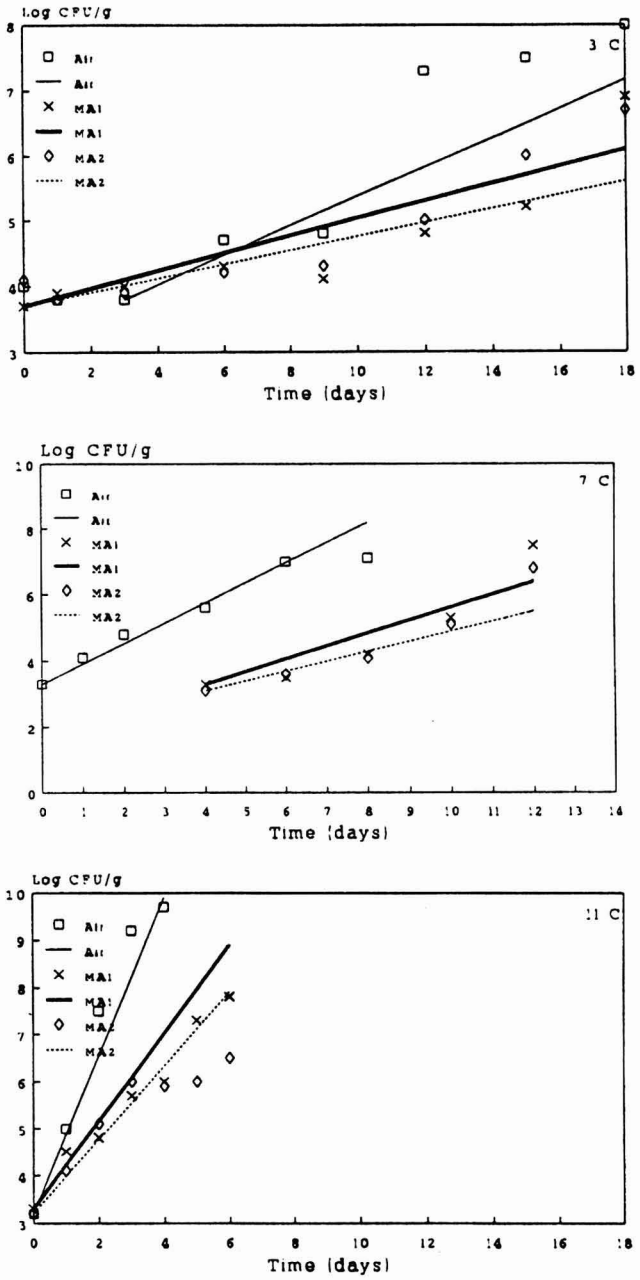


FIG. 4. COMPARISON OF OBSERVED (SYMBOL) AND PREDICTED (LINE) GROWTH OF *P. FLUORESCENS* POPULATION AT 3, 7, AND 11C USING A MODIFIED AND ADDITIVE ARRHENIUS EQUATION (EQ. 10)

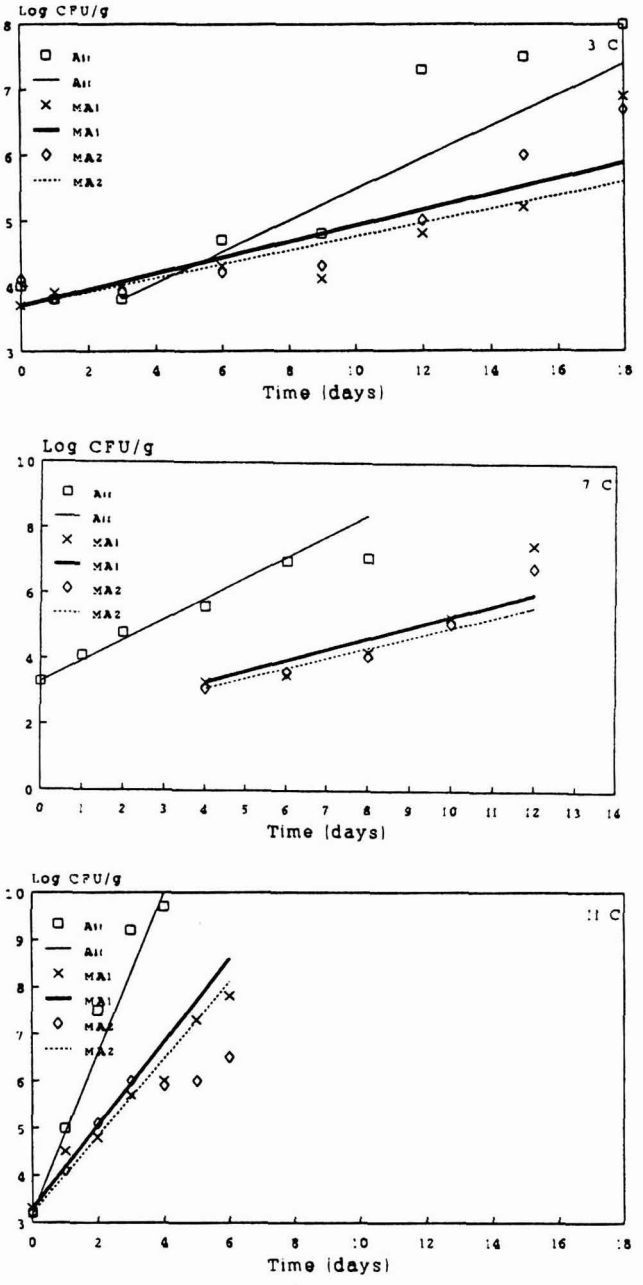


FIG. 5. COMPARISON OF OBSERVED (SYMBOL) AND PREDICTED (LINE) GROWTH OF *P. FLUORESCENS* POPULATION AT 3, 7, AND 11C USING MODIFIED ARRHENIUS TEMPERATURE CHARACTERISTIC EQUATION (EQ. 12)

present study, nine groups of experimental data were used, thereby limiting the parameters of Eq. (8) that could be estimated.

It must be noted that Eq. (10) and Eq. (12) are empirical. From a practical standpoint, therefore, use of these descriptions will be predicated on how successfully they fit data over a wide range temperatures and gas compositions. Also, the easy of equation usage must be considered. With respect to these criteria, the equations presented have the advantage that they can be fit to data using statistical software that is available on most computers. The mathematical formulation of the equations do not preclude application in a wide variety of conditions, but have only been demonstrated for ranges of $[O_2]$ from 0% to 20.99% and $[CO_2]$ from 0.03% to 80% under refrigeration temperatures.

It is noteworthy that when Eq. (10) and Eq. (12) are used to predict bacterial population during the log phase, such equations are limited in determination of lag phase and by the choice of the initial point of log phase from experimental observations. The degree of difficulty in selecting the range of log phase growth increases with the nonlinearity of experimental observations. Modified atmosphere storage significantly lengthens the lag phase; therefore, different times must be chosen as the initial growth time for log phase predictions depending on atmosphere composition and temperature. For example, the initial lag time for *L. monocytogenes* at 3C in air is three days, but extends to six days for modified atmosphere 1. Further discussion of lag phase extension is presented by Marshall *et al.* (1991).

Equations (10) and (12) have been constructed based on experimental data for *L. monocytogenes* and *P. fluorescens*. Since *L. monocytogenes* is facultatively anaerobic, and *P. fluorescens* is aerobic, it is not clear if these equations are applicable to strict anaerobic organisms. Furthermore, other species of bacteria are likely to have different magnitudes of regression parameters for similar growth conditions. More experimental data are needed to confirm the potential of using Eq. (10) and Eq. (12) for organisms and conditions extrapolated beyond the limits given in Tables 1 and 2.

## CONCLUSIONS

Two mathematical descriptions based on modifications of the Arrhenius equation were shown to predict the effect of temperature and percent concentration ratio of oxygen to carbon dioxide on the population growth rate coefficient of *L. monocytogenes* and *P. fluorescens* in chicken nuggets. The present amount of experimental data appropriate to equation development limited derivation of a widely applicable mathematical equation. Care must be taken when using the proposed equations in extrapolations beyond the previously defined limits. The

equations were sensitive to determination of the beginning of log phase growth and initial cell concentration. Future studies should be designed in a manner to yield data that lends itself to modelling.

## ACKNOWLEDGMENTS

Partial financial support provided by the Southeastern Poultry & Egg Association Project #478. The authors thank the following individuals for technical assistance: L.S. Andrews, H.K. Salman, S. Donnelly, and P.L. Wiese-Lehigh.

## NOMENCLATURE

| | |
|---|---|
| A | Collision factor in Arrhenius equation |
| b,c | Quantity of parameters related to bacterial growth rate coefficient |
| $[CO_2]$ | Percent concentration of carbon dioxide |
| $C_N$ | Concentration of NaCl in Eq. (2) |
| $\mu$ | Arrhenius temperature characteristic term, cal/mol |
| G | Generation time, day |
| $H_A$,$H_L$ | Constants in Eq. (8) describing the enthalpy for microbial growth |
| k | Rate coefficient for bacterial growth, $day^{-1}$ |
| N | Number of viable microorganisms |
| $[O_2]$ | Percent concentration of oxygen |
| $pH_I$ | Initial pH value [Eq. (2)] |
| R | Universal gas constant, 1.987 cal/(mol K) |
| $T_{1/2L}$ | Absolute temperature, K describing 50% low temperature interaction of the growth rate [Eq. (8)] |
| T | Absolute temperature K |
| t | Time, day |
| $\alpha_w$ | Water activity |
| $\rho_{(25)}$ | Growth rate at 25C [Eq. (8)] |

### Subscripts

| | |
|---|---|
| min | Minimum |
| max | Maximum |
| o | Initial condition |

## REFERENCES

BROUGHALL, J.M., ANSLOW, P.A. and KILSBY, D.C. 1983. Hazard analysis applied to microbial growth in foods: Development of mathematical models describing the effect of water activity. J. Appl. Bacteriol. *55*, 101–110.

BROUGHALL, J.M. and BROWN, C. 1984. Hazard analysis applied to microbial growth in foods: Development and application of three-dimensional models to predict bacterial growth. Food Microbiol. *1*, 13–22.

CHANDLER, R.E. and McMEEKIN, T.A. 1989a. Modelling the growth response of *Staphylococcus xylosus* to changes in temperature and glycerol concentration/water activity. J. Appl. Bacteriol. *66*, 543–548.

CHANDLER, R.E. and McMEEKIN, T.A. 1989b. Combined effect of temperature and salt concentration/water activity on the growth rate of *Halobacterium spp.* J. Appl. Bacteriol. *67*, 71–76.

DAVEY, K.R. 1989. A predictive model for combined temperature and water activity on microbial growth during the growth phase. J. Appl. Bacteriol. *67*, 483–488.

FARBER, J.M. 1991. Microbiological aspects of modified-atmosphere packaging: A review. J. Food Prot. *54*, 58–70.

GILL, C.O. and TAN, K.H. 1980. Effect of carbon dioxide on growth of meat spoilage bacteria. Appl. Environ. Microbiol. *39*, 317–319.

LABUZA, T.P. 1984. Application of chemical kinetics to deterioration of foods. J. Chem. Educ. *61*(4), 348–353.

MARSHALL, D.L. and SCHMIDT, R.H. 1988. Growth of *Listeria monocytogenes* at 10°C in milk preincubated with selected *Pseudomonas*. J. Food Prot. *51*, 277–282.

MARSHALL, D.L., WIESE-LEHIGH, P.L., WELLS, J.H. and FARR, A.J. 1991. Comparative growth of *Listeria monocytogenes* and *Pseudomonas fluorescens* on precooked chicken nuggets stored under modified atmospheres. J. Food Prot. *54*, 841–843, 851.

McMEEKIN, T.A. *et al.* 1987. Model for combined effect of temperature and salt concentration/water activity on the growth rate of *Staphylococcus xylosus*. J. Appl. Bacteriol. *62*, 543–550.

RATKOWSKY, D.A., LOWRY, R.K., McMEEKIN, T.A., STOKES, A.N. and CHANDLER, R.E. 1983. Model for bacterial culture growth rate throughout the entire biokinetic temperature range. J. Bacteriol. *154*, 1222–1226.

RATKOWSKY, D.A., OLLEY, J., McMEEKIN, T.A. and BALL, A. 1982. Relationship between temperature and growth rate of bacterial cultures. J. Bacteriol. *149*, 1–5.

ROBERTS, T.A. 1989. Combinations of antimicrobials and processing methods. Food Technol. *43*, 156–163.

SAGUY, I. and KAREL, M. 1980. Modeling of quality deterioration during food processing and storage. Food Technol. *34*, 78–85.

SAS Institute Inc. 1988. *SAS/STAT User's Guide*, Release 6.03 Ed., SAS Institute, Cary, NC.

SCHOOLFIELD, R.M., SHARPE, P.J.H. and MAGNUSON, C.E. 1981. Nonlinear regression of biological temperature-dependent rate models based on absolute reaction-rate theory. J. Theor. Biol. *88*, 719–731.

THAYER, D.W., MULLER, W.S., BUCHANAN, R.L. and PHILLIPS, J.C. 1987. Effect of NaCl, pH, temperature, and atmosphere on growth of *Salmonella typhimurium* in glucose-mineral salts medium. Appl. Environ. Microbiol. *53*, 1311–1315.

WIMPFHIMER, L., ALTMAN, N.S. and HOTCHKISS, J.H. 1990. Growth of *Listeria monocytogenes* Scott A, serotype 4 and competitive spoilage organisms in raw chicken packaged under modified atmospheres and in air. Int. J. Food Microbiol. *11*, 205–214.

# AUTHOR INDEX



Journal of Food Process Engineering **15** (1992) 319–320. *All Rights Reserved.*

# SUBJECT INDEX




Journal of Food Process Engineering **15** (1992) 321-322. *All Rights Reserved.*

# F N P PUBLICATIONS IN FOOD SCIENCE AND NUTRITION

## Journals

JOURNAL OF FOOD LIPIDS, F. Shahidi
JOURNAL OF RAPID METHODS AND AUTOMATION IN MICROBIOLOGY, D.Y.C. Fung and M.C. Goldschmidt
JOURNAL OF MUSCLE FOODS, N.G. Marriott and G.J. Flick, Jr.
JOURNAL OF SENSORY STUDIES, M.C. Gacula, Jr.
JOURNAL OF FOODSERVICE SYSTEMS, C.A. Sawyer
JOURNAL OF FOOD BIOCHEMISTRY, J.R. Whitaker, N.F. Haard and H. Swaisgood
JOURNAL OF FOOD PROCESS ENGINEERING, D.R. Heldman and R.P. Singh
JOURNAL OF FOOD PROCESSING AND PRESERVATION, D.B. Lund
JOURNAL OF FOOD QUALITY, J.J. Powers
JOURNAL OF FOOD SAFETY, T.J. Montville and A.J. Miller
JOURNAL OF TEXTURE STUDIES, M.C. Bourne and P. Sherman

## Books

MICROWAVE FOODS: NEW PRODUCT DEVELOPMENT, R.V. Decareau
DESIGN AND ANALYSIS OF SENSORY OPTIMIZATION, M.C. Gacula, Jr.
NUTRIENT ADDITIONS TO FOOD, J.C. Bauernfeind and P.A. Lachance
NITRITE-CURED MEAT, R.G. Cassens
THE POTENTIAL FOR NUTRITIONAL MODULATION OF THE AGING PROCESSES, D.K. Ingram *et al.*
CONTROLLED/MODIFIED ATMOSPHERE/VACUUM PACKAGING OF FOODS, A.L. Brody
NUTRITIONAL STATUS ASSESSMENT OF THE INDIVIDUAL, G.E. Livingston
QUALITY ASSURANCE OF FOODS, J.E. Stauffer
THE SCIENCE OF MEAT AND MEAT PRODUCTS, 3RD ED., J.F. Price and B.S. Schweigert
HANDBOOK OF FOOD COLORANT PATENTS, F.J. Francis
ROLE OF CHEMISTRY IN THE QUALITY OF PROCESSED FOODS, O.R. Fennema, W.H. Chang and C.Y. Lii
NEW DIRECTIONS FOR PRODUCT TESTING AND SENSORY ANALYSIS OF FOODS, H.R. Moskowitz
PRODUCT TESTING AND SENSORY EVALUATION OF FOODS, H.R. Moskowitz
ENVIRONMENTAL ASPECTS OF CANCER: ROLE OF MACRO AND MICRO COMPONENTS OF FOODS, E.L. Wynder *et al.*
FOOD PRODUCT DEVELOPMENT IN IMPLEMENTING DIETARY GUIDELINES, G.E. Livingston, R.J. Moshy, and C.M. Chang
SHELF-LIFE DATING OF FOODS, T.P. Labuza
ANTINUTRIENTS AND NATURAL TOXICANTS IN FOOD, R.L. Ory
UTILIZATION OF PROTEIN RESOURCES, D.W. Stanley *et al.*
VITAMIN $B_6$: METABOLISM AND ROLE IN GROWTH, G.P. Tryfiates
POSTHARVEST BIOLOGY AND BIOTECHNOLOGY, H.O. Hultin and M. Milner

## Newsletters

MICROWAVES AND FOOD, R.V. Decareau
FOOD INDUSTRY REPORT, G.C. Melson
FOOD, NUTRITION AND HEALTH, P.A. Lachance and M.C. Fisher
FOOD PACKAGING AND LABELING, S. Sacharow

# Statement of Ownership, Management and Circulation

*(Required by 39 U.S.C. 3685)*

| 1A. Title of Publication | 1B. PUBLICATION NO. | 2. Date of Filing |
|---|---|---|
| JOURNAL OF FOOD PROCESS ENGINEERING | 0 1 4 5 8 8 7 6 | Oct. 1, 1992 |
| 3. Frequency of Issue | 3A. No. of Issues Published Annually | 3B. Annual Subscription Price |
| Quarterly | 4 | $120.00 |

4. Complete Mailing Address of Known Office of Publication (Street, City, County, State and ZIP+4 (Not printers)

2 Corporate Drive, POB 374, Trumbull, Fairfield, CT 06611

5. Complete Mailing Address of the Headquarters of General Business Offices of the Publisher (Not printers)

2 Corporate Drive, POB 374, Trumbull, CT 06611

6. Full Names and Complete Mailing Address of Publisher, Editor, and Managing Editor (This item MUST NOT be blank)

Publisher (Name and Complete Mailing Address)

John J. O'Neil, 2 Corporate Drive, POB 374, Trumbull, CT 06611

Editor (Name and Complete Mailing Address)

Dr. Dennis R. Heldman, 83 Gordon Avenue, Lawrenceville, NJ 08648

Editor (Name and Complete Mailing Address)

Dr. R. Paul Singh, Univ. of California, Dept. of Agricultural Eng., Davis, CA 95616

7. Owner (If owned by a corporation, its name and address must be stated and also immediately thereunder the names and addresses of stockholders owning or holding 1 percent or more of total amount of stock. If not owned by a corporation, the names and addresses of the individual owners must be given. If owned by a partnership or other unincorporated firm, its name and address, as well as that of each individual must be given. If the publication is published by a nonprofit organization, its name and address must be stated.) (Item must be completed.)

| Full Name | Complete Mailing Address |
|---|---|
| Food & Nutrition Press, Inc. | 2 Corporate Drive, POB 374, Trumbull, CT 06611 |
| John J. O'Neil | 53 Stonehouse Road, Trumbull, CT 06611 |
| Michael J. Tully | 3 No. Slope, Union Gap Village, Clinton, NJ 088 |
| Kathryn O. & Christopher R. Ziko | 8 Maria Alicia Dr., Huntington, CT 06484 |
| John J. O'Neil, Jr. | 115 Maureen Sr., Srrarford, CT 06497 |

8. Known Bondholders, Mortgagees, and Other Security Holders Owning or Holding 1 Percent or More of Total Amount of Bonds, Mortgages or Other Securities (If there are none, so state)

| Full Name | Complete Mailing Address |
|---|---|
| None | |
| | |
| | |
| | |
| | |

9. For Completion by Nonprofit Organizations Authorized To Mail at Special Rates (DMM Section 424.12 only)
The purpose, function, and nonprofit status of this organization and the exempt status for Federal income tax purposes (Check one)

(1) ☐ Has Not Changed During Preceding 12 Months (2) ☐ Has Changed During Preceding 12 Months (If changed, publisher must submit explanation of change with this statement.)

| 10. Extent and Nature of Circulation (See instructions on reverse side) | Average No. Copies Each Issue During Preceding 12 Months | Actual No. Copies of Single Issue Published Nearest to Filing Date |
|---|---|---|
| A. Total No. Copies (Net Press Run) | 400 | 400 |
| B. Paid and/or Requested Circulation 1. Sales through dealers and carriers, street vendors and counter sales | 0 | 0 |
| 2. Mail Subscription (Paid and/or requested) | 239 | 239 |
| C. Total Paid and/or Requested Circulation (Sum of 10B1 and 10B2) | 239 | 239 |
| D. Free Distribution by Mail, Carrier or Other Means Samples, Complimentary, and Other Free Copies | 53 | 53 |
| E. Total Distribution (Sum of C and D) | 292 | 292 |
| F. Copies Not Distributed 1. Office use, left over, unaccounted, spoiled after printing | 108 | 108 |
| 2. Return from News Agents | 0 | 0 |
| G. TOTAL (Sum of E, F1 and 2—should equal net press run shown in A) | 400 | 400 |

11. I certify that the statements made by me above are correct and complete

Signature and Title of Editor, Publisher, Business Manager, or Owner

John J. O'Neil, Publisher

# GUIDE FOR AUTHORS

Typewritten manuscripts in triplicate should be submitted to the editorial office. The typing should be double-spaced throughout with one-inch margins on all sides.

Page one should contain: the title, which should be concise and informative; the complete name(s) of the author(s); affiliation of the author(s); a running title of 40 characters or less; and the name and mail address to whom correspondence should be sent.

Page two should contain an abstract of not more than 150 words. This abstract should be intelligible by itself.

The main text should begin on page three and will ordinarily have the following arrangement:

**Introduction:** This should be brief and state the reason for the work in relation to the field. It should indicate what new contribution is made by the work described.

**Materials and Methods:** Enough information should be provided to allow other investigators to repeat the work. Avoid repeating the details of procedures which have already been published elsewhere.

**Results:** The results should be presented as concisely as possible. Do not use tables *and* figures for presentation of the same data.

**Discussion:** The discussion section should be used for the interpretation of results. The results should not be repeated.

In some cases it might be desirable to combine results and discussion sections.

**References:** References should be given in the text by the surname of the authors and the year. *Et al.* should be used in the text when there are more than two authors. All authors should be given in the Reference section. In the Reference section the references should be listed alphabetically. See below for style to be used.

DEWALD, B., DULANEY, J.T., and TOUSTER, O. 1974. Solubilization and polyacrylamide gel electrophoresis of membrane enzymes with detergents. In *Methods in Enzymology,* Vol. xxxii, (S. Fleischer and L. Packer, eds.) pp. 82–91, Academic Press, New York.

HASSON, E.P. and LATIES, G.G. 1976. Separation and characterization of potato lipid acylhydrolases. Plant Physiol. *57,*142–147.

ZABORSKY, O. 1973. *Immobilized Enzymes,* pp. 28–46, CRC Press, Cleveland, Ohio.

Journal abbreviations should follow those used in *Chemical Abstracts.* Responsibility for the accuracy of citations rests entirely with the author(s). References to papers in press should indicate the name of the journal and should only be used for papers that have been accepted for publication. Submitted papers should be referred to by such terms as "unpublished observations" or "private communication." However, these last should be used only when absolutely necessary.

Tables should be numbered consecutively with Arabic numerals. The title of the table should appear as below:

Table 1. Activity of potato acyl-hydrolases on neutral lipids, galactolipids, and phospholipids

Description of experimental work or explanation of symbols should go below the table proper. Type tables neatly and correctly as tables are considered art and are not typeset. Single-space tables.

Figures should be listed in order in the text using Arabic numbers. Figure legends should be typed on a separate page. Figures and tables should be intelligible without reference to the text. Authors should indicate where the tables and figures should be placed in the text. Photographs must be supplied as glossy black and white prints. Line diagrams should be drawn with black waterproof ink on white paper or board. The lettering should be of such a size that it is easily legible after reduction. Each diagram and photograph should be clearly labeled on the reverse side with the name(s) of author(s), and title of paper. When not obvious, each photograph and diagram should be labeled on the back to show the top of the photograph or diagram.

**Acknowledgments:** Acknowledgments should be listed on a separate page.

Short notes will be published where the information is deemed sufficiently important to warrant rapid publication. The format for short papers may be similar to that for regular papers but more concisely written. Short notes may be of a less general nature and written principally for specialists in the particular area with which the manuscript is dealing. Manuscripts which do not meet the requirement of importance and necessity for rapid publication will, after notification of the author(s), be treated as regular papers. Regular papers may be very short.

Standard nomenclature as used in the engineering literature should be followed. Avoid laboratory jargon. If abbreviations or trade names are used, define the material or compound the first time that it is mentioned.

**EDITORIAL OFFICES:** DR. D.R. HELDMAN, COEDITOR, *Journal of Food Process Engineering,* Weinberg Consulting Group Inc., 1220 19th St., N.W., Washington, D.C. 20036 USA; or DR. R.P. SINGH, COEDITOR, *Journal of Food Process Engineering,* University of California, Davis, Department of Agricultural Engineering, Davis, CA 95616 USA.

# CONTENTS